



Hochschule für Angewandte Wissenschaften Hamburg
Hamburg University of Applied Sciences

Project

Department of Automotive and Aeronautical Engineering

**Mach number, relative thickness, sweep and
lift coefficient of the wing -
An empirical investigation of parameters and equations**

Author: Simona Ciornei

Examiner: Prof. Dr.-Ing. Dieter Scholz, MSME

Delivered: 31.05.2005

Abstract

12 equations were investigated to calculate the relative thickness t/c of the wing of an aircraft. The calculated relative thickness was taken as the average relative thickness of the wing. The data obtained from these 12 equations was checked against the given average relative thickness of 29 carefully selected aircraft, spanning a space of the parameters Mach number, lift coefficient, sweep, and type of airfoil. Some equations selected are empirical in their nature (partly based on aerodynamic derivation) other equations are purely statistical. Whenever equations had free parameters, these were optimized against the aircraft data. The best equation turned out to be an equation based on nonlinear regression. It achieved a Standard Error of Estimate of only 0.75 % for the average relative thickness of the wing. Torenbeek's equation will probably be preferred by those that like to see an equation that is based on aerodynamic considerations. It achieved a Standard Error of Estimate of 0.80 % when all its free parameters were considered for optimization. The worst equation produced an Standard Error of Estimate of 8 %. For an airfoil with 10 % relative thickness this would give an unacceptable 10 % \pm 8 % band of values for t/c which renders equations like this quite useless.





FACHBEREICH FAHRZEUGTECHNIK UND FLUGZEUGBAU

Mach number, relative thickness, sweep and lift coefficient of the wing

- an empirical investigation of parameters and equations

Aufgabenstellung zum *Projekt* gemäß Prüfungsordnung

Background

In aircraft design, the wing parameters "relative thickness" and "sweep" follow from a demand for a certain cruise Mach number at low wave drag. In addition, the cruise lift coefficient and the type of airfoil have an influence on the aerodynamics of the wing. If there is a demand for a higher cruise Mach number during aircraft design, the sweep has to be increased or the relative thickness has to be decreased. The transonic flow around a wing can not be described with simple equations. For this reason, the relationship between the parameters as given above will be based in preliminary aircraft design on statistics of known aircrafts.

Task

Equations based on statistical data relating Mach number, relative thickness, sweep and lift coefficient of the wing have to be investigated, checked and improved for their suitability in preliminary aircraft design. The project's task includes these subtasks:

- Introduction to transonic flow around wings.
- Literature search for equations dealing with the relationship of named parameters.
- Theoretical substantiation of the empirical equations as far as possible.
- Investigation of aircraft parameters for sample calculations with equations from the literature.
- Comparison of equations based on sample calculations. Selection of the most suitable equation.
- Adaptation of this equation to further improve the accuracy based on given aircraft parameters.

The report has to be written according to German DIN standards on report writing!

Table of Contents

	page
List of Figures	8
List of Tables	10
List of Symbols	11
List of Key Words and Definitions	13
1 Introduction	15
1.1 Motivation	15
1.2 Definitions	15
1.3 Task	18
1.4 Literature	19
1.5 Structure of Work	19
2 Transonic Flow	21
2.1 Transonic Flow Phenomena	21
2.2 Compressibility Corrections	23
2.3 Critical Mach Number and Critical Pressure Coefficient	24
2.4 Drag –Divergence Mach Number	28
2.5 Development of the Supercritical Airfoil	31
2.6 Swept Wings	34
2.7 Relative Thickness	37
3 Equations for the Calculation of Relative Thickness	38
3.1 Equation based on Torenbeek	38
3.2 Equations from Aerodynamic Similarity based on Anderson	40
3.3 Equation based on Shevell	41
3.4 Equation based on Kroo	44
3.5 Equation from Howe	47
3.6 Equation from Jenkinson	48
3.7 Equation from Weisshaar	49
3.8 Equation based on Böttger	50
3.9 Equation based on Raymer	54
3.10 Equation based on Linear Regression	59
3.11 Equation based on Nonlinear Regression	60
3.12 Substantiation of the Equation from Torenbeek	61
4 Investigation Comparison and Adaptation of Equations	65
4.1 Input from Aircraft Data	65
4.2 Calculation, Optimization and Results	66

5	Conclusions	70
6	Recommendations	71
	List of References	72
	Appendix A Three-View Drawings	77
	Appendix B Investigation of Aircraft Parameters from Different Sources	107
	Appendix C Summary of Aircraft Parameters	137
	Appendix D Calculation of Relative Thickness / Optimization of Equations	142
	Appendix E Schaufele's Method	151

List of Figures

Figure 1.1	Definition of sweep angles on a tapered inner and outer wing	17
Figure 2.1	Physical mechanism of drag divergence	22
Figure 2.2	Variation of (a) lift coefficient and (b) drag coefficient versus Mach number with angle of attack as a parameter for an NACA 2315 airfoil.....	22
Figure 2.3	Several compressibility corrections compared with experimental results for an NACA 4412 airfoil at an angle of attack $\alpha = 1^\circ 53'$	24
Figure 2.4	Illustration of critical Mach number.....	25
Figure 2.5	Illustration of critical pressure coefficient.....	26
Figure 2.6	Critical pressure coefficient and critical Mach numbers for airfoils of different thickness	26
Figure 2.7	Sketch of the variation of profile drag coefficient with freestream Mach number, illustrating the critical and drag-divergence Mach number and showing the large drag rise near Mach 1	29
Figure 2.8	Definition of critical Mach number.....	30
Figure 2.9	Peaky upper surface pressure distribution.....	32
Figure 2.10	Standard NACA 64-series airfoil compared with a supercritical airfoil at cruise lift conditions	33
Figure 2.11	Effect of swept wing on critical Mach number	34
Figure 2.12	Sketch of the variation of minimum wing-drag coefficient versus Mach number with different sweep angles and relative thickness	36
Figure 2.13	Wing sweep historical trend.....	36
Figure 2.14	Wing thickness spanwise distribution.....	37
Figure 3.1	Explanation of M_{CC}	42
Figure 3.2	The ratio of M_{DIV} and M_{CC} versus sweep.....	42
Figure 3.3	Crest critical Mach number (M_{CC}) as a function of relative thickness t/c and lift coefficient C_L can be compared	44
Figure 3.4	The crest critical Mach number versus relative thickness for $C_L = 0$	45
Figure 3.5	Crest Critical Mach number versus relative thickness for all five values of C_L	46
Figure 3.6	Drag divergence Mach number M_{DD} versus lift coefficient C_L	50
Figure 3.7	Drag divergence Mach number M_{DD} versus relative thickness t/c	51
Figure 3.8	Drag divergence Mach number M_{DD} versus sweep ϕ_{25}	52
Figure 3.9	The M_{DD} versus C_L converted in Excel	53
Figure 3.10	Wing drag-divergence Mach number.....	55

Figure 3.11	Lift adjustment for M_{DD}	55
Figure 3.12	Representation of Figure 3.10 for $t/c = 0.12$ with equation (3.50).....	56
Figure 3.13	Representation of Figure 3.10 with equation (3.50)	57
Figure 3.14	Influence of t/c in Figure 3.10 given by equation (3.51).....	57
Figure 3.15	Representation of Figure 3.11 for $t/c = 0.14$ with equation (3.52).....	58
Figure 3.16	Representation of Figure 3.11 with equation (3.52)	58
Figure 3.17	Influence of t/c in Figure 3.11 given by equation (3.53).....	59
Figure 3.18	Minimum pressure coefficient at zero lift for selected NACA airfoils as a function of relative thickness	61
Figure A.1	Three-view drawing: IAI 1124A Westwind 2.....	77
Figure A.2	Three-view drawing: Sud Aviation Caravelle.....	78
Figure A.3	Three-view drawing: VFW 614	79
Figure A.4	Three-view drawing: HFB 320.....	80
Figure A.5	Three-view drawing: Gates Lear Jet Model 23	81
Figure A.6	Three-view drawing: Lockheed C-141 Starlifter	82
Figure A.7	Three-view drawing: Lockheed Jetstar II.....	83
Figure A.8	Three-view drawing: Dassault Falcon 20.....	84
Figure A.9	Three-view drawing: BAC One–Eleven Series 500.....	85
Figure A.10	Three-view drawing: McDonnell Douglas DC-9 Series 30	86
Figure A.11	Three-view drawing: Vickers Super VC-10.....	87
Figure A.12	Three-view drawing: McDonnell Douglas DC-8 Series 63	88
Figure A.13	Three-view drawing: McDonnell Douglas DC-10 Series 10	89
Figure A.14	Three-view drawing: Lockheed C-5A.....	90
Figure A.15	Three-view drawing: Mitsubitshi Diamond I	91
Figure A.16	Three-view drawing: Airbus A300-600	92
Figure A.17	Three-view drawing: Boeing 767-200.....	93
Figure A.18	Three-view drawing: Cessna 650 Citation VI.....	94
Figure A.19	Three-view drawing: Airbus A310-300	95
Figure A.20	Three-view drawing: Raytheon Hawker 800XP	96
Figure A.21	Three-view drawing: Raytheon Beechjet 400A	97
Figure A.22	Three-view drawing: Beriev Be-40	98
Figure A.23	Three-view drawing: Bombardier Global Express.....	99
Figure A.24	Three-view drawing: Bombardier Challenger CRJ 200 LR.....	100
Figure A.25	Three-view drawing: Tupolev Tu-204-300.....	101
Figure A.26	Three-view drawing: BAe RJ85.....	102
Figure A.27	Three-view drawing: Embraer EMB-145.....	103
Figure A.28	Three-view drawing: Airbus A321-200	104
Figure A.29	Three-view drawing: Airbus A340-300	105

List of Tables

Table 3.1	Variation of divergence Mach number (ΔM_{DIV}) depending on the type of airfoil	47
Table 4.1	Comparison of different equations used to calculate the relative thickness of a wing based on Standard Errors of Estimate	69
Table B.1	Investigation of aircraft parameters from different sources – IAI 1124A Westwind	108
Table B.2	Investigation of aircraft parameters from different sources – Caravelle	109
Table B.3	Investigation of aircraft parameters from different sources – VFW 614	110
Table B.4	Investigation of aircraft parameters from different sources – HFB 320	111
Table B.5	Investigation of aircraft parameters from different sources – Lear Jet Model 23	112
Table B.6	Investigation of aircraft parameters from different sources – Lockheed C-141 Starlifter	113
Table B.7	Investigation of aircraft parameters from different sources – Lockheed Jetstar II	114
Table B.8	Investigation of aircraft parameters from different sources – Dassault Falcon 20	115
Table B.9	Investigation of aircraft parameters from different sources – BAC One –Eleven Series 500	116
Table B.10	Investigation of aircraft parameters from different sources – McDonnell Douglas DC-9 Series 30	117
Table B.11	Investigation of aircraft parameters from different sources – Vickers Super VC10	118
Table B.12	Investigation of aircraft parameters from different sources – McDonnell Douglas DC-8 Series 63	119
Table B.13	Investigation of aircraft parameters from different sources – McDonnell Douglas DC-10 Series 10	120
Table B.14	Investigation of aircraft parameters from different sources – Lockheed C-5A	121
Table B.15	Investigation of aircraft parameters from different sources – Mitsubitshi Diamond I 15	122
Table B.16	Investigation of aircraft parameters from different sources – Airbus A300-600	123

Table B.17	Investigation of aircraft parameters from different sources – Boeing 767-200	124
Table B.18	Investigation of aircraft parameters from different sources – Cessna 650 Citation VI	125
Table B.19	Investigation of aircraft parameters from different sources – A310-300	126
Table B.20	Investigation of aircraft parameters from different sources – Raytheon Hawker 800XP	127
Table B.21	Investigation of aircraft parameters from different sources – Raytheon Beechjet 400A	128
Table B.22	Investigation of aircraft parameters from different sources – Beriev Be-40	129
Table B.23	Investigation of aircraft parameters from different sources – Bombardier Global Express	130
Table B.24	Investigation of aircraft parameters from different sources – Bombardier Challenger CRJ 200 LR	131
Table B.25	Investigation of aircraft parameters from different sources – Tupolev Tu-204-300	132
Table B.26	Investigation of aircraft parameters from different sources – BAe RJ85	133
Table B.27	Investigation of aircraft parameters from different sources – Embraer EMB-145	134
Table B.28	Investigation of aircraft parameters from different sources – A321-200	135
Table B.29	Investigation of aircraft parameters from different sources – A340-300	136
Table C.1	Summary of data for aircraft with conventional airfoils	138
Table C.2	Summary of data for aircraft with peaky airfoils	139
Table C.3	Summary of data for aircraft with older supercritical airfoils	140
Table C.4	Summary of data for aircraft with modern supercritical airfoils	141
Table D.1	Relative thickness of a wing - aircraft with conventional airfoils (1)	143
Table D.1	Relative thickness of a wing - aircraft with conventional airfoils (2)	144
Table D.1	Relative thickness of a wing - aircraft with peaky airfoils (1)	145
Table D.1	Relative thickness of a wing - aircraft with peaky airfoils (2)	146
Table D.1	Relative thickness of a wing - aircraft with supercritical airfoils (1)	147
Table D.1	Relative thickness of a wing - aircraft with supercritical airfoils (2)	148
Table D.1	Relative thickness of a wing - aircraft with modern supercritical airfoils (1)	149
Table D.1	Relative thickness of a wing - aircraft with modern supercritical airfoils (2)	150

List of Symbols

M_∞	free stream Mach number
a	speed of sound
Fr	Froude number
c_l	lift coefficient
c_d	drag coefficient
M	Mach number
C_p	pressure coefficient
$C_{p,0}$	incompressible pressure coefficient
$C_{p,cr}$	critical pressure coefficient
M_{cr}	critical Mach number
M_{DD}	drag divergence Mach number
M_{CR}	cruise Mach number
M_{eff}	effective Mach number
t/c	relative thickness
V	local velocity
M^*	factor use in Torenbeek equation
$M_{DD,eff}$	effective drag-divergence Mach number
A_F	factor use in Howe equation
M_{NCRIT}	the critical Mach number for a given form of two-dimensional aerofoil
C_{Ldes}	design lift coefficient
$M_{DDL=0}$	drag divergence Mach number for $C_L = 0$
LF_{DD}	factor use in Raymer equation
u, v, w	factors use in solving the Raymer equation
a, b	factors use in solving the Raymer equation
M_{DIV}	drag divergence Mach number
ΔC_{Dc}	incremental drag coefficient due to compressibility
M_{CC}	crest critical Mach number
ϕ_{25}	sweepback angle of the quarter chord in degrees
K_A	factor use in Weisshaar equation

Geek Symbols

γ	specific heat
Ω	sweep angle
Λ	sweepback angle of the quarter chord in degrees

Indices

∞	freestream
l	lift
d	drag
p	pressure
cr	critical
p, cr	critical pressure
DD	drag divergence
DIV	drag divergence
$D0$	parasite drag
CC	crest critical
eff	effective
max	maximum

List of Key Words and Definitions

sweep

The angle in plan view between a specified spanwise line along an aerodynamic surface and the normal to the plane of symmetry. For an aerodynamic surface as a whole, the quarter-chord line is preferred, but any other specified line, such as the leading or trailing edge, may be taken for a particular purpose. (AGARD 1980)

Mach Cone

The cone-shaped shock wave theoretically emanating from an infinitesimally small particle moving at the supersonic speed through a fluid medium. It is the locus of the mach lines: the cone shaped shock wave generated by a sharp pointed body, as the nose of a high speed aircraft. (AGARD 1980)

Mach number

The ratio of the true airspeed to the speed of sound under prevailing atmospheric conditions. (AGARD 1980)

Drag

The component along the longitudinal axis of the resultant of all external forces action on ACV due to its motion. (AGARD 1980)

Drag coefficient

The ratio of the drag to the product of dynamic pressure and a reference area. (AGARD 1980)

Lift coefficient

A coefficient representing the lift of a given aerofoil or other body. The lift coefficient is obtained by dividing the lift by the free-stream dynamic pressure and by the representative area under consideration. (AGARD 1980)

Lift/drag ratio

The ratio of the lift to drag obtained by dividing the lift by the drag or the lift coefficient by the drag coefficient. (AGARD 1980)

The drag-divergence Mach

The drag divergence Mach number is that Mach number where the wave drag coefficient reaches 20 drag counts ($\Delta C_{D,wave} = 0.002$). (AGARD 1980)

The free stream Mach

The free stream Mach number is the Mach number of the moving body $M = M_\infty = V/a$ with a being the speed of sound. (**Anderson 1989**)

1 Introduction

1.1 Motivation

The aim of this project is to search and develop equations that relate the parameters Mach number, relative thickness, sweep, and lift coefficient to one another. In general the dependence from two or more than two parameters can be establish in three ways:

1. based on calculations and statistical considerations
2. based on physical reasoning without using the statistical evidence and
3. using both ways.

In aircraft design an accurate sizing of the wing has a significant importance. A good explanation of this is given in **Hepperle 2003** “The size of the wing depends on the aerodynamic lift requirements, mainly during takeoff and landing as well as on the required fuel volume.” Mach number, relative thickness, sweep and lift coefficient are all related and involve a complex series of studies to achieve an optimum design for a specified set of requirements. It is well know that for maximum fuel volume, a large relative thickness is recommended. But for a higher cruise Mach number the relative thickness has to be decreased or the sweep has to be increased.

In order to establish the dependence between these parameters and to settle the contribution of each of them, 12 equations were used. The equations used in the calculation are taken from different source: some of them are given in the authentic form of the equation taken from literature, others were determine base on regression calculation.

The parameters of 29 aircraft have been used.

The project tries not only to settle the dependence between the parameters only on the equations as found in the literature, but tries also to improve these equation to achieve better results. The final result of the project gives not only a comparison between all these equations and but also new improved equations.

1.2 Definitions

The key words in the title of the project should be defined for a common understanding. The project is about: *Mach number*, *relative thickness*, *lift coefficient* and *sweep* of the wing. These aerodynamic parameters will be explained here.

The **Mach number** is according to **AGARD 1980**: "The ratio of the true airspeed to the speed of sound under prevailing atmospheric conditions."

$$M = V / a \quad (1.1)$$

with

V true airspeed
 a speed of sound.

The speed of sound which was used in the calculations had been calculated with the next equations valid for both troposphere and stratosphere

$$a = \sqrt{\gamma \cdot R \sqrt{T}} \quad (1.2)$$

$$\sqrt{\gamma \cdot R} = 20.0468 \text{ 1/}\sqrt{k} \cdot \frac{m}{s} \quad (1.3)$$

$$R = 287.053 \frac{J}{Kg \cdot K} \quad (1.4)$$

$$\gamma = 1.4 \quad (1.5)$$

$$a_0 = 340.294 \text{ m/s} = 1225.06 \text{ km/h} = 661.48 \text{ kt} \quad (1.6)$$

The next important two parameters used in the calculations are the **relative thickness** t/c and the effective relative thickness t/c_{eff} . The relative thickness is the ratio of the thickness of the wing divided by the chord of the wing. In the case of the swept wings c is in flow direction. The effective relative thickness t/c_{eff} is also the thickness of the wing but divided by the chord of the wing c_{eff} perpendicular to quarter chord line.

Some interesting explications about the distribution of the thickness of the wing are given in **Kroo 2001**:

"The distribution of thickness from wing root to tip is selected as follows:

1. We would like to make the t/c as large as possible to reduce wing weight (thereby permitting larger span, for example).
2. Greater t/c tends to increase $C_{L,max}$ up to a point, depending on the high lift system, but gains above about 12% are small if there at all.
3. Greater t/c increases fuel volume and wing stiffness.
4. Increasing t/c increases drag slightly by increasing the velocities and the adversity of the pressure gradients.

5. The main trouble with thick airfoils at high speeds is the transonic drag rise which limits the speed and C_L at which the airplane may fly efficiently.

Lift: According to **AGARD 1980**: "A coefficient representing the lift of a given aerofoil or other body." In cruise C_L follows from the equations below:

$$L = W = m \cdot g \quad (1.7)$$

we also know that

$$L = 1/2 \cdot \rho \cdot v^2 \cdot C_L \cdot S \quad (1.8)$$

Combining the both equations a convenient expression for the lift coefficient has been determined

$$C_L = \frac{2 \cdot m \cdot g}{\rho \cdot v^2 \cdot S} \quad (1.9)$$

Wing sweep. Each %-line on the wing has its sweep. It is its angle normal to the plane of symmetry. Figure 1.1 shows the sweep of the quarter chord line on an inner and outer tapered wing. The quarter chord sweep of the outer wing is given as the sweep for the total wing.

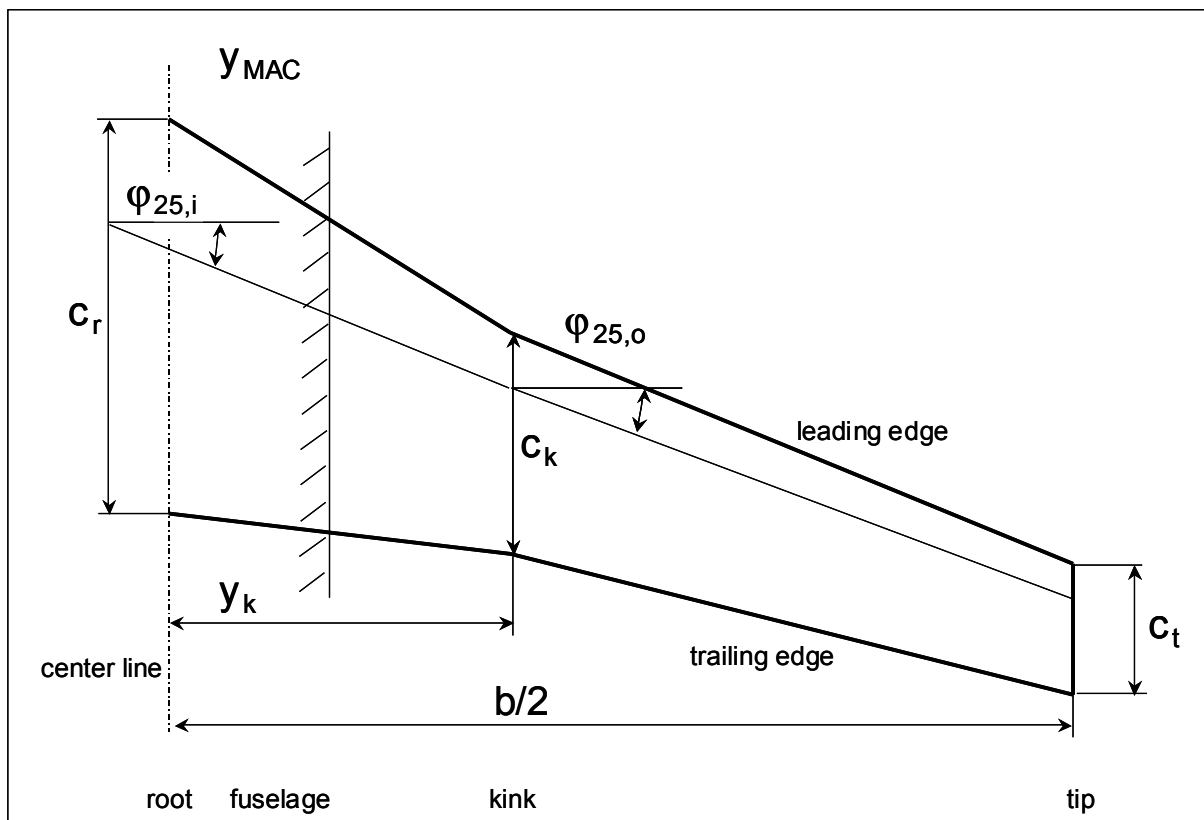


Figure 1.1 Definition of sweep angles on a tapered inner and outer wing (adapted from **Scholz 2005**)

A good explication of the use of the swept wing is offered in **Kroo 2001**:

“Wing sweep is chosen almost exclusively for its desirable effect on transonic wave drag. (Sometimes for other reasons such as a c.g. problem or to move winglets back for greater directional stability.)

1. It permits higher cruise Mach number, or greater thickness or C_L at a given Mach number without drag divergence.
2. It increases the additional loading at the tip and causes span wise boundary layer flow, exacerbating the problem of tip stall and either reducing $C_{L,max}$ or increasing the required taper ratio for good stall.
3. It increases the structural weight - both because of the increased tip loading, and because of the increased structural span.
4. It stabilizes the wing aero elastically but is destabilizing to the airplane.
5. Too much sweep makes it difficult to accommodate the main gear in the wing.

Much of the effect of sweep varies as the cosine of the sweep angle, making forward and aft-swept wings similar.”

The project is also about **empirical investigations**. This means in this context, to check the equations against statistical data taken from existing passenger aircraft.

1.3 Task

The aim of this project is to search and develop equations that relate the parameters Mach number, relative thickness, sweep and lift coefficient to one another. The project's task includes these subtasks:

- Introduction to transonic flow around wings and the complex effects which characterize this type of flow.
- Presentations of all parameters that are related to transonic flow base on the literature statements and the way that they are depending on one another.
- Presentations of all equations which had been found and which are dealing with these parameters.
- Theoretical substantiation of a selected empirical equation.
- Calculation of one chosen parameter (the relative thickness) based on the equations that had been found.
- Improvement of the equations by modifying their coefficients and to find a best fit to the collected data of aircraft parameters.

1.4 Literature

There are a number of empirical or semi-empirical equations presented in the literature trying to establish a relationship among the parameters of interest in this project (sweep, Mach number, relative thickness, sweep and lift coefficient). The different equations are in detail presented in Chapter 3. No reference has been found that

- a) extensively compares these equations with one another or
- b) tries to check the equations against a large set of statistical data.

Equations from literature could be grouped according to the level of aerodynamic detail included. One extreme are the equations that draw strongly from aerodynamic theory. This is the method based on **Torenbeek 1988** and the method that was deduced from **Anderson 1990**. The other extreme are the methods purely based on statistical considerations and data regression. Also **Jenkinson 1999** follows this approach.

The investigated equations are quite different. Some authors are taking into account the type of airfoil, other authors neglect this influence and just give a general equation for all types of airfoils.

Some equations are given without considering the effect of sweep whereas some take this effect into account.

Somewhere in between are equations that show a structure that well represents agreed aerodynamic wisdom and adjust the structure of the equations with parameter that were fit to statistical aircraft data. **Shevell 1980** follows this approach. His equations have not only a theoretical foundation but are also based on wind tunnel data.

1.5 Structure of Work

Chapter 2 presents an introduction to transonic flow and the complex effects which characterized it, a short describes of the parameters which are used in the equations: critical Mach number and the critical pressure, drag divergence Mach number, the sweep, relative thickness. This Chapter also shows how the different parameters influence each other. The development of the supercritical airfoil is presented.

Chapter 3 describes not only the equation that had been found in literature but also the equation that had been produced based on equations which have been found

in literature. A discussion of each equation is given. A subchapter of its own is dedicated to the theoretical substantiation of Torenbeek's equation.

Chapter 4

contains the calculation of relative thickness based on all equations that had been found or determined, the results are presented in form of tables and illustrated in graphical form if deemed necessary. This last chapter also contains the solutions for improving the equations that had been found in literature by modifying their coefficients and the adaptation of these equations to further improve the accuracy based on given aircraft parameters.

2 Transonic Flow

2.1 Transonic Flow Phenomena

An excellent explanation of transonic flow phenomena is given by John D. Anderson. This project puts much emphasis on information given in **Anderson 1989** and **Anderson 1991**. Anderson covers the theory together with the applications related to airfoil design and aircraft layout considerations. Transonic flow is one of the most challenging topics in aerodynamics.

Transonic flow is highly nonlinear, and theoretical transonic aerodynamics is a challenging and sophisticated subject. (Anderson 1991, p 547)

The analysis of transonic flows has been one of the major challenges in modern aerodynamics. Only in recent years, since about 1970, have computer solutions for transonic flows over airfoils come into practical use; these numerical solutions are still in a state of development and improvement. (Anderson 1989, p 209)

In transonic and supersonic flow we will encounter the effect of shock waves. They form when an object is approaching $M = 1$. Pressure disturbances which are created at the body surface and which propagate away at the speed of sound *cannot* work their way upstream. Instead, these disturbances coalesce at a finite distance from the body and form a natural phenomenon called a shock wave. The flow upstream of the shock wave does not feel the pressure disturbance. (**Anderson 1989**, p 123). We are very familiar with this phenomenon when we think of a boat going through the water. Here we have a clear indication of the formation of waves. Indeed, it can be shown that through similarity parameters both flow phenomena can be related to one another. In open channel flow the Froude number Fr takes up the function of the Mach number. In open channel flow $Fr = 1$ indicates the change in the character of the flow from subcritical to supercritical. (**Fox 1985**, p. 508)

Transonic flow is characterized by some very complex effects as indicated in Figure 2.1. In transonic flow we notice a large variation of both c_l and c_d as a function of Mach number Figure 2.2.

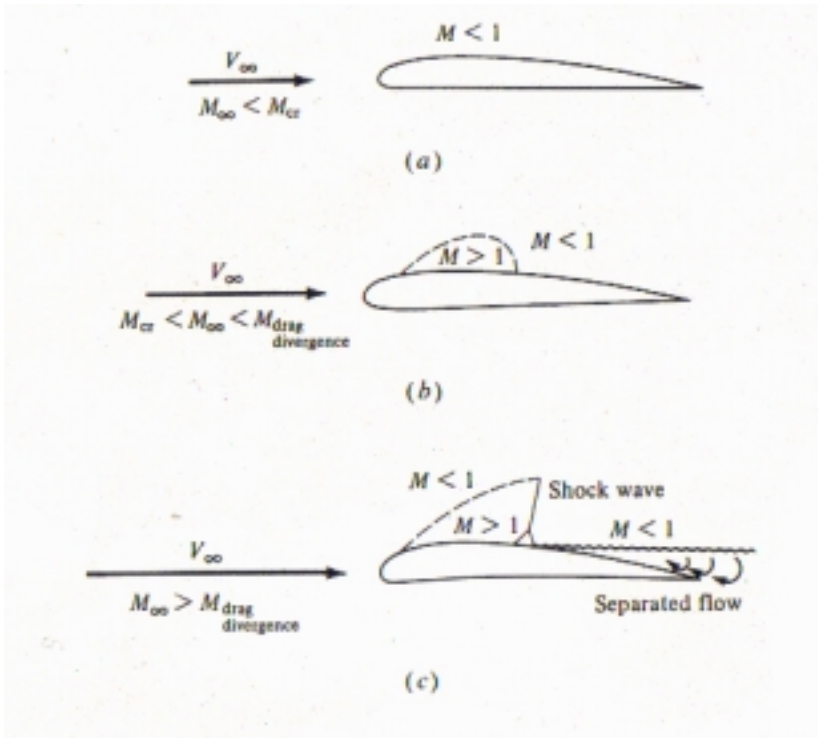


Figure 2.1 Physical mechanism of drag divergence (Anderson 1989)

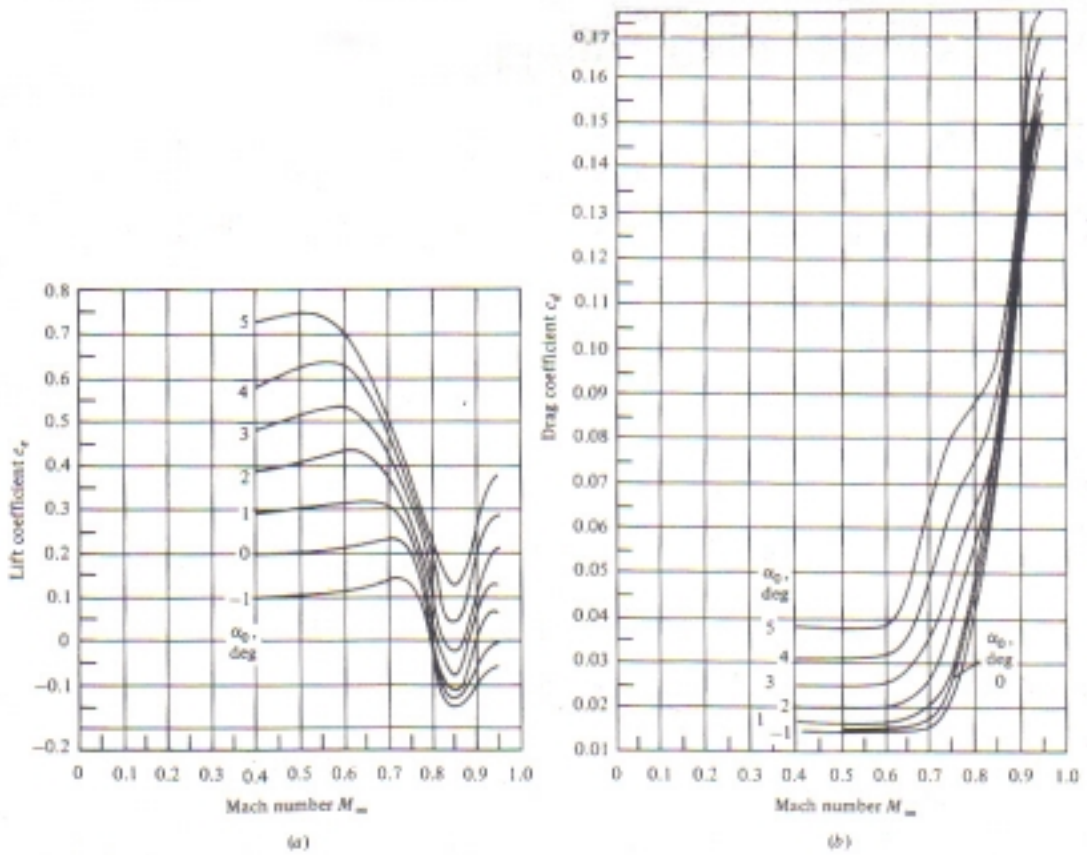


Figure 2.2 Variation of (a) lift coefficient and (b) drag coefficient versus Mach number with angle of attack as a parameter for an NACA 2315 airfoil (Anderson 1989)

When calculating the drag in transonic or supersonic flow, the effects due to the formation of shock waves have to be considered. *Zero-lift drag* is not only composed of skin-friction drag (as in incompressible flow) but in addition consists of wave (or pressure related) drag at zero lift. Similarly, *lift-dependent drag* is not only composed of induced drag (drag due to lift) but also of wave (or pressure-related) drag due to lift. (**Dailey 2005**)

In subsonic flow as well as in supersonic flow there are adequate theories than can predict the aerodynamic forces and moments present. On the contrary, is much less predictable. “Often, in transonic flow, the flow is unsteady, and the shock waves on the body surface may jump back and forth along the surface, thus disrupting and separating the flow over the wing surface. This sends pulsing, unsteady flow back to the tail surfaces of the airplane... With proper design, however, airplane configurations gradually evolved to the point where flying through the transonic region posed little or no difficulty in terms of wing buffeting or loss of lift.” (**Dailey 2005**)

“There are a number of ways of delaying the transonic wave drag rise (or equivalently, increasing the drag-divergence Mach number closer to 1). These include:

- Use of thin airfoils
- Use of a forward or backward swept wing
- Low-aspect ratio wing
- Removal of boundary layer and vortex generators;and
- Supercritical and area-rule technology” (**Dailey 2005**)

2.2 Compressibility Corrections

Equation

$$C_p = \frac{C_{p,0}}{\sqrt{1-M_\infty^2}} \quad (2.1)$$

is called the Prandtl-Glauert rule. “It states that, if we know the incompressible pressure distribution over an airfoil, then the compressible pressure distribution over the same airfoil can be obtain from (2.1).Therefore, equation(2.1) is truly a compressibility correction to incompressible data.” (**Anderson 1991**, p. 545)

Other compressibility corrections are (**Anderson 1991**, p. 546) the Karman-Tsien rule

$$C_p = \frac{C_{p,0}}{\sqrt{1-M_\infty^2} + \left[\frac{M_\infty^2}{1 + \sqrt{1-M_\infty^2}} \right] C_{p,0} / 2}} \quad (2.2)$$

and Laitone's rule

$$C_p = \frac{C_{p,0}}{\sqrt{1-M_\infty^2 + \left(M_\infty^2 \left\{ 1 + \frac{(\gamma-1)}{2} M_\infty^2 \right\} / 2\sqrt{1-M_\infty^2} \right) C_{p,0}}} \quad (2.3)$$

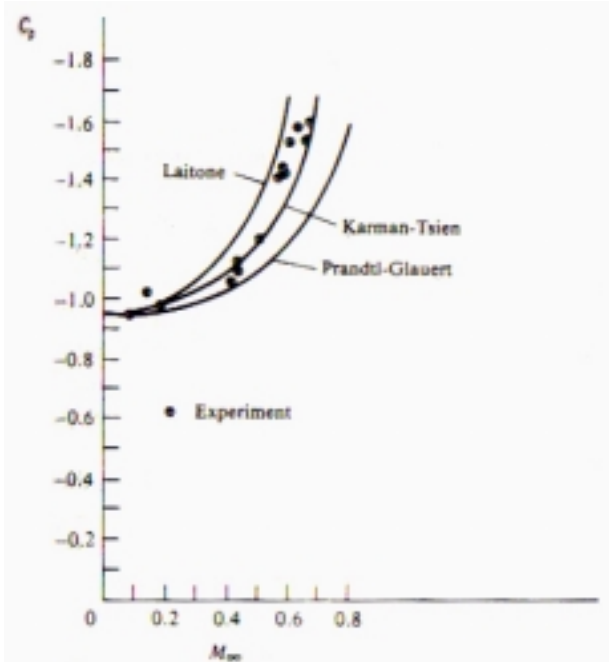


Figure 2.3 Several compressibility corrections compared with experimental results for an NACA 4412 airfoil at an angle of attack $\alpha = 1^\circ 53'$ (**Anderson 1991**)

“These compressibility corrections are compared in Figure 2.3, which also shows experimental data for the C_p variation with M_∞ at the 0.3-chord location on an NACA 4412 airfoil. Note that the Prandtl-Glauert rule, although the simplest to apply, underpredicts the experimental data, whereas the improved compressibility corrections are clearly more accurate. Recall that the Prandtl-Glauert rule is based on linear theory. In contrast, both the Laitone and Karman-Tsien rules attempt to account for some of nonlinear aspects of the flow.” (**Anderson 1991**, p. 547)

2.3 Critical Mach number and Critical Pressure Coefficient

Definition of Critical Mach Number

Anderson 1989 (p. 201) explains and defines the term Critical Mach Number: “Consider the flow of air over on airfoil. We know that, as the gas expands around the top surface near the leading edge, the velocity and hence the Mach number will increase rapidly. Indeed, there are regions on the airfoil surface where the local number is greater than M_∞ . Imagine that we put a given airfoil in a wind tunnel where $M_\infty = 0.3$ and that we observe the peak local Mach number on the top of surface of the airfoil to be 0.435. This is sketched in Figure 2.4a. Imag-

ine that we now increase M_∞ to 0.5; the peak local Mach number will correspondingly increase to 0.772, as shown in Figure 2.4b. If we further increase M_∞ to a value of 0.61, we observe that the peak local Mach number is 1.0, locally sonic flow on the surface of the airfoil. This is sketched in Figure 2.4c. Note that the flow over an airfoil can be locally sonic (or higher), even though the freestream Mach number is subsonic. By definition, the freestream Mach number at which sonic flow is first obtained somewhere on the airfoil surface is called the critical Mach number of the airfoil.”¹

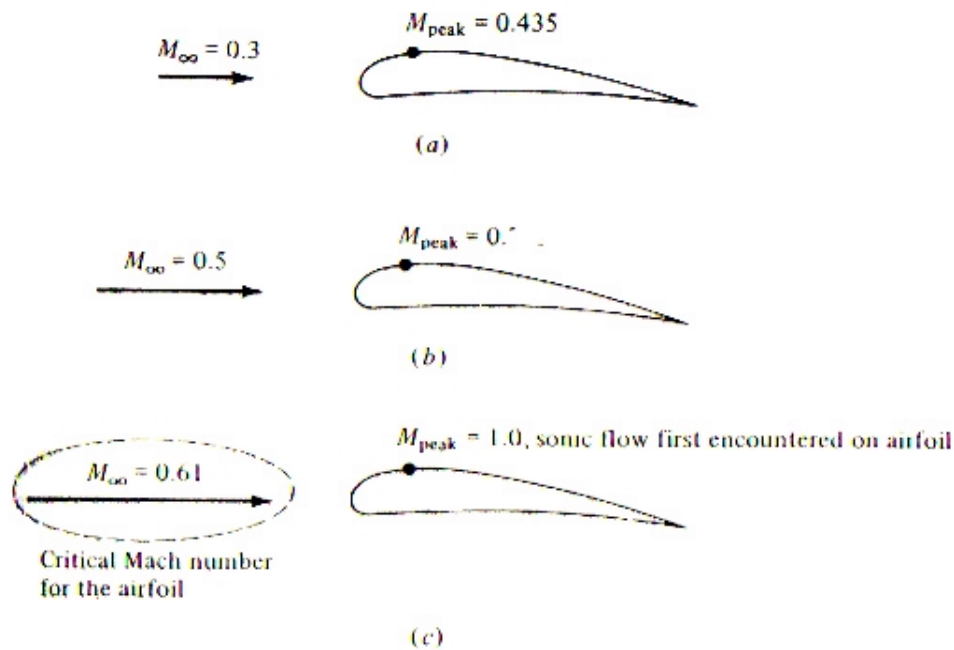


Figure 2.4 Illustration of critical Mach number (Anderson 1989)

Definition of Critical Pressure Coefficient

The relation between Mach number and pressure and the explanation and definition of the critical pressure coefficient $C_{p,cr}$ is present by Anderson 1989 (p. 202): “Returning to Figure 2.4, the point on the airfoil where the local M is a peak value is also the point of minimum surface pressure ... Moreover, according to the Prandtl-Glauert rule ... as M_∞ is increase from 0.3 to 0.61, the value of C_p at this point will become increasingly negative. This is sketched in Figure 2.5. The specific value of C_p that corresponds to sonic flow is defined as the critical pressure coefficient $C_{p,cr}$. In Figures 2.4a and 2.4b C_p at the minimum pressure point on the airfoil is less negative than $C_{p,cr}$; however, in Figure 2.4c, $C_p = C_{p,cr}$ (by definition).”¹

¹ Figure numbers changed in the quote to figure numbers related to this text.

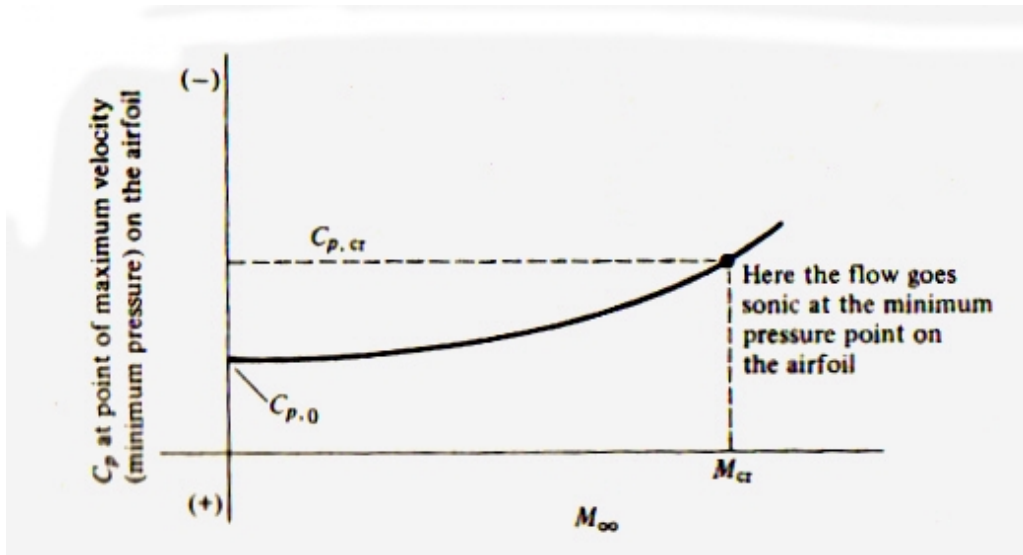


Figure 2.5 Illustration of critical pressure coefficient (Anderson 1989)

Method to Determine the Critical Mach Number

The Critical Mach number can be found from

1. the variation of pressure coefficient with Mach number for a given airfoil following e.g. from the Prandtl-Glauert compressibility correction,
2. the general variation of critical pressure coefficient $C_{p,cr}$ with Mach number
3. the intersection of the two curves following from 1. and 2.

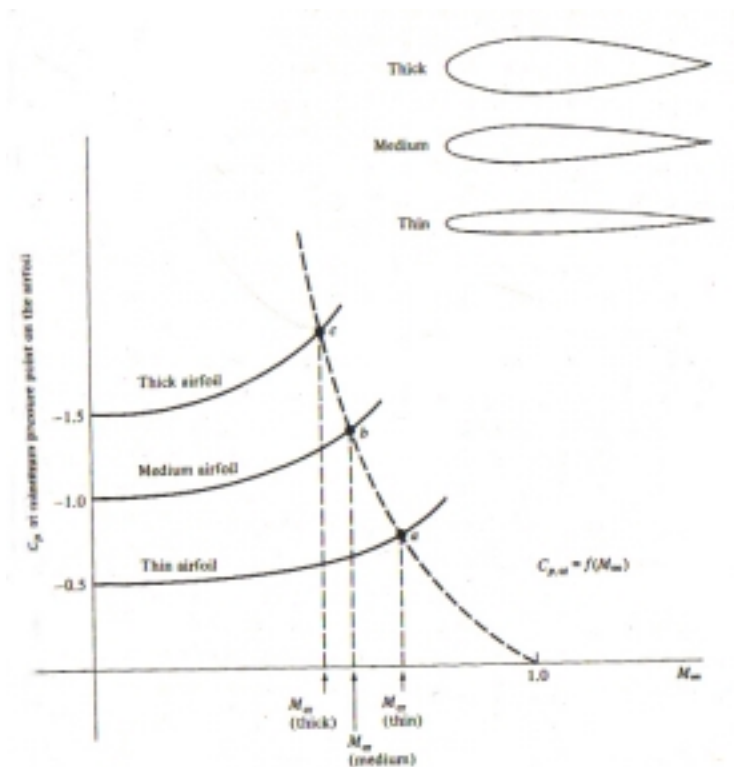


Figure 2.6 Critical pressure coefficient and critical Mach numbers for airfoils of different thickness (Anderson 1989)

Related to point 1 and point 3. Information on the variation of pressure coefficient with Mach numbers for airfoils of different thickness can be found in **Anderson 1989** (p.202): “Consider now three different airfoils ranging from thin to thick, as shown in Figure 2.6. Concentrate first on the thin airfoil. Because of the thin, streamlined profile, the flow over the thin airfoil is only slightly perturbed from its freestream values. The expansion over the top surface is mild, the velocity increases only slightly, the pressure decreases only a relative small amount, and hence the magnitude of C_p at the minimum pressure point is small. Thus, the variation of C_p with M_∞ is shown as the bottom curve in Figure 2.6. For the thin airfoil, $C_{p,0}$ is small in magnitude, and the rate of increase of C_p as M_∞ increases is also relatively small. In fact, because the flow expansion over the thin airfoil surface is mild, M_∞ can be increased to a large subsonic value before sonic flow is encountered on the airfoil surface. The point corresponding to sonic flow conditions on the thin airfoil is labeled point *a* in Figure 2.6. The values of C_p and M_∞ at point *a* are $C_{p,cr}$ and M_{cr} , respectively, for the thin airfoil, by definition. Now consider the airfoil of medium thickness. The flow expansion over the leading edge for this medium airfoil will be stronger, the velocity will increase to larger values, the pressure will decrease to lower values, and the absolute magnitude of C_p is larger. Thus, the pressure coefficient curve for the medium thickness airfoil will lie above that for a thin airfoil, as demonstrated in Figure 2.6. Moreover, because the flow expansion is stronger, sonic conditions will be obtain sooner (at a lower M_∞). Sonic conditions for the medium airfoil are labeled as point *b* in Figure 2.6. Note that the point *b* is to the left of point *a*, that is, the critical Mach number for the medium-thickness airfoil is less than M_{cr} for the thin airfoil. The same logic holds for the pressure coefficient curve for the thick airfoil, where $C_{p,cr}$ and M_{cr} are given by point *c*. Emphasis is made that the thinner airfoils have higher values of M_{cr} . As we will see, this is desirable, and hence all airfoils on modern, high-speed airplanes are thin. The pressure coefficient curves in Figure 2.6 are shown as solid curves. On these curves, only points *a*, *b*, and *c* are critical pressure coefficients, by definition. However, these critical points by themselves form a locus represented by the dotted curve in Figure 2.6; i.e., the critical pressure coefficients themselves are given by a curve of $C_{p,cr} = f(M_\infty)$ as labeled in Figure 2.6.”

Related to point 2. For a given freestream Mach number M_∞

$$C_p = \frac{2}{\gamma M_\infty^2} \left[\left(\frac{1 + \frac{1}{2}(\gamma-1)M_\infty^2}{1 + \frac{1}{2}(\gamma-1)M^2} \right)^{\gamma/(\gamma-1)} - 1 \right] \quad (2.4)$$

relates the local value of C_p to the local M at any point in the field, hence at the given point on the airfoil surface (**Anderson 1989**, p.204). If we pick a particular point on the surface where $M = 1$, then, by definition, $C_p = C_{p,cr}$. Substituting $M = 1$ into equation (2.4), we obtain with

$$C_p = \frac{2}{\gamma M_\infty^2} \left[\left(\frac{2 + (\gamma - 1)M_\infty^2}{\gamma + 1} \right)^{\gamma/(\gamma-1)} - 1 \right] \quad (2.5)$$

the desired relation $C_{p,cr} = f(M_\infty)$. When numbers are fed into equation (2.5), the dotted curve in Figure 2.6. results. Note that, as M_∞ increases, $C_{p,cr}$ decreases.

2.4 Drag -Divergence Mach Number

Anderson 1991 (p. 551 ff) gives an inside into the drag as a function of Mach number, drag-divergence Mach number and shock waves: “Imagine that we have a given airfoil at a fixed angle of attack in a wind tunnel, and we wish to measure its drag coefficient c_d as a function of M_∞ . To begin with, we measure the drag coefficient at low subsonic speed to be $c_{d,0}$, shown in Figure 2.7. Now, as we gradually increase the freestream Mach number, we observe that c_d remains relatively constant all the way to the critical Mach number, as illustrated in. The flow fields associated with points a , b , and c in Figure 2.7 are represented by Figure 2.8 a , b , and c , respectively Figure 2.8. As we very carefully increase M_∞ slightly above M_{cr} , say, to point d in Figure 2.7, a finite region of supersonic flow appears on the airfoil, as shown in Figure 2.8d. The Mach number in this bubble of supersonic flow is only slightly above Mach 1, typically 1.02 to 1.05. However, as we continue to nudge M_∞ , higher, we encounter a point where the drag coefficient suddenly starts to increase. This is given as point e in Figure 2.7. The value of M_∞ at which this sudden increase in drag starts is defined as the drag-divergence Mach number. Beyond the drag-divergence Mach number, the drag coefficient can become very large, typically increasing by a factor of 10 or more. This large increase in drag is associated with an expressive region of supersonic flow over the airfoil, terminating in a shock wave, as sketched in the insert in Figure 2.7. Corresponding to point f on the drag curve, this insert shows that as M_∞ approaches unity, the flow on the both the top and bottom surfaces can be supersonic, both terminated by shock waves. For example, consider the case of a reasonably thick airfoil, designed originally for low-speed applications, when M_∞ is beyond drag-divergence; in such a case, the local Mach number can reach 1.2 or higher. As a result, the terminating shock waves can be relatively strong. These shocks generally cause severe flow separation downstream of the shocks, with an attendant large increase in drag.”¹

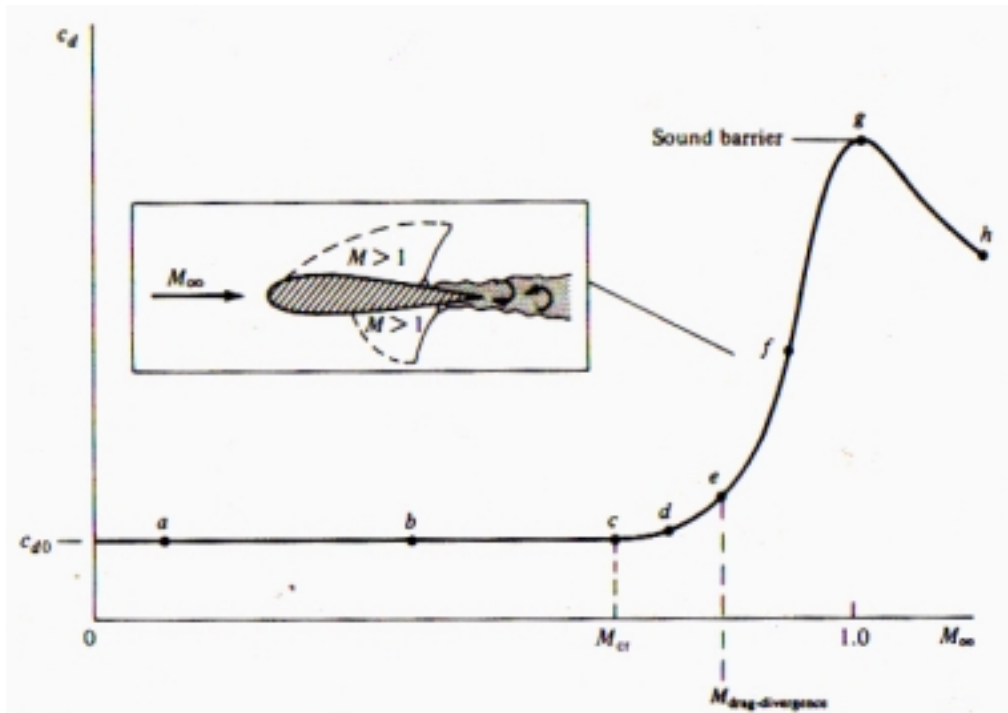


Figure 2.7 Sketch of the variation of profile drag coefficient with freestream Mach number, illustrating the critical and drag-divergence Mach number and showing the large drag rise near Mach 1 (**Anderson 1991**)

The shock pattern is characteristic of the transonic flight regime. **Anderson 1989** (p.123) gives some more inside into this phenomenon: "... the shock wave is a thin boundary in a supersonic flow, across which major changes in flow properties take place and which divides the region of undisturbed flow upstream from the region of disturbed flow downstream ... Within the thin structure of a shock wave itself, very large friction and thermal conduction effects are taking place ... A major consequence is that the total pressure p_0 is smaller behind the shock than in front of it."

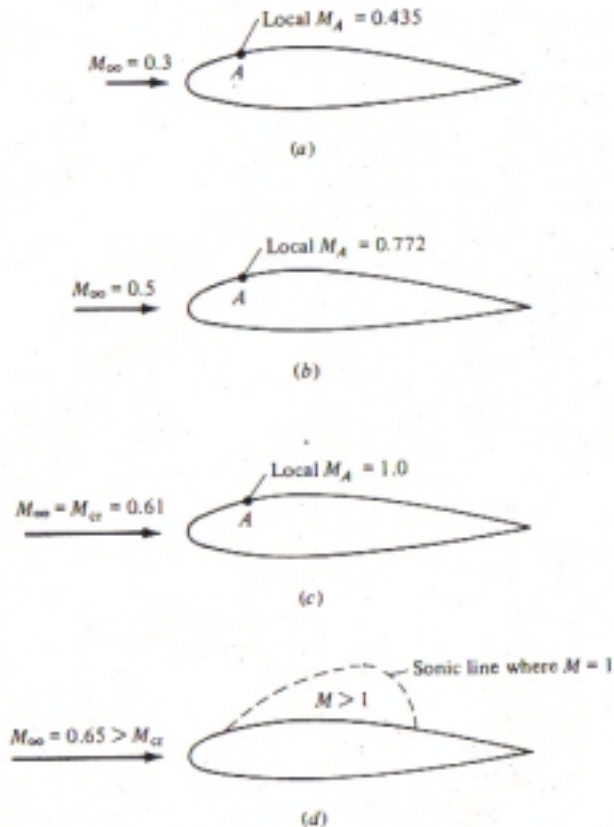


Figure 2.8 Definition of critical Mach number (Anderson 1991)

In the literature we see much confusion when it comes to the definition of the terms critical Mach number and drag divergence Mach number. The generally accepted definition of the critical Mach number is that given by Anderson (see also Chapter 3). The drag divergence Mach number has seen different definitions in history depending also on the respective aircraft manufacturer in question. Today we know two major manufacturers of big passenger aircraft. They agree in their definition of drag divergence Mach number

The Boeing view is stated in **Raymer 1989** (p. 294): “The Boeing definition is that M_{DD} is where the drag rise reaches 20 counts.” **Howe 2000** (p. 117) supports this view (only that he talks about critical Mach number when he expresses a parameter with properties of the drag divergence Mach number).

In the past also other definitions have been used. “The Douglas definition, also used by the Air Force ... is, that M_{DD} is the Mach number at which the rate of change in parasite drag with Mach number (dC_{D0}/dM) first reaches 0.10” (**Raymer 1989**, p. 294). **Jenkinson 1999** (p. 115) supports this view on the M_{DD} –definition of the Douglas company. **Shevell 1980** introduces another M_{DD} –definition similar to that from Douglas. He states that M_{DD} is the Mach number at which (dC_{D0}/dM) first reaches 0.05.

The aircraft designer has to decide how much the aircraft should penetrate the flight regime where the aircraft experiences wave drag during cruise flight. Various philosophies have been expressed and applied

- *Boeing*: $M_{DD} = M_{CR}$ **Raymer 1989**, p. 294
- *Airbus*: $M_{DD} = M_{CR}$
- *Fokker*: $M_{DD} \approx M_{CR} + 0.02$ **Obert 1997**
- *University of Kansas* aircraft design classes:
 $M_{DD} \approx M_{CR} + 0.1$ **Roskam 1989**

2.5 Development of the Supercritical Airfoil

The evolution of the airfoil from NACA 64 series to the appearance of the supercritical airfoil, the comparison of them in cruise flight, drag-divergence properties, and the proposal of the supercritical airfoil are presented by **Anderson 1991**:

”A natural conclusion ... from Figure 2.7 is that an airfoil with a high critical Mach number is very desirable, indeed necessary, for high-speed subsonic aircraft. If we can increase M_{cr} , then we can increase $M_{drag-divergence}$, which follows closely after M_{cr} . This was the philosophy employed in aircraft design from 1945 to approximately 1965. Almost by accident, the NACA 64-series airfoils ... , although originally designed to encourage laminar flow, turned out to have relative high values of M_{cr} in comparison with other NACA shapes. Hence, the NACA 64 series has seen wide application on high-speed airplanes. Also, we know that thinner airfoils have higher values of M_{cr} ... ; hence, aircraft designers have used relatively thin airfoils on high-speed airplanes. However, there is a limit to how thin a practical airfoil can be. For example, considerations other than aerodynamic influence the airfoil thickness; the airfoil requires a certain thickness for structural strength, and there must be room for the storage of fuel. This prompts the following question: For an airfoil of given thickness, how can we delay the large drag rise to higher Mach numbers? To increase M_{cr} is one obvious tack, as described above, but there is another approach. Rather than increasing M_{cr} , let us strive to increase the Mach number increment between M_{cr} and $M_{drag-divergence}$. That is, referring to Figure 2.7, let us increase the distance between point's e and c .”

The first attempt to modify the general airfoil shape to increase the distance between M_{cr} and M_{DD} was achieved with the invention of the “peaky airfoils”. A interesting explanation of this type of airfoil is given by **Torenbeek 1988**: ”A peaky pressure distribution ... pioneered by

Piercy ... and by others, intentionally creates supersonic velocities and suction forces close to the leading edge. The airfoil nose is carefully designed so that near-isentropic compression and a weak shock are obtained. The suction forces have a large forward component and the drag rise is postponed to high speeds. As compared with conventional sections of the same thickness ratio, the value of M_{crD} is approximately .03 and .05 higher and the off-design behavior is improved. This type of airfoil has been used on the BAC 1-11, VC-10 and DC-9 aircraft. The technique employed in designing peaky airfoils was highly empirical.”

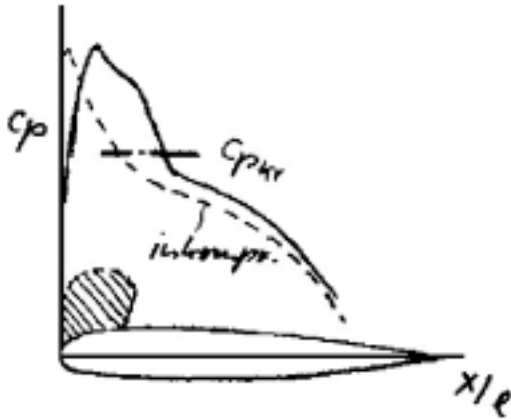


Figure 2.9 Peaky upper surface pressure distribution (Thorbeck 2001)

Kroo 2001 adds that “Shocks on the upper surface near the leading edge produce much less wave drag than shocks aft of the airfoil crest and it is feasible, although not always best, to design sections with forward shocks. Such sections are known as peaky airfoils and were used on many transport aircraft.”

In 1965 a new family of airfoils called supercritical airfoils were invented. “The purpose of supercritical airfoils is to increase the value of $M_{drag-divergence}$, although M_{cr} may change very little. The shape of a supercritical airfoil is compared with an NACA 64-series airfoil in figure 2.10. Here, an NACA 64₂-A215 airfoil is sketched in figure 2.10a, and 13-percent thick supercritical airfoil is shown in (Figure 2.10c). ... The supercritical airfoil has a relatively flat top, thus encouraging a region of supersonic flow with lower local values of M than the NACA 64 series. In turn, the terminating shock is weaker, thus creating less drag. Similar trends can be seen by comparing the C_p distribution for the NACA 64 series Figure 2.10b and the supercritical airfoil Figure 2.10d. Indeed, Figure 2.10a and b for the NACA 64-series airfoil pertain to a lower freestream Mach number, $M_\infty = 0.69$, than Figure 2.10c and d, which pertain to the supercritical airfoil at a higher freestream Mach number, $M_\infty = 0.79$. In spite of the fact the 64-series airfoil is at a lower M_∞ , the extent of the supersonic flow reaches farther above the airfoil, the local supersonic Mach numbers are higher, and the terminating shock wave is stronger. Clearly, the supercritical airfoil shows more desirable flow-field characteris-

tics; namely, the extent of the supersonic flow is closer to the surface, the local supersonic Mach numbers are lower, and the terminating shock wave is weaker. As a result, the value of ... $M_{\text{drag-divergence}}$ is 0.79 for the supercritical airfoil in comparison with 0.67 for NACA 64 series.

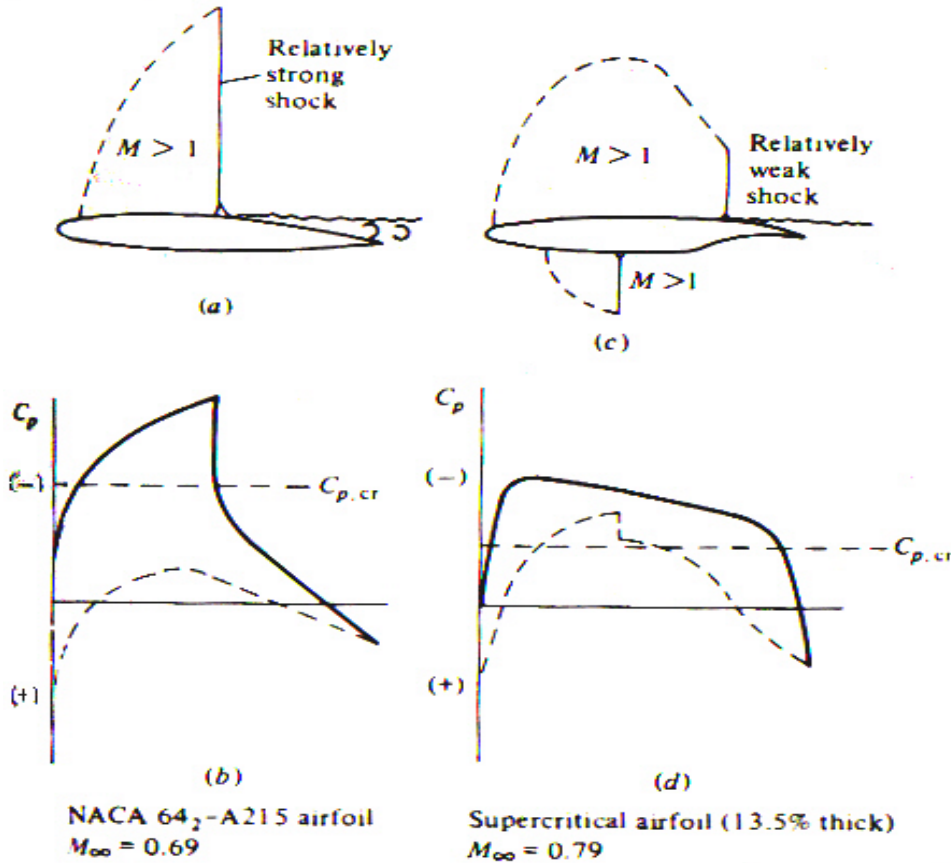


Figure 2.10 Standard NACA 64-series airfoil compared with a supercritical airfoil at cruise lift conditions (Anderson 1991)

Because the top of the supercritical airfoil is relatively flat, the forward 60 percent of the airfoil has negative camber, which lowers the lift. To compensate, the lift is increased by having extreme positive camber on the rearward 30 percent of the airfoil. This is the reason for the cusplike shape of the bottom surface near the trailing edge.

The supercritical airfoil was developed by Richard Whitcomb in 1965 at the NASA Langley Research Center ... The supercritical airfoil, and many variations of such, are now used by the aircraft industry on modern high-speed airplane designs. Examples are the Boeing 757 and 767 and the latest model Lear jets. The supercritical airfoil is one of ... [the] major breakthroughs made in transonic airplane aerodynamics since 1945.” (Anderson 1991)

2.6 Swept Wings

The main idea of swept wings, the advantages and the disadvantages of swept wings, and a clear presentation of the flow around swept and unswept wings can be found in **Anderson 1989**, p. 226: “Consider the plan view of a straight wing, as sketched in Figure 2.11a. Assume this wing has an airfoil cross section with a critical Mach number $M_{cr} = 0.7$. Now assume that we sweep the wing back through an angle of, say, 30° , as shown in figure 2.11b. The airfoil, which still has a value of $M_{cr} = 0.7$, now ‘sees’ essentially only the component of the flow normal to the leading edge of the wing; i.e., the aerodynamic properties of the local section of the swept wing are governed mainly by the flow normal to the leading edge. Hence, if M_∞ is the free stream Mach number, the airfoil in figure 2.11b is seeing effectively a smaller Mach number, $M_\infty \cdot \cos 30^\circ$. As a result, the actual free stream Mach number can be increased above 0.7 before critical Mach number for the swept wing itself would be as high as $0.7 / \cos 30^\circ = 0.808$, as shown in figure 5.38. This means that the large increase in drag ... would be delayed to M_∞ much than 0.7, and maybe even as high as 0.808. By sweeping the wings of subsonic aircraft, drag divergence is delayed to higher Mach numbers .”

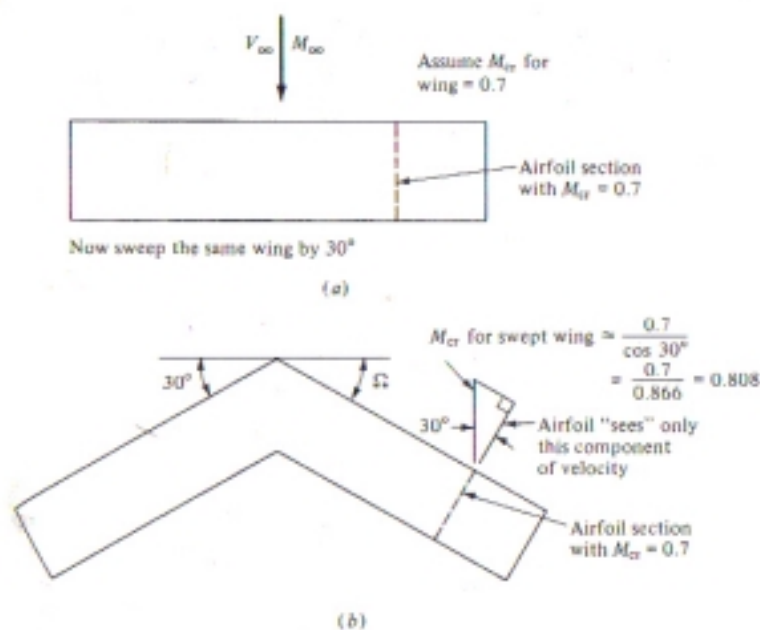


Figure 2.11 Effect of swept wing on critical Mach number (**Anderson 1989**)

The actual critical Mach number for the swept wing is according to the **Anderson 1989**, p. 226

$$M_{cr} \text{ for airfoil} < \text{actual } M_{cr} \text{ for wing} < M_{cr} \text{ for airfoil} / \cos \Omega$$

where the Ω is the sweep angle.

Following the same reasoning we can define the effective mach number as:

$$M_{eff} = M \cdot (\cos \varphi_{25})^x \quad (2.6)$$

where x is according to **Torenbeek 1988**: 0.5, according to **Staufenbiel ca. 1992**: 0.75 and by the cosine rule:1.0. In light of (2.6) **Anderson 1989** states that $0 < x < 1$. **Jenkinson 1999** chooses $x = 1.0$, stating: "For the same thickness/chord ratio, sweepback (Λ) will increase drag divergence Mach number (Mn) as follows: $(Mn_{sweep})/(Mn_{zerosweep}) = 1/\cos \Lambda$ "

Jenkinson 1999 (p. 113) presents not only the aerodynamic main characteristics of sweepback but also the aerodynamics effects that the sweepback causes to the wing aerodynamics: "Sweepback is mainly used to reduce drag from local flow velocities at or close to supersonic speed." "The spanwise drift of the flow reduces lift, increases boundary layer thickness, increases drag, reduces aileron effectiveness and increases risk of tip stall." "Flap effectiveness is reduced by the sweep trailing edge which reduces the maximum lift coefficient from the deflected flap." "Its primary purpose is to delay the drag divergence Mach number, but at the expense of the decrease in that maximum lift coefficient achievable by the wing." The result of sweepback on $C_{L_{max}}$ is as follows

$$(C_{L_{max}})_{sweep} / (C_{L_{max}})_{zerosweep} = \cos \Lambda \quad (2.7)$$

Also we can define the effective velocity, chord and relative thickness as

$$V_{eff} = V \cdot \cos \varphi_{25} \quad (2.8)$$

$$M_{eff} = M \cdot \cos \varphi_{25} \quad (2.9)$$

$$c_{eff} = c \cdot \cos \varphi_{25} \quad (2.10)$$

$$t_{eff} = t \quad (2.11)$$

$$(t/c)_{eff} = (t/c) / \cos \varphi_{25} \quad (2.12)$$

"Therefore, the advantage of sweeping the wings for supersonic flight is in general to obtain a decrease in wave drag, and if the wing is swept inside the Mach cone, a considerable decrease can be obtained. The quantitative effects of maximum thickness and wing sweep on wave-drag coefficient are shown in Figure 2.12a and b." (**Anderson 1989**, p. 228)

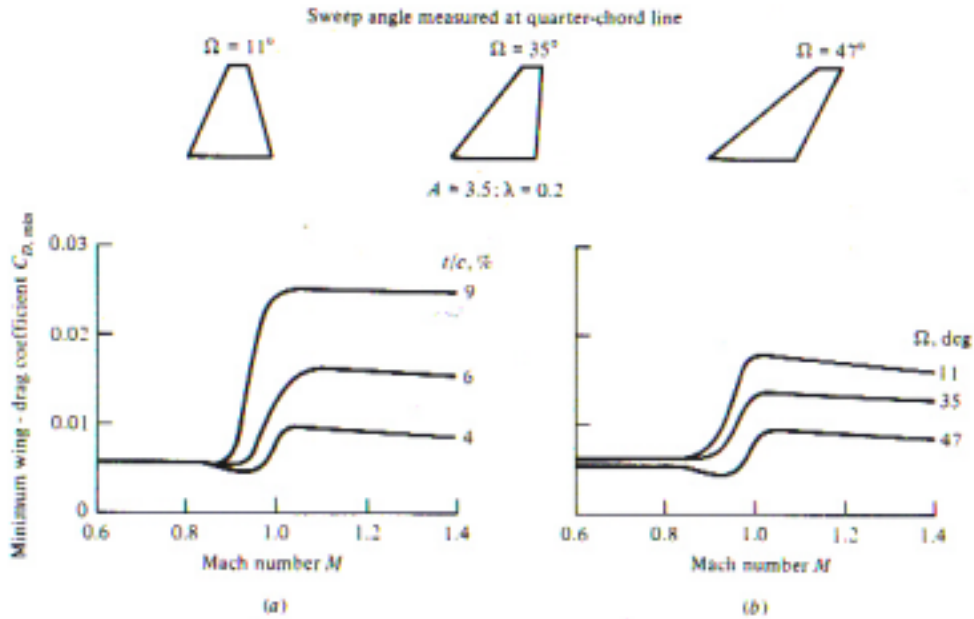


Figure 2.12 Sketch of the variation of minimum wing-drag coefficient versus Mach number with different sweep angles and relative thickness (**Anderson 1989**)

Raymer 1992 (p. 53) Figure 2.13 “... shows a historical trend line for wing leading-edge sweep vs Mach number ... the sweep is defined aft of a line perpendicular to the flight direction ... line labeled ‘90-arcsin (1/ Mach No.)’ is the wing sweep required to place the wing leading edge exactly on the Mach cone.” “The historical trend differs from this theoretical results for two reasons. In the high-speed range, it becomes structurally impractical to sweep the wing past the Mach cone. In this speed regime, over about Mach 2.5, it is necessary to use sharp or nearly sharp airfoils”

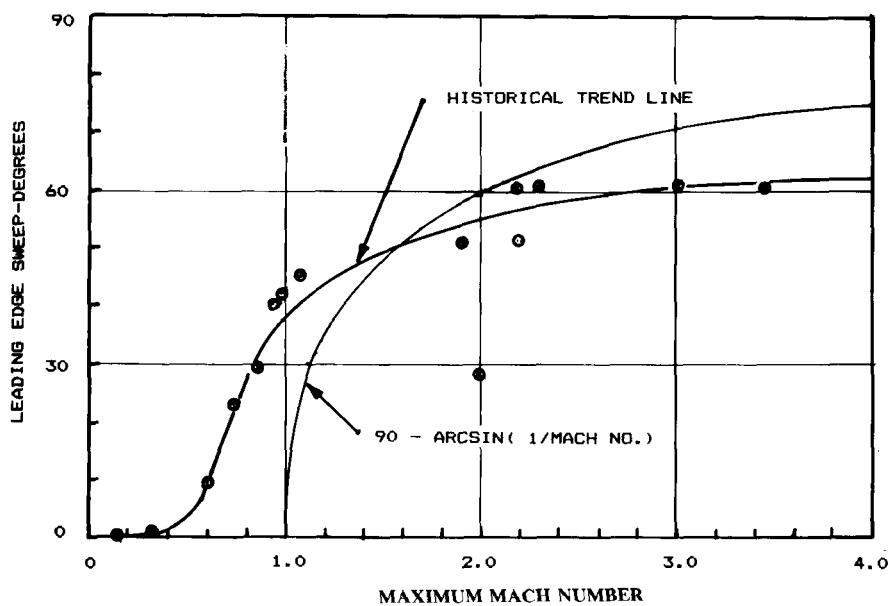


Figure 2.13 Wing sweep historical trend (**Raymer 1992**)

2.7 Relative Thickness

A good explication of dependence between the thickness ratio and the regime of flow is given by **Howe 2000** (p. 117): “In incompressible flow conditions relatively high thickness to chord ratios up to 0.2 are acceptable at the root of the wing and give a good structural depth with a small profile drag penalty. The value at the tip is typically about two-thirds of that at the root. At higher Mach numbers, where compressibility effects become important, it is usual to use somewhat thinner aerofoil and root values in the range 0.10 to 0.15 are typical. Again the tip value is usually about two-thirds of that at the root, but the spanwise variation is not necessarily linear especially if the wing trailing edge is cranked.”

Jenkinson 1999 (p. 112) offers an interesting affirmation about the distribution of thickness along span: “Thickness is normally variable along the span to suit the local flow conditions.” He also comments about the variation of the bending moment and the shear force on the wing: “Wing bending moment and shear force gradually increase from the tip to the root; therefore wing thickness is frequently chosen to be smaller at the tip and progressively increased along the span to the fuselage shear connections at the root.”

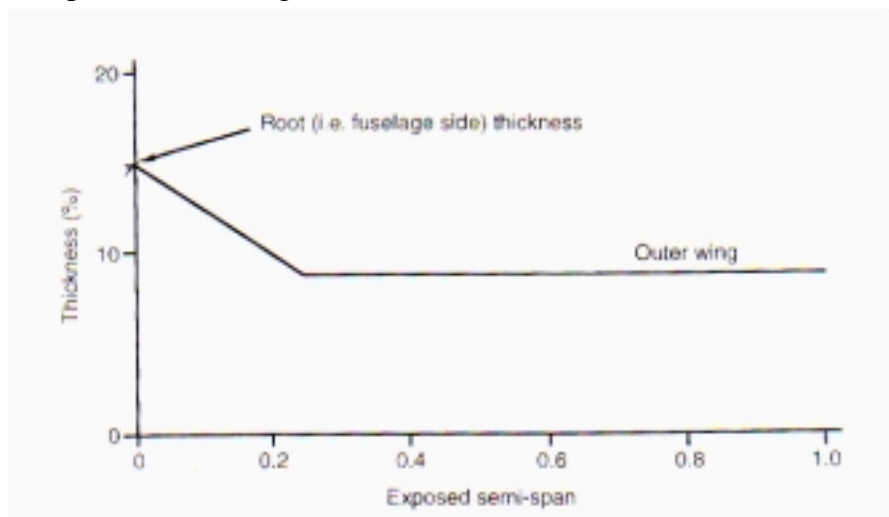


Figure 2.14 Wing thickness spanwise distribution (**Jenkinson 1999**)

“A typical spanwise thickness distribution is shown in Figure 2.14. This can be used as typical for initial project studies.” **Jenkinson 1999** proposes an average thickness ratio t/c

$$(\text{average thickness ratio}) = \frac{(3 \times \text{outer wing value}) + \text{root wing value}}{4} . \quad (2.13)$$

3 Equations for the Calculation of Relative Thickness

A literature search for equations dealing with the relationship between Mach number, relative thickness, sweep, and lift coefficient of the wing leads to several sources. The equations from these sources are explained in this Chapter.

3.1 Equation based on Torenbeek

Torenbeek 1988 (p. 246) gives an equation in which we see the dependence between the relative thickness and the design Mach number for two-dimensional flow

$$\frac{t}{c} = 0.30 \left\{ \left[1 - \left\{ \frac{5 + M^2}{5 + (M^*)^2} \right\}^{3.5} \right] \frac{\sqrt{1 - M^2}}{M^2} \right\}^{2/3} \quad (3.1)$$

“In this equation M denotes the design (drag-critical) Mach number for which the airfoil is to be designed. The factor M^* in (3.1) has no physical meaning and is merely a figure defining the aerodynamic sophistication employed to obtain supercritical flow at the design condition. Good results are obtained by taking:

- $M^* = 1.0$, conventional airfoils; maximum t/c at about $0.30c$
- $M^* = 1.05$, high-speed (peaky) airfoils, 1960-1970 technology
- $M^* = 1.12$ to 1.15 , supercritical airfoils.“

As we observe in this equation we don't see the influence of the lift coefficient, but **Torenbeek 1988** allows us to include this influence too, through the next paragraph from his book: “It is difficult to make adequate allowance for the effects of airfoil camber and lift. Provided the airfoil operates at the design c_l , it is possible to use an approximation by reducing M^* ... by .25 times the design c_l for c_l up to .7.” and the equation (3.1) becomes:

$$\frac{t}{c} = 0.30 \left\{ \left[1 - \left\{ \frac{5 + M^2}{5 + (M^* - 0.25c_l)^2} \right\}^{3.5} \right] \frac{\sqrt{1 - M^2}}{M^2} \right\}^{2/3} \quad (3.2)$$

Equation (3.2) may be extended to swept wings by including equation (2.6) with a value of $x = 0.5$ as proposed by **Torenbeek 1988**. Substituting M_{DD} for M into equation (2.6), we obtain an effective drag-divergence Mach number

$$M_{DD,eff} = M_{DD} \cdot \sqrt{\cos \varphi_{25}} \quad . \quad (3.3)$$

Now all values in (3.2) are considered to be effective (*eff*) values. Knowing that $(t/c)_{eff} = (t/c)/\cos \varphi_{25}$ (2.11) and using the new expression of $M_{DD,eff}$ the equation (3.2) becomes

$$\frac{t}{c} = 0.30 \cos \varphi_{25} \left\{ \left[1 - \frac{5 + M_{DD,eff}^2}{5 + (k_M - 0.25c_l)^2} \right]^{3.5} \left[\frac{\sqrt{1 - M_{DD,eff}^2}}{M_{DD,eff}^2} \right]^{2/3} \right\} \quad (3.4)$$

The lift coefficient can also be considered to be an effected value and would need to be modified if the effect of sweep is considered. The expression of this contribution is explain next.

It is $v_{eff} = v/\cos \varphi_{25}$ (2.8), $c_{eff} = c/\cos \varphi_{25}$ (2.10), $t_{eff} = t$ (2.11). Lift must support weight (times load factor) no matter if the wing is swept or not. Hence

$$L_{eff} = L \quad . \quad (3.5)$$

From the definition of lift coefficient

$$L = \frac{1}{2} \cdot \rho \cdot v^2 \cdot C_L \cdot S \quad (3.6)$$

or for swept wings

$$L_{eff} = \frac{1}{2} \cdot \rho \cdot v_{eff}^2 \cdot C_{L,eff} \cdot S \quad . \quad (3.7)$$

Setting equal these two equations (3.6) and (3.7) base on equation (3.5) results in

$$v_{eff}^2 \cdot C_{L,eff} = v^2 \cdot C_L \quad . \quad (3.8)$$

Solving for $C_{L,eff}$ yields

$$C_{L,eff} = C_L \cdot \frac{v^2}{v_{eff}^2} \quad (3.9)$$

From equation (2.8) based on geometric considerations

$$\frac{v_{eff}}{v} = \cos \varphi_{25} \quad (3.10)$$

But considering aerodynamic effects as explained with equation (2.6) of applied in (3.3)

$$\frac{v_{eff}}{v} = \sqrt{\cos \varphi_{25}} \quad (3.11)$$

Substituting (3.11) in (3.9) the contribution of the lift coefficient it's determine

$$C_{L,eff} = \frac{C_L}{\cos \varphi_{25}} \quad (3.12)$$

Hence we could also - as a variation to (3.4) - substitute (3.12) into (3.4) and in this way also account for the effect of sweep on lift coefficient.

3.2 Equations from Aerodynamic Similarity based on Anderson

The “transonic similarity equation” offered by **Anderson 1990**

$$K = \frac{1 - M_\infty}{\tau^{2/3}} \quad (3.13)$$

gives the possibly of a new calculation of the relative thickness. τ in this equation is the relative thickness.

The “transonic similarity equation” states: ”Consider two flows at different values of M_∞ (but both transonic) over two bodies with different values of τ , but with M_∞ and τ for both flows such that the transonic similarity parameter K is the same for both flows. Then Equation (3.15) states that the solution for both flows ... will be the same.” (**Anderson 1990** p. 434)

The relative thickness $\tau = t/c$ was determined considering two cases: with or without considering the effect of sweep. Based on Equation (3.13), the first case was made without consider-

ing the effect of sweep. Here M_{DD} was used in place of M_∞ and hence the effect of sweep was not considered

$$t/c = \left(\frac{1 - M_{DD}}{K} \right)^{3/2} \quad (3.14)$$

In the second case the effect of sweep was considered by using the effective drag divergence Mach number $M_{DD,eff}$. The equation is this time

$$t/c = \left(\frac{1 - M_{DD,eff}}{K} \right)^{3/2} \quad (3.15)$$

The value of the parameter K was determined based on selected aircraft parameters by using the EXCEL solver.

3.3 Equation based on Shevell

Shevell 1980 offers “An analytical method, based upon theory and empirical results” “developed to predict the drag divergence Mach number M_{DIV} , and the incremental drag coefficient due to compressibility, ΔC_{D_c} , for an airplane with optimally designed wing. The method needs only four inputs: lift coefficient, C_L , sweep angle, $\Lambda_{C/4}$, thickness ratio, t/c , and type of wing, conventional or supercritical.” Two equations are given by Shevell. The first equation is

$$M_{DIV} = M_{CC} [1.025 + (1 - \cos \Lambda) \cdot 0.08] \quad (3.16)$$

M_{CC} , the crest critical Mach number, “is the freestream Mach number at which the local Mach number, at the airfoil crest, perpendicular to the isobars, is 1.0. The crest is the point on the upper surface of the airfoil tangent to the freestream direction.” (See Figure 3.1).



Figure 3.1 Explanation of M_{cc} (Shevell 1980)

Equation (3.16) is represented in Figure 3.2.

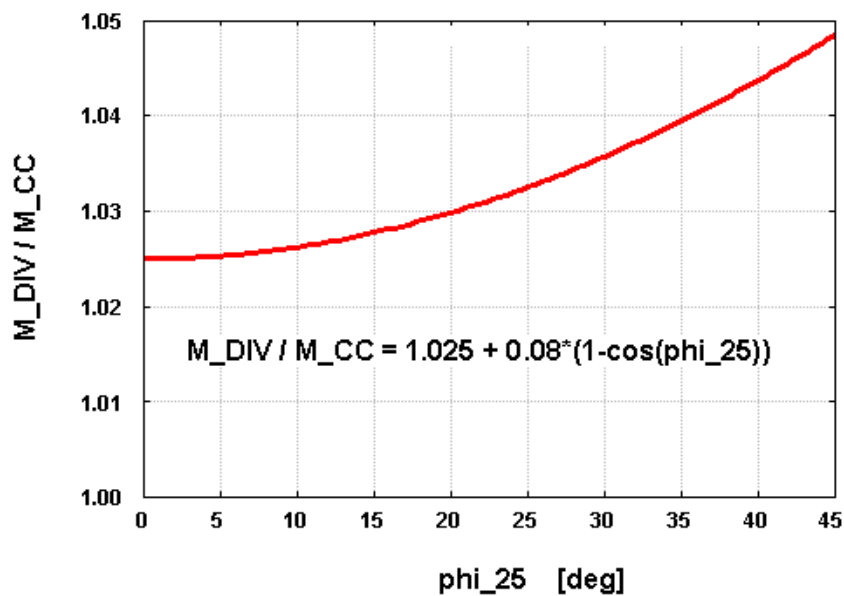


Figure 3.2 The ratio of M_{DIV} and M_{CC} versus sweep

“ M_{DIV} is defined qualitatively as the Mach number at which the drag coefficient starts to rise abruptly. Quantitatively M_{DIV} is defined in this report as the Mach number at which $\frac{dC_D}{dM} = 0.05$.” Hence, M_{DIV} is in fact also a drag-divergence Mach number, but following a different definition as applied for previous equations where an M_{DD} was defined at a drag rise of 20 drag counts. Without knowing the shape of the drag rise curve, there is no way to convert M_{DIV} to M_{DD} . From Figure 2 in Shevell 1980 it can be concluded that $M_{DIV} < M_{DD}$. A very crude estimate would be to assume that $M_{DD} = M_{DIV} + 0.02$. If Shevell’s approach is to

be compared with the results of other authors and with aircraft data, this crude assumption should be applied in view of a missing better relation.

Shevell's second equations is

$$\begin{aligned}
& \frac{M_{\infty}^2 \cos^2 \Lambda}{\sqrt{1 - M_{\infty}^2 \cos^2 \Lambda}} \left[\left(\frac{\gamma+1}{2} \right) \frac{2.64(t/c)_{\infty}}{\cos \Lambda} + \left(\frac{\gamma+1}{2} \right) \frac{2.64(t/c)_{\infty} (0.34C_L)}{\cos^3 \Lambda} \right] \\
& + \frac{M_{\infty}^2 \cos^2 \Lambda}{1 - M_{\infty}^2 \cos^2 \Lambda} \left[\left(\frac{\gamma+1}{2} \right) \left[\frac{1.32(t/c)_{\infty}}{\cos \Lambda} \right]^2 \right] \\
& + M_{\infty}^2 \cos^2 \Lambda \left[1 + \left(\frac{\gamma+1}{2} \right) \frac{(0.68C_L)}{\cos^2 \Lambda} + \frac{\gamma+1}{2} \left(\frac{0.34C_L}{\cos^2 \Lambda} \right)^2 \right] - 1 = 0
\end{aligned} \tag{3.17}$$

with $M_{\infty} = M_{CC}$, $\Lambda = \varphi_{25}$, and $(t/c)_{\infty}$ simply being t/c .

The advantage of this method to calculate M_{DD} is "Its simplicity – only four inputs [φ_{25} , t/c , c_l , γ] – makes it very easy to use, and allows a rapid approximation ..." "The method first calculates the crest critical Mach number, M_{CC} , from two-dimensional airfoil characteristics, simple sweep theory and one dimensional compressible flow equations ... The method is evaluated by comparison to flight test drag results for airplanes with different wing geometries" (Shevell 1980).

With $M_{DIV} = M_{CC} [1.025 + (1 - \cos \varphi_{25}) \cdot 0.08]$ and knowing that $M_{CC} = f(\varphi_{25}, t/c, C_l)$, M_{DIV} can be calculated from these two equations. By the same token the relative thickness t/c can be calculated from an iteration of

$$t/c = f(M_{CC}, \varphi_{25}, C_l) \tag{3.18}$$

with

$$M_{CC} = \frac{M_{DIV, conventional}}{1.025 + 0.08(1 - \cos \varphi_{25})} \tag{3.19}$$

and

$$M_{DIV, conventional} = M_{DIV, supercritical} - 0.06 \quad . \tag{3.20}$$

Equation (3.20) was obtained by Shevell 1980 from a comparison of data related to aircraft with conventional wings and wind tunnel data from a supercritical wing. He concludes that the wave drag curve of a wing with a conventional airfoil is shifted up by 0.06 Mach if a supercritical airfoil is used. For this reason also M_{DD} is shifted up that amount.

In this project the iteration of t/c is again performed with EXCEL and the modified Newton method of the “Solver”.

3.4 Equation based on Kroo

The origin of this equation is based on a graph given by **Kroo 2001** (Figure 7). This graph is based on **Shevell 1989** (page 199) and adapted to swept wings. It is given in this text as Figure 3.3. **Kroo 2001** explains “This graph displays M_{cc} as a function of the airfoil mean thickness ratio t/c and C_L . It is based on studies of the M_{cc} of various airfoils representing the best state of the art for conventional ‘Peaky’ type airfoils typical of all existing late model transport aircraft.”

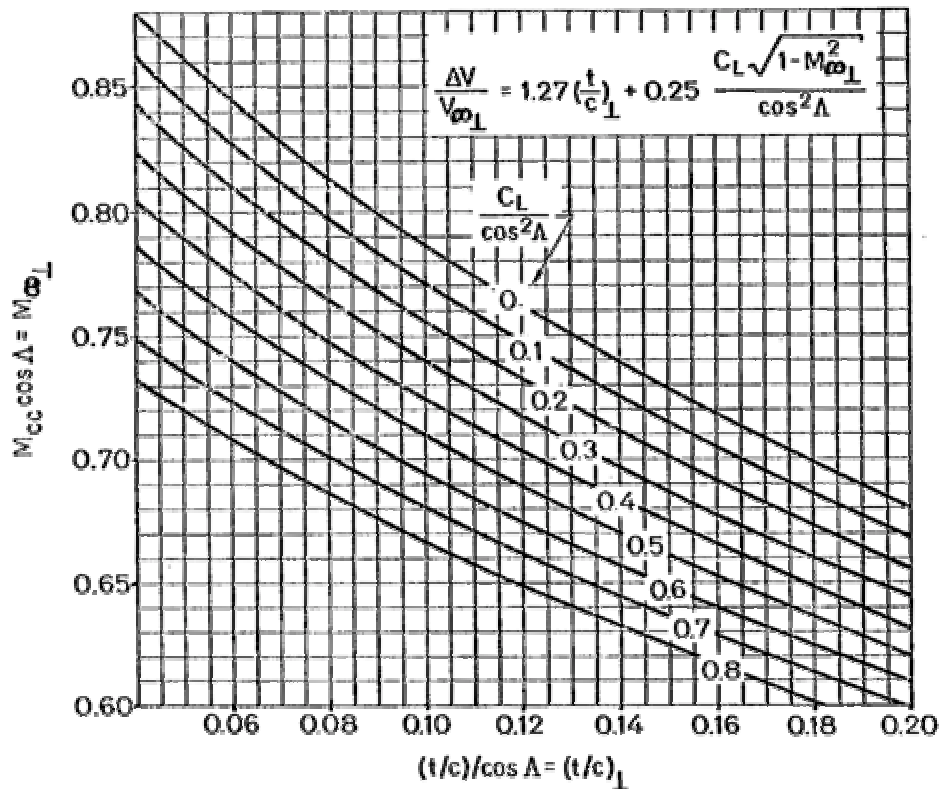


Figure 3.3 Crest critical Mach number (M_{cc}) as a function of relative thickness t/c and lift coefficient C_L (**Kroo 2001**)

The aim here was to convert this graph to an equation in order to use the information in an easy comparison of the different methods. In a first step, the line in the graph for $C_L = 0$ was transformed into an equation with help of EXCEL. This is shown in Figure 3.4. With help of EXCEL a representation was found in the form

$$y = f((t/c)/\cos(\varphi_{25}), C_L = 0) \quad (3.21)$$

With

$$y = M_{CC} \cdot \cos \varphi_{25} \quad (3.22)$$

$$x = (t/c) / \cos \varphi_{25} \quad (3.23)$$

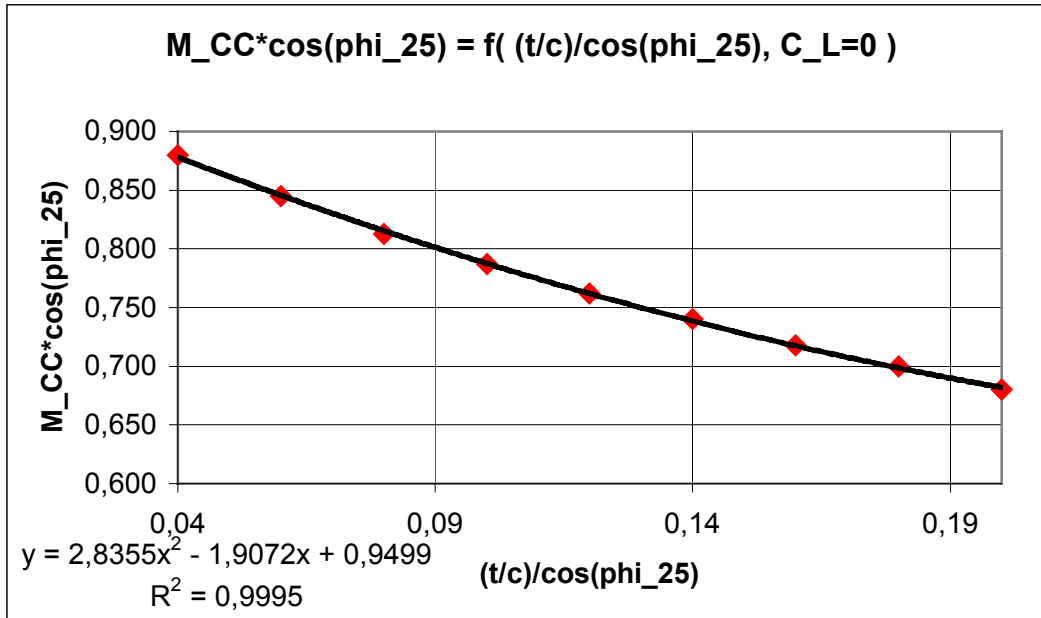


Figure 3.4 The crest critical Mach number versus relative thickness for $C_L = 0$

In order to also include the influence of lift coefficient C_L , Equation 3.23 is extended (using some intuition) with the term $a(1-b)y$ giving

$$M_{CC} \cdot \cos \varphi_{25} = 2.8355 \cdot x^2 - 1.9072 \cdot x + 0,9499 - a(1-bx)y \quad (3.24)$$

where $x = (t/c) / \cos(\varphi_{25}) \quad (3.25)$

and now redefined $y = C_L / (\cos \varphi_{25})^2 \quad (3.26)$

Using the EXCEL solver and this time considering the suitable values of M_{CC} not only for one value of C_L but for five, the discovered values for the a and b terms are:

$$a = 0,200 \quad (3.27)$$

$$b = 2,131. \quad (3.28)$$

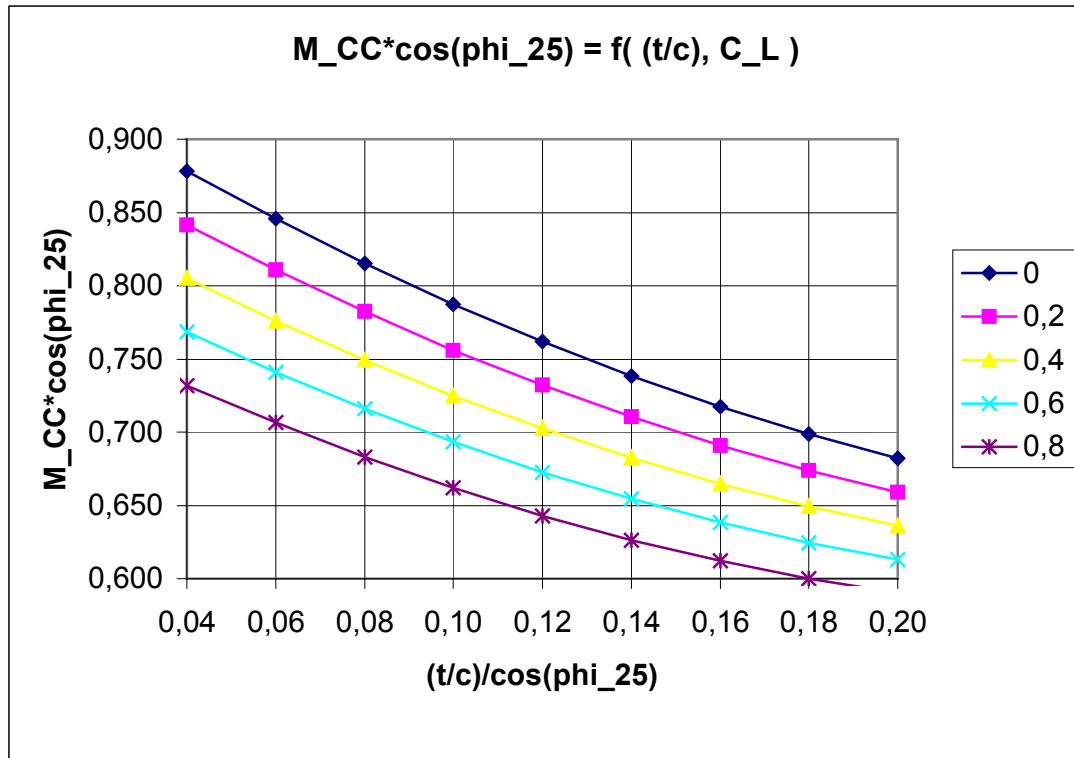


Figure 3.5 Crest Critical Mach number versus relative thickness for all five values of C_L

Introducing this values in equation 3.24 the equation becomes

$$u \cdot x^2 + v \cdot x + w = 0 \quad (3.29)$$

with

$$\begin{aligned} u &= 2.8355 \\ v &= -1.9072 + 0,2 \cdot 2.131y \\ w &= 0,9499 - 0,2y - M_{CC} \cdot \cos \varphi_{25} \end{aligned}$$

solving the quadratic equation

$$x = \frac{-v - \sqrt{v^2 - 4uw}}{2u} \quad (3.29a)$$

finally

$$t/c = x \cos \varphi_{25} \quad (3.25)$$

But one aspect has to be mentioned: "Figure 7 does not apply directly to airfoils with distributions that look significantly different from the peaky airfoil family. Modern supercritical airfoils,..., can achieve higher drag divergence Mach numbers than those suggested by the figure. Although the performance of such airfoil families is often a closely guarded company secret, the effect can be approximated by adding an increment to the value of M_{CC} shown in the figure. A very aggressive supercritical section might achieve a drag divergence Mach number increment of 0.06, while more typically the increment is 0.03 to 0.04 above the peaky sections." (Kroo 2001)

Kroo's diagram and his information are given for M_{CC} . Therefore the calculations of all equations were made with a M_{DD} or a M_{CC} which was obtained using the equation already known from Shevell

$$M_{CC} = \frac{M_{DIVPeakY}}{1,025 + 0,08(1 - \cos \varphi_{25})} \quad (3.30)$$

where

$$M_{DIVPeakY} = M_{DIVNACA} + \Delta M_{DIV} \quad (3.31)$$

The values of the term ΔM_{DIV} were being obtained by using literature information. For a better understanding the next table was produced:

Table 3.1 Variation of divergence Mach number (ΔM_{DIV}) depending on the type of airfoil

Type of airfoil	ΔM_{DIV}	Source
NACA	+0,04	Torenbeek 2001
PEAKY	0	Kroo 2001
Supercritical I	-0,04	Kroo 2001
Supercritical II	-0,06	Kroo 2001 / Shevell 1980 / Schauffele 2000

3.5 Equation from Howe

Howe 2000 (p. 117) offers a relationship between the lift coefficient, the thickness to chord ratio and the critical Mach number:

$$M_{NCRIT} = A_F - 0.1C_L - (t/c) = A_f - (t/c) \quad (3.32)$$

With

- M_{NCRIT} the critical Mach number for a given form of two-dimensional aerofoil
- C_L lift coefficient
- (t/c) thickness to chord ratio

Note, that Howe has an understanding of what he calls M_{NCRIT} that differs from what was introduced in Chapter 2 as M_{crit} . Howe's M_{NCRIT} is in effect what was introduced in Chapter 2 as M_{DD} ! This becomes apparent from his text "There is no generally accepted definition of critical Mach number [M_{NCRIT}], but it is the Mach number at which the rate of drag increase due to compressibility becomes unacceptable ... that is the Mach number at which the wave drag due to compressibility results in an increment of 20 drag counts (0.002) to the zero lift

drag coefficient”. Furthermore, we must note that Howe just considers the two-dimensional case, so M_{NCRIT} has to be taken in the context of this report as $M_{DD,eff}$. In the interest of a uniform notation equation (3.32) is thus rewritten

$$M_{DD,eff} = A_F - 0.1 C_L - t/c \quad (3.33)$$

“ A_F is a number, which depends upon the design standard of the aerofoil section. For older aerofoil A_F was around 0.8 but a value of 0.95 should be possible with an optimized advanced aerofoil.” In effect, we can think of as A_F being the drag-divergence Mach number of an airfoil of zero thickness at zero angle of attack. Once the angle of attack is increased and hence the lift coefficient, the drag-divergence Mach number will decrease. This is due to the super velocities on the top of the airfoil. According to (3.33) the drag-divergence Mach number also decreases with an increase of relative thickness. These general phenomena were explained already in Chapter 2 and are well represented in Howe’s equation. The extend to which these phenomena have an influence on the drag-divergence Mach number is given in (3.33) by the factor 0.1 for C_L and the factor 1.0 for t/c . If these factors will in fact result in an optimum representation of measured parameters will be investigated in Chapter 4 . Here the interest is first of all to calculate relative thickness giving

$$t/c = A_F - 0.1 C_L - M_{DD,eff} \quad (3.34)$$

3.6 Equation from Jenkinson

Another equations is given by **Jenkinson 1999** (p. 116):

$$M_n = 0,877 - (1,387 \cdot T) + (0.431 \cdot \Lambda \cdot 10^{-4}) + (0.1195 - 0.18 \cdot C_{Ldes}) \quad (3.35)$$

or

$$M_n = 0,9965 - 1,387 \cdot T + 4.31 \cdot 10^{-5} \Lambda - 0.18 \cdot C_{Ldes} \quad (3.36)$$

With

- Λ sweepback angle of the quarter chord in degrees
- T thickness ratio
- C_{Ldes} design lift coefficient

The equation considers the effect of sweep, so the calculated Mach number is M_{DD} (and not $M_{DD,eff}$). Using the notation of this report

$$M_{DD} = 0,9965 - 1,387 \cdot t/c + 4,31 \cdot 10^{-5} \varphi_{25} - 0,18 \cdot C_L \quad (3.37)$$

Again we can think of $M_{DD} = 0.9965$ for a wing

- with a of zero thickness
- at zero angle of attack ($C_L = 0$)
- with sweep $\varphi_{25} = 0$.

Once the angle of attack is increased and hence the lift coefficient, the drag-divergence Mach number will decrease. The drag-divergence Mach number also decreases with an increase of relative thickness, but it is increased with sweep. The extend to which these phenomena have an influence on the drag-divergence Mach number is given in (3.37) by the factors in front of each parameter in question. Unfortunately, the author does not give an explanation about how these parameters were obtained. If these factors will in fact result in an optimum representation of measured parameters will be investigated in Chapter 4. Solving for relative thickness

$$t/c = \frac{1}{1.387} (0.9965 + 4.31 \cdot 10^{-5} \varphi_{25} - 0.18 \cdot C_L - M_{DD}) \quad (3.38)$$

$$t/c = 0.7185 + 3.107 \cdot 10^{-5} \varphi_{25} - 0.1298 \cdot C_L - 0.7210 \cdot M_{DD} \quad (3.39)$$

3.7 Equation from Weisshaar

Weisshaar 2000 presents an equation to calculate the drag divergence Mach number:

$$M_{DD} = \frac{K_A}{\cos \Lambda} - \frac{t/c}{\cos^2 \Lambda} - \frac{C_L}{10 \cos^3 \Lambda} \quad (3.40)$$

where $K_A \cong 0.80 - 0.90$ and $\Lambda = \varphi_{25}$.

As a matter of interest also the critical Mach number may be estimate

$$M_{Crit} = M_{DD} - \left(\frac{0.1}{80} \right)^{1/3} \quad (3.41)$$

In effect, we can think of K_A as being the drag-divergence Mach number of an unswept wing of zero thickness at zero angle of attack. Once the angle of attack is increased and hence the

lift coefficient, the drag-divergence Mach number will decrease. According to (3.40) the drag-divergence Mach number also decreases with an increase of relative thickness. M_{DD} increases with sweep by a factor of $1/\cos(\Lambda)$. The relative thickness t/c can then be calculated from

$$t/c = K_A \cos \Lambda - M_{DD} \cos^2 \Lambda - \frac{C_L}{10 \cos \Lambda} \quad (3.42)$$

3.8 Equation based on Böttger

Böttger 1993 (in his thesis prepared at Airbus) presents three graphs. These three graphs can be used to determine the drag divergence Mach number M_{DD} (called M_{20} by **Böttger 1993**). The graphs are reproduced here in this text as

- **Figure 3.6:** M_{DD} versus C_L
- **Figure 3.7:** Variation 1 to M_{DD} : ΔM_{DD} as function of t/c
- **Figure 3.8:** Variation 2 to M_{DD} : ΔM_{DD} as function of φ_{25}

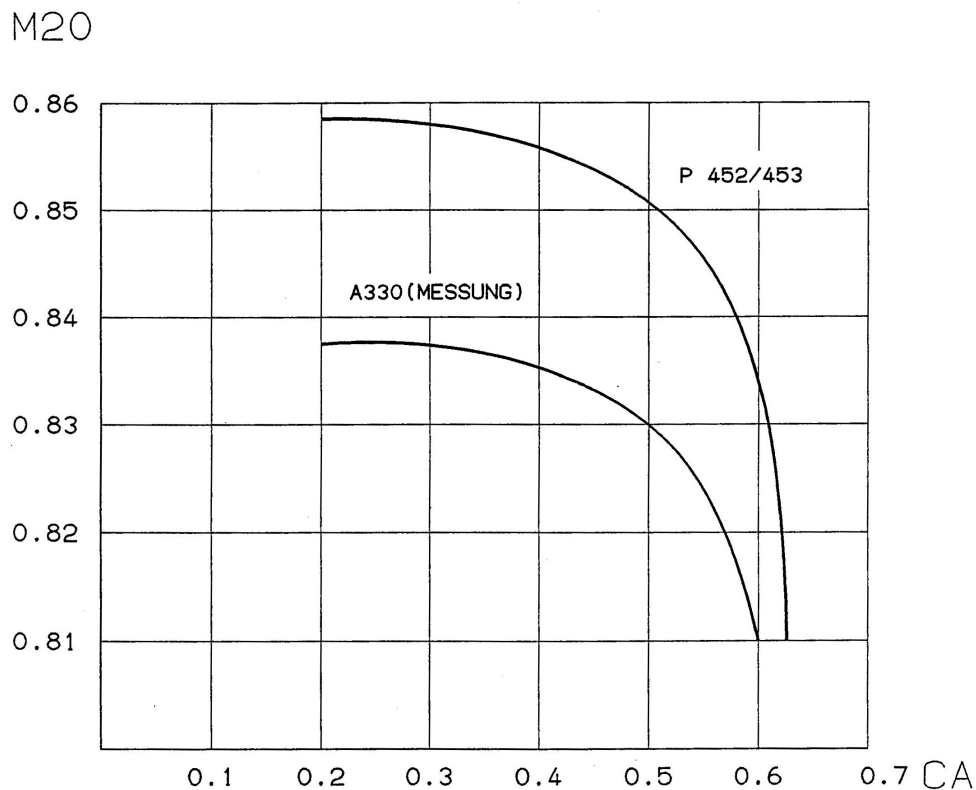


Figure 3.6 Drag divergence Mach number M_{DD} versus lift coefficient C_L (named here C_A)

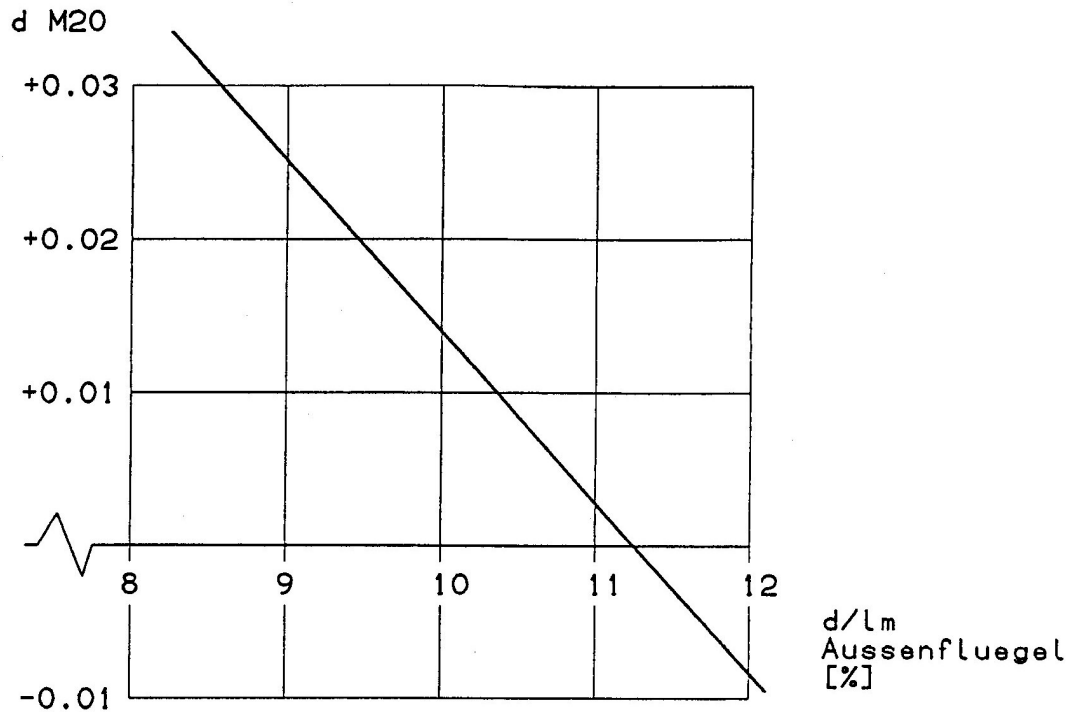


Figure 3.7 Drag divergence Mach number M_{DD} versus relative thickness t/c (named here d/lm)

d M20

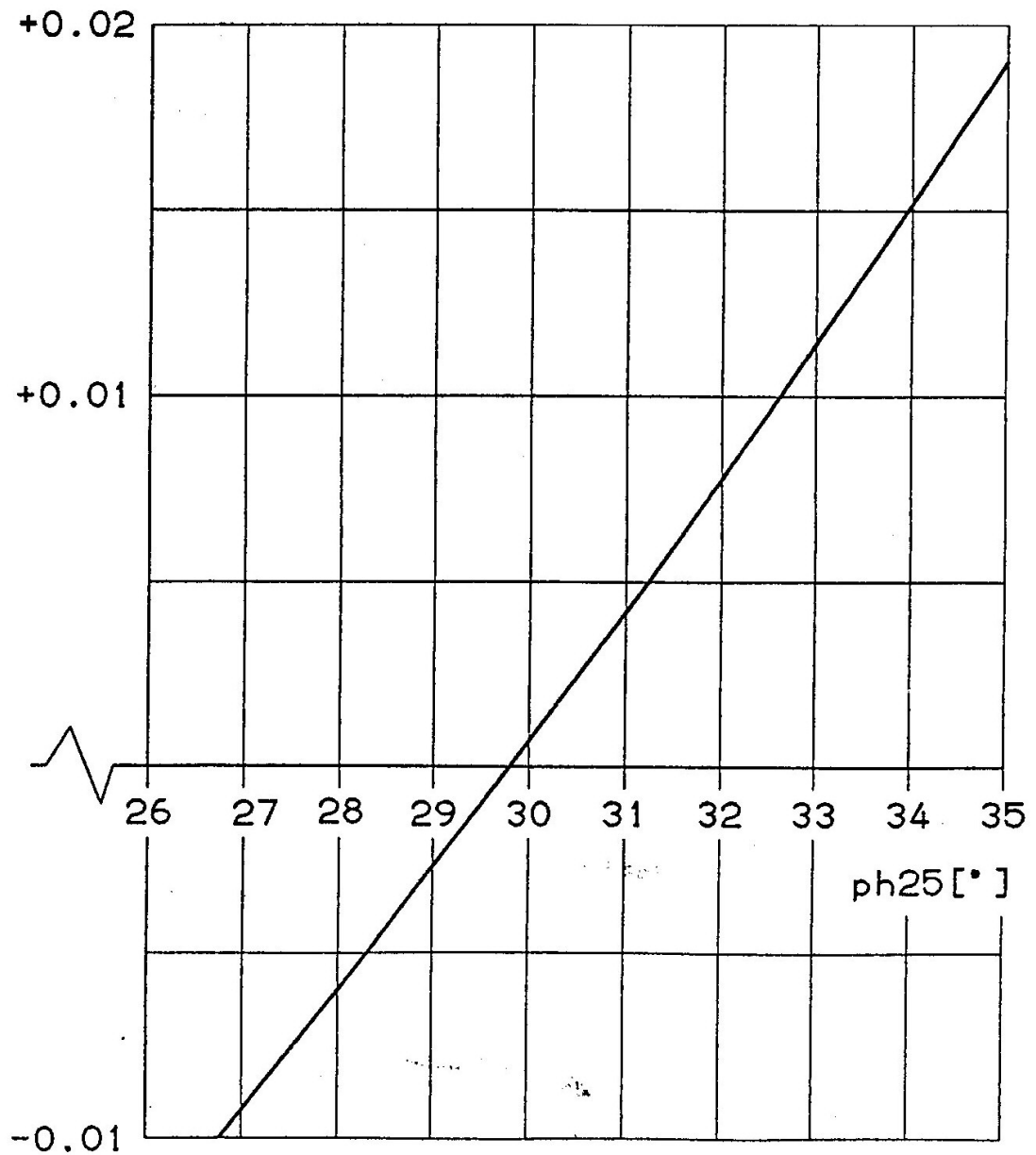


Figure 3.8 Drag divergence Mach number M_{DD} versus sweep ϕ_{25} (named here ph25[°])

The aim here was to convert the graphs to an equation in order to use the information in an easy comparison of the different methods.

The first graph from Figure 3.6 was converted to an equation. Its structure follows intuition.

$$M_{DD} = a(C_L - b)^d + c \quad (3.43)$$

with

$$\begin{aligned}
 a &= -1.147 \\
 b &= 0.200 \\
 c &= 0.838 \\
 d &= 4.057
 \end{aligned}$$

where the parameters b and c were read from the graph “A330 (Messung)” shown in Figure 3.6 and the other two parameters of the equation were determined by using the EXCEL solver. The results are shown in Figure 3.9.

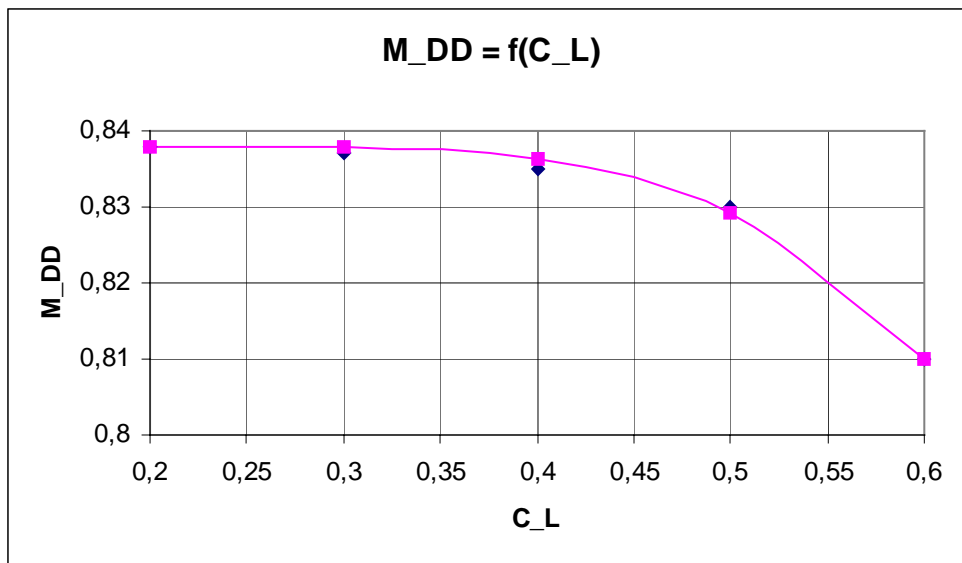


Figure 3.9 The M_{DD} versus C_L converted in Excel

The influence of the sweep was read directly from the graph shown in Figure 3.8 giving

$$\Delta M_{DD} = 0.00288 \cdot (\varphi_{25} - 29.8^\circ). \quad (3.44)$$

The influence of the relative thickness was directly read from the graph shown in Figure 3.7 giving

$$\Delta M_{DD} = -30/27 \cdot (t/c - 0.113). \quad (3.45)$$

Combining all three equation results in

$$M_{DD} = a(C_L - b) \cdot d + c - 30/27 \cdot (t/c - 0.113) + 0.00288 \cdot (\varphi_{25} - 29.8^\circ) \quad (3.46)$$

Solved for the relative thickness the equation becomes

$$t/c = \frac{27}{30} [a(C_L - b)^d + c + 0.00288(\phi_{25} - 29,8^\circ) - M_{DD}] + 0.113 \quad . \quad (3.47)$$

3.9 Equation based on Raymer

Another equation which gives a relationship between the parameters can be found in **Raymer 1992** who gives "A preliminary estimate of wing M_{DD} " where M_{DD} is calculated to fit the Boeing definition (20 drag counts) of a conventional wing

$$M_{DD} = M_{DD_{L=0}} LF_{DD} - 0.05C_{L_{design}} \quad . \quad (3.48)$$

Figures 3.10 and 3.11 are used in this equation. Figure 3.10 provides the wing drag-divergence Mach number of a wing at zero lift as a function of sweep and relative thickness. Figure 3.11 adjusts M_{DD} by a factor LF_{DD} to the actual lift coefficient. Relative thickness has to be considered again in Figure 3.11. In equation (3.48) the last term is an adjustment for the wing design lift coefficient. "Initially it can be assumed that the design lift coefficient is the same as the lift coefficient at cruise". No explanation is given how the lift coefficient in Figure 3.11 is to be calculated. For simplicity, the calculations presented in Chapter 4 take this lift coefficient also to be the design lift coefficient. **Raymer 1992** states how an adjustment to the airfoil quality should be made: "If the wing uses a supercritical airfoil the actual thickness ratio should be multiplied by 0.6 before using these figures."

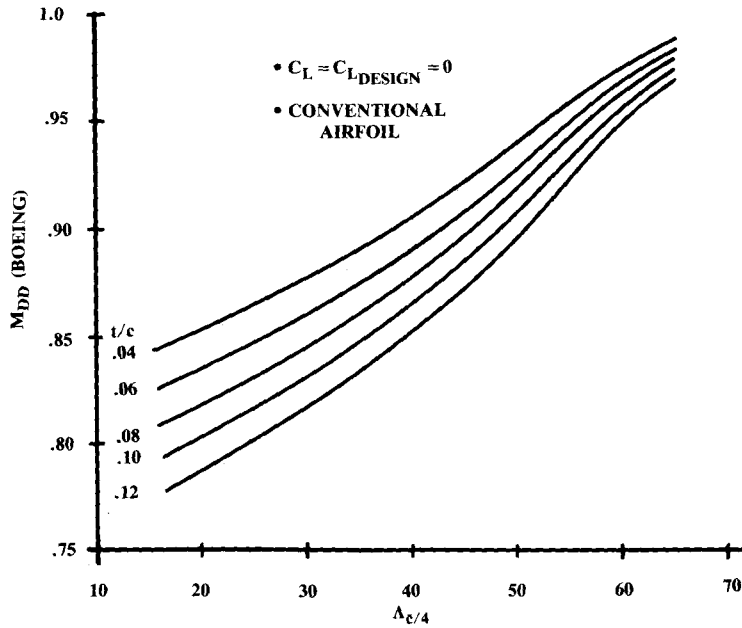


Figure 3.10 Wing drag-divergence Mach number (Raymer 1992)

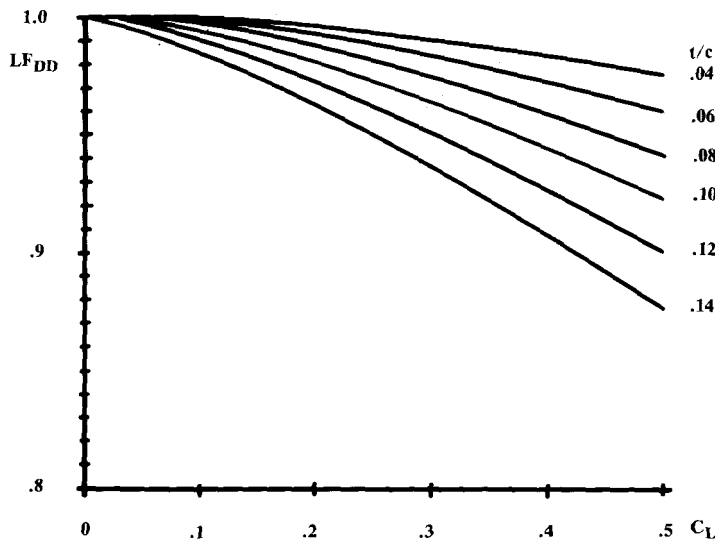


Figure 3.11 Lift adjustment for M_{DD} (Raymer 1992)

In order to compare Raymer’s equation with that of the other authors, it is handy to calculate the relative thickness. This obviously is not that easy, since t/c is included in both, Figure 3.10 and 3.11. The approach followed here is to convert the two figures into equations. Once that is done the relative thickness can be calculated iteratively. A modified Newton method given in EXCEL by means of the “Solver” has been used here to calculate for t/c .

The detailed procedure is this:

$$M_{DD} = M_{DD}(C_L = 0) LF_{DD} - 0,05C_L \tag{3.49}$$

$$M_{DD}(C_L = 0) = 1 + k_{M,DD} \left(u(90^\circ - \rho_{25})^3 + v(90^\circ - \rho_{25})^2 + w(90^\circ - \rho_{25}) \right) \quad (3.50)$$

with $u = 8.029 \cdot 10^{-7}$, $v = -1.126 \cdot 10^{-4}$, $w = 8.437 \cdot 10^{-4}$

$$k_{M,DD} = 1317 (t/c)^3 - 324,3(t/c)^2 + 28,948(t/c) - 0,0782 \quad (3.51)$$

$$LF_{DD} = k_{LF,DD} (a C_L^2 + b C_L) + 1 \quad (3.52)$$

with $a = -0,1953$, $b = -0.1494$

$$k_{LF,DD} = 23,056(t/c)^2 + 3,889(t/c) \quad (3.53)$$

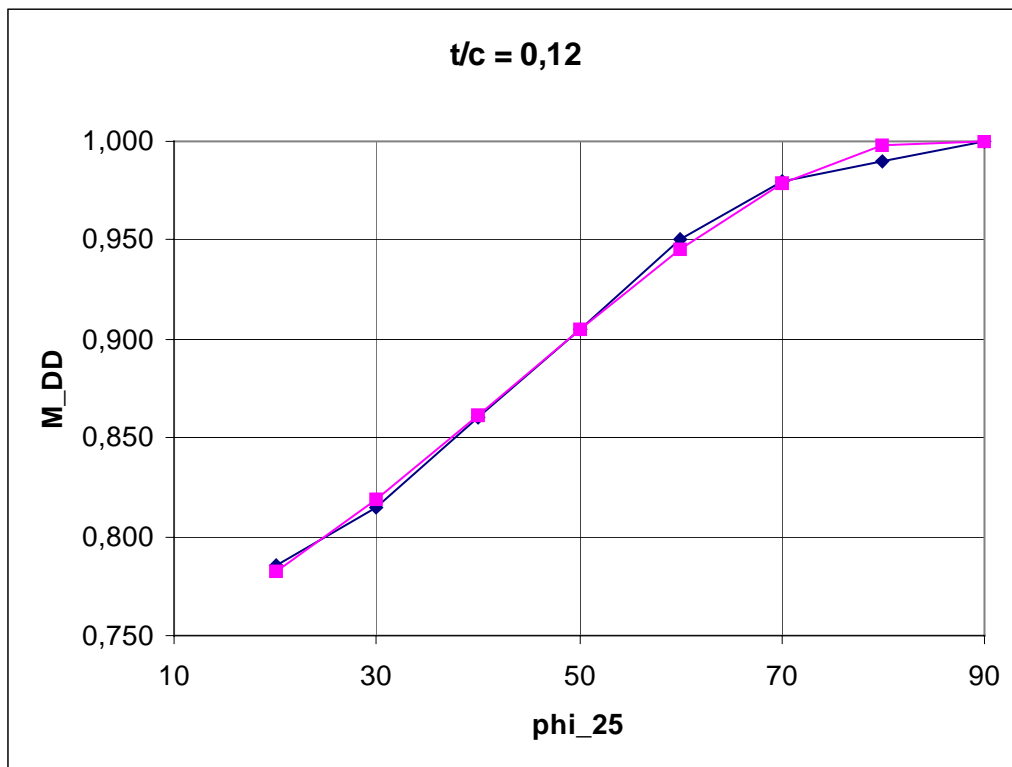


Figure 3.12 Representation of Figure 3.10 for $t/c = 0.12$ with equation (3.50) – measured data points (blue) and calculated data points (purple) can be compared

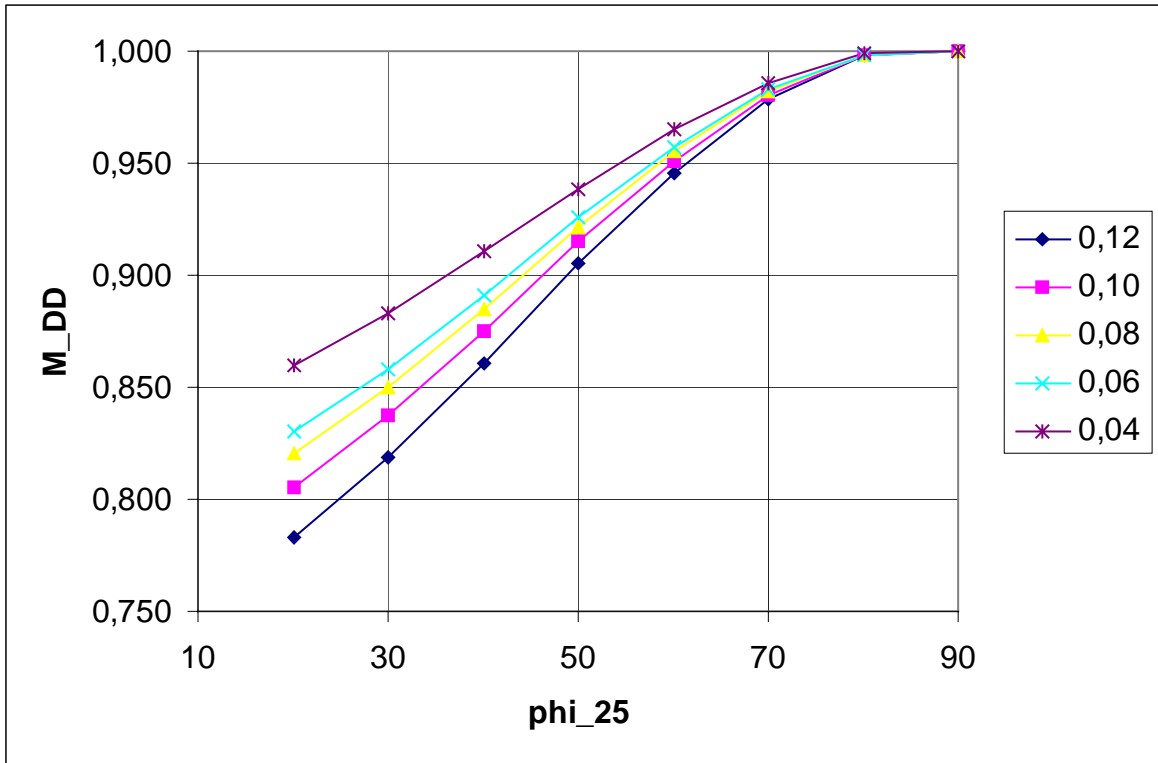


Figure 3.13 Representation of Figure 3.10 with equation (3.50)

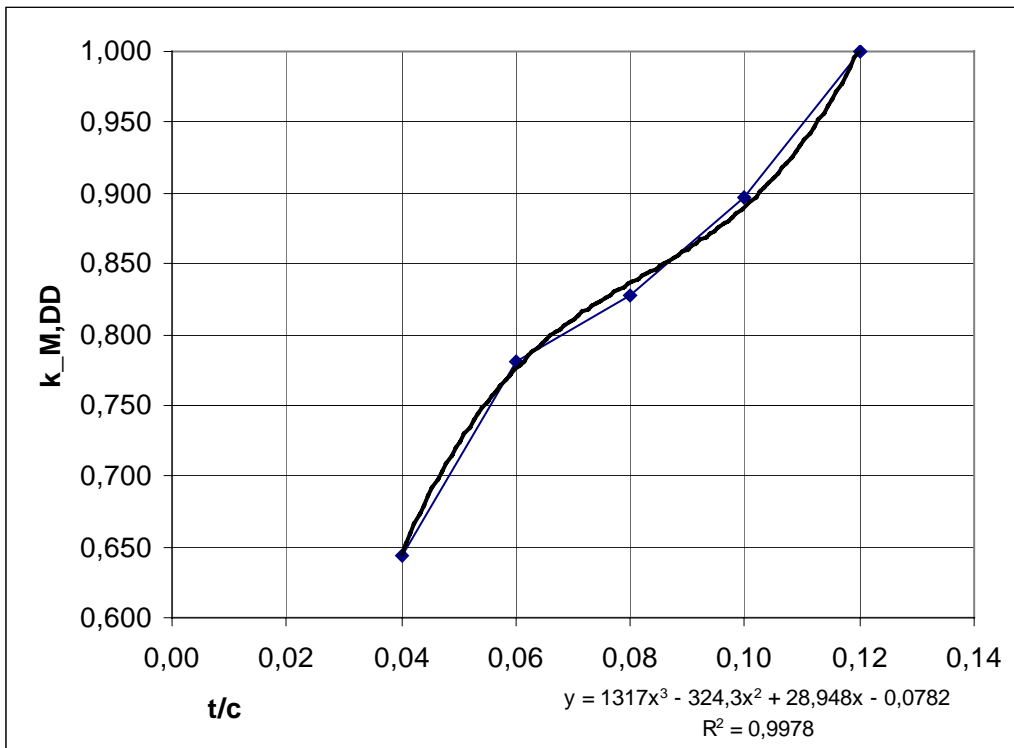


Figure 3.14 Influence of t/c in Figure (3.10) given by equation (3.51) – data points measured from Figure 3.10(blue) can be compared with the curve fit from EXCEL (solid black line)

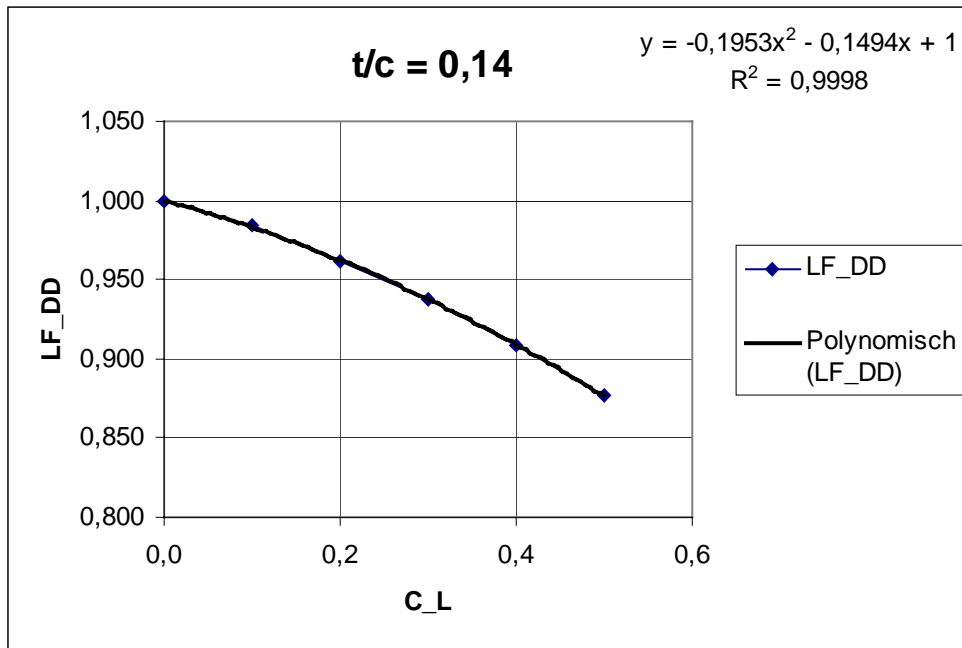


Figure 3.15 Representation of Figure 3.11 for $t/c = 0.14$ with equation (3.52) – data points measured from Figure 3.11 (blue) can be compared with the curve fit from EXCEL (solid black line)

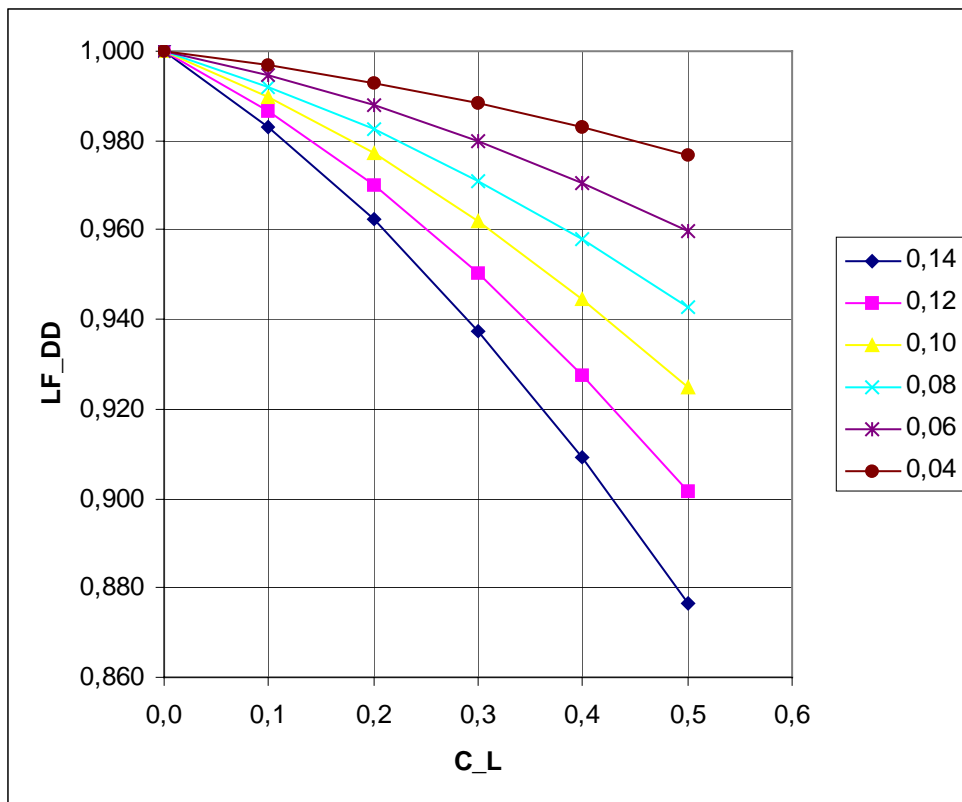


Figure 3.16 Representation of Figure 3.11 with equation (3.52)

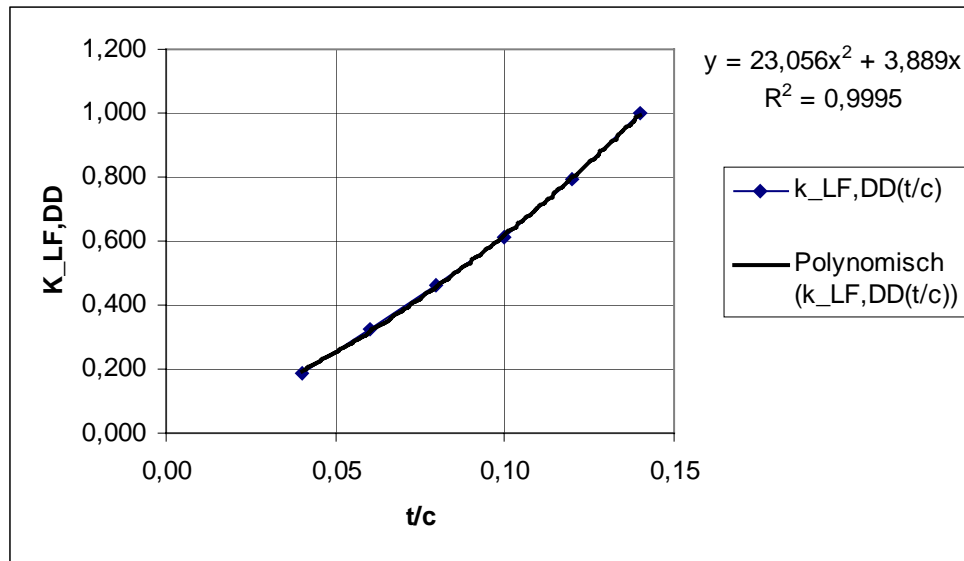


Figure 3.17 Influence of t/c in Figure (3.11) given by equation (3.53) – data points measured from Figure 3.11 (blue) can be compared with the curve fit from EXCEL (solid black line)

3.10 Equation based on Linear Regression

The investigations in this project relate the parameters relative thickness, Mach number, sweep, lift coefficient and type of airfoil (represented by a parameter k_m – see Chapter 3.1) to one another.

It was decided that the relation should be solved for relative thickness. This means that we consider relative thick as dependent variable whereas the remaining variables are considered independent. The independent variables can be selected free of choice the value of the dependent variable is than fixed by the established relationship.

The first approach applies *linear* regression. It is presented in this Chapter. A second approach applies *nonlinear* regression and is explained in the next Chapter. In both cases it is a form of *multiple* regression (compare with **Menascé 1995**), because the model is based on more than one independent parameter.

In linear regression, the model is built as a linear combination of the independent variables. In this case treated here, a multiple regression model could be set up like

$$t/c = a M_{DD} + b \varphi_{25} + c C_L + d k_m \quad . \quad (3.54)$$

This is a 5-dimensional data modeling exercise, because 4 independent plus one dependent variable are involved.

The task in multiple regression is to find a set of parameters a, b, c, and d that best fit the given data. So it is an optimization process that needs to be used to find this best fit. **Matulsky 2003** describes several optimisation techniques used in curve fitting: The method of the steepest descent, the Gauss-Newton method, and the Levenberg-Marquardt method. The parameters are fit to the data in this project by help of the EXCEL-solver that works with a modified Newton method.

Here we follow a slightly modified approach to linear regression. Instead of using M_{DD} and φ_{25} separately as in (3.54), we use the nonlinear combination of the two parameters

$$M_{DD,eff} = M_{DD} \cdot \sqrt{\cos \varphi_{25}} \quad (3.3)$$

following aerodynamic proven evidence. This than yields a modified regression model

$$t/c = a M_{DD,eff} + b C_L + c k_m \quad (3.55)$$

3.11 Equation based on Nonlinear Regression

In nonlinear regression the regression equation is of nonlinear form. **Phillips 2005** could be consulted as a source for equations to chose from. Virtually any function know from mathematics could be used for curve fitting. The technical understanding about the particular problem should lead to a suitable equation. Popular are among others Taylor Series Equations, Polynomial Equations, or Power Family Equations – just to name a few. Here a standard approach is followed using a variant of the Power Family Equations

$$t/c = k_t \cdot M_{DD}^t \cdot \cos \varphi_{25}^u \cdot c_L^v \cdot k_M^w \quad (3.56)$$

It was decided to take $\cos \varphi_{25}$ as one of the independent parameters instead of φ_{25} , in order to resemble the flow phenomena better (see Chapter 3.10).

As in all the other cases, the parameters are fit to the data again with the EXCEL-solver.

3.12 Theoretical Substantiation of Torenbeek's Equation

The starting point in the theoretical substantiation of Torenbeek's derivation is based on the sectional data which indicates that the lowest pressure coefficient of the symmetrical sections at zero lift is

$$(c_{p_i})_{\min} = c_{p_{ier}} = \text{const} \left(\frac{t}{c} \right)^{1.5} . \quad (3.57)$$

This equation given by **Torenbeek 1988** was checked with airfoil data from **Riegels 1958**. The results are presented in Figure 3.18. The data points can be fitted by a curve (blue line in Figure 3.18)

$$(c_{p_i})_{\min} = -3.03 \left(\frac{t}{c} \right)^{0.914} . \quad (3.58)$$

Hence Torenbeek's assumption is not in close agreement with NACA airfoil data. The exponent in Torenbeek's Equation (3.2) of $2/3 = 0.67$ should be $1/0.914 = 1.094$ if based on (3.58).

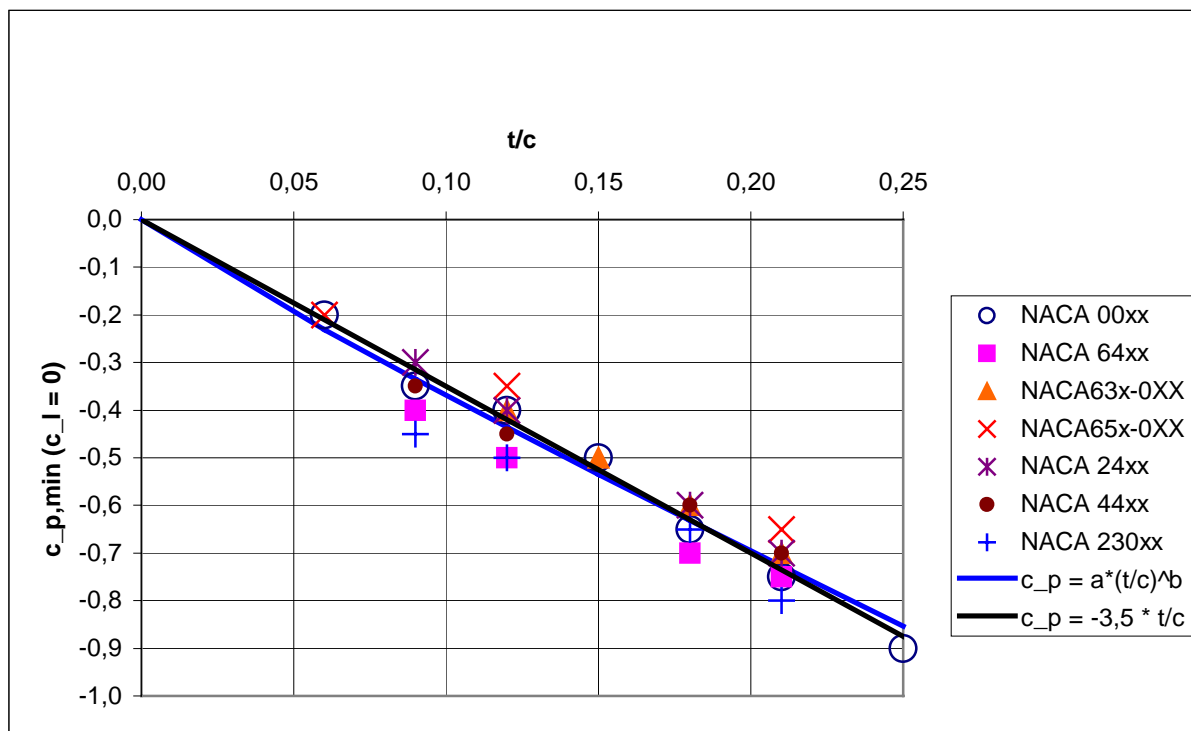


Figure 3.18 Minimum pressure coefficient at zero lift for selected NACA airfoils as a function of relative thickness

In Equation (3.57) we name the constant k_{cp} and the equation becomes

$$\left(c_{p_i}\right)_{\min} = c_{p_{i_{cr}}} = -k_{cp} \left(\frac{t}{c}\right)^{1.5} \quad (3.59)$$

with $k_{cp} > 0$. From the Prandtl- Glauert correction we have

$$c_{p_{cr}} = \frac{c_{p_{i_{cr}}}}{\sqrt{1-M_{cr}^2}} \quad (3.60)$$

The

$$c_{p_{cr}} = \frac{2}{\gamma M_{cr}^2} \left[\left\{ \frac{2 + (\gamma - 1) M_{cr}^2}{\gamma + 1} \right\}^{\gamma/(\gamma-1)} - 1 \right] \quad (3.61)$$

Substituting 3.59 into 3.60 we get with 3.61 two expressions for $c_{p_{cr}}$. Setting them equal yields

$$\frac{-k_{cp} \left(\frac{t}{c}\right)^{3/2}}{\sqrt{1-M_{cr}^2}} = \frac{-2}{\gamma M_{cr}^2} \left[1 - \left\{ \frac{2 + (\gamma - 1) M_{cr}^2}{\gamma + 1} \right\}^{\gamma/(\gamma-1)} \right] \quad (3.62)$$

Solving for t/c

$$\frac{t}{c} = \left(\frac{1}{k_{cp}}\right)^{2/3} \left\{ \frac{2}{\gamma M_{cr}^2} \left[1 - \left(\frac{2 + (\gamma - 1) M_{cr}^2}{\gamma + 1} \right)^{\gamma/(\gamma-1)} \right] \sqrt{1 - M_{cr}^2} \right\}^{2/3} \quad (3.63)$$

Next we define a new constant just for simplicity

$$\left(\frac{1}{k_{cp}}\right)^{2/3} = k_{tc} \quad (3.64)$$

the above equation becomes

$$\frac{t}{c} = k_{tc} \left\{ \frac{2}{\gamma M_{cr}^2} \left[1 - \left(\frac{2 + (\gamma - 1) M_{CR}^2}{\gamma + 1} \right)^{\gamma/(\gamma-1)} \right] \sqrt{1 - M_{cr}^2} \right\}^{2/3} \quad (3.65)$$

$$\frac{t}{c} = k_{tc} \left\{ \frac{2}{\gamma} \left[1 - \left(\frac{2 + (\gamma - 1) M_{cr}^2}{\gamma + 1} \right)^{\gamma/(\gamma-1)} \right] \frac{\sqrt{1 - M_{cr}^2}}{M_{cr}^2} \right\}^{2/3} \quad (3.66)$$

$$\frac{t}{c} = k_{tc} \left(\frac{2}{\gamma} \right)^{2/3} \left\{ \left[1 - \left(\frac{2 + (\gamma - 1) M_{cr}^2}{\gamma + 1} \right)^{\gamma/(\gamma-1)} \right] \frac{\sqrt{1 - M_{cr}^2}}{M_{cr}^2} \right\}^{2/3} \quad (3.67)$$

Now knowing that $\gamma = \frac{C_p}{C_v} = 1.4$ for air, we can make the simple calculation

$$\frac{\gamma}{\gamma - 1} = \frac{1.4}{1.4 - 1} = \frac{1.4}{0.4} = 3.5 \quad (3.68)$$

If we assume that $k_{tc} \left(\frac{2}{\gamma} \right)^{2/3} = 0.3$ – as proposed by Torenbeek – the equation becomes

$$\frac{t}{c} = 0.3 \cdot \left\{ \left[1 - \left(\frac{2 + (\gamma - 1) M_{cr}^2}{\gamma + 1} \right)^{3.5} \right] \frac{\sqrt{1 - M_{cr}^2}}{M_{cr}^2} \right\}^{2/3} \quad (3.69)$$

We see that at this stage the only term which has not the same expression as in Torenbeek's equation is

$$\frac{2 + (\gamma - 1) M_{cr}^2}{\gamma + 1} \quad (3.70)$$

We go to Equation 11.58 from **Anderson 1991** on page 549

$$C_{p,A} = \frac{2}{\gamma \cdot M_{\infty}^2} \left[\left(\frac{1 + [(\gamma - 1)/2] \cdot M_{\infty}^2}{1 + [(\gamma - 1)/2] \cdot M_A^2} \right)^{\gamma/(\gamma-1)} - 1 \right] \quad (3.71)$$

Transforming the expression which includes the contribution of the local maximum Mach number on the surface M_A by dividing the equation by 0.2

$$\frac{1 + [(\gamma - 1)/2] \cdot M_{\infty}^2}{1 + [(\gamma - 1)/2] \cdot M_A^2} = \frac{1 + 0.2 \cdot M_{\infty}^2}{1 + 0.2 \cdot M_A^2} = \frac{5 + M_{\infty}^2}{5 + M_A^2} = \frac{5 + M_{DD}^2}{5 + (M^*)^2} \quad (3.72)$$

The final form of the above equation has been obtain by considering flight with a free stream Mach number M_{DD} leading to a maximum Mach number on the surface of $M_A = M^*$. This gives even a physical meaning to M^* ! M^* is the local maximum Mach number on the surface (of an unswept wing) when the aircraft flies with a speed of M_{DD} . The better the airfoil, the higher is M^* (compare with Chapter 3.1!).

By replacing the term from (3.72) in equation (3.69) we obtain Tornbeek's equation

$$\frac{t}{c} = 0.3 \left\{ \left[1 - \left(\frac{5 + M_{DD}^2}{5 + (M^*)^2} \right)^{3.5} \right] \frac{\sqrt{1 - M_{cr}^2}}{M_{cr}^2} \right\}^{2/3} \quad (3.73)$$

Neglecting the difference between M_{DD} and M_{cr}

$$\frac{t}{c} = 0.3 \left\{ \left[1 - \left(\frac{5 + M_{DD}^2}{5 + (M^*)^2} \right)^{3.5} \right] \frac{\sqrt{1 - M_{DD}^2}}{M_{DD}^2} \right\}^{2/3} \quad (3.74)$$

Considering the effect of the lift coefficient and dropping the subscript DD , the equation becomes

$$\frac{t}{c} = 0.30 \left\{ \left[1 - \left\{ \frac{5 + M^2}{5 + (M^* - 0.25c_l)^2} \right\}^{3.5} \right] \frac{\sqrt{1 - M^2}}{M^2} \right\}^{2/3} \quad (3.2)$$

M^* is called k_M in this project. This is to underline that $M^* = k_M$ is just a parameter to fit (3.2) to airfoil data.

4 Investigation, Comparison, and Adaptation of Equations

A complete evaluation of all 12 equations presented in Chapter 3 is the next step in the investigation. The idea is to check the equations given and to optimize free parameters based on data of 29 carefully selected aircraft. These aircraft are presented with their three-view drawing in Appendix A. Aircraft data is presented in Appendix B. Often different sources do not agree on specific aircraft data. For this reason it was necessary to consult several sources and to decide which given data is the correct one. The aircraft selected are grouped according to their airfoil class: conventional airfoil, peaky airfoil, older supercritical airfoil (called here: supercritical I), and newer supercritical airfoil (called here: supercritical II). For each of these aircraft classes a summary of the aircraft parameters is given in Appendix C. The calculations based on the 12 equations are presented in detail in Appendix D. Here in Chapter 4 only the main ideas and principles of these calculations are presented together with the final result (see Table 4.1).

4.1 Input from Aircraft Data

With the idea that free parameters of equations shall be fitted to aircraft data, it is evident that **aircraft had to be selected** carefully. A selected inadequate set of aircraft (and aircraft data) could easily lead to wrong results when fitting (optimizing) parameters. So the aim was to select a set of aircraft that

- ... span well the parameter range in question,
- ... well represent the history of aerodynamic evolution.

The aircraft chosen cover a range of different values of sweep (from 0° to 35°), different Drag Divergence Mach numbers (from 0,65 to 0,88), different average relative wing thickness (from 9% to 13,4%), cruise lift coefficient (from 0,22 to 0,73), and type of airfoil (conventional, peaky, older transonic, and modern transonic airfoils). Again: Every parameter was taken from more than two sources of documentation so that there is some assurance of the accuracy of the aircraft data.

As pointed out in Chapter 3, the equations under investigation relate Mach number, relative thickness, sweep and lift coefficient of the wing to one another. It was decided to consider the relative thickness t/c as the unknown and the other parameters as known inputs. But also these **input parameters** had to be evaluated first. The calculations for each aircraft are given in Appendix B. The ideas behind these calculations are discussed next:

The **Mach number** to enter calculations of the relative thickness is the drag divergence Mach number M_{DD} . Given in aircraft literature are the maximum cruising speed V_{MO} and/or the maximum operating Mach number M_{MO} . If V_{MO} was given, a Mach number called $M_{CR,max}$ (maximum cruise Mach number) was calculated depending also on the cruise altitude h up to which V_{MO} may be flown. Ideally when all parameters are given, we would assume that $M_{CR,max} = M_{MO}$. With a lack of data or the maximum cruise altitude h for a flight with V_{MO} not being specified, a decision had to be made on the selection of $M_{CR,max}$ respectively M_{MO} . This Mach number was assumed to be a reasonable Mach number for cruise flight. Furthermore it was assumed that at this cruise Mach number the aircraft would experience 20 drag counts (following Boeing and Airbus design principles). In other words:

- M_{DD} was taken as M_{MO} if M_{MO} was known,
- M_{DD} was taken as $M_{CR,max}$ (calculated from V_{MO} and h) if M_{MO} was unknown or considered to be unrealistic.

The **lift coefficient** C_L to enter further calculations was calculated from

- ... the mass in cruise flight m_{CR} . m_{CR} was assumed to be equal to the maximum take-off mass m_{MTO} ,
- ... the cruise speed calculated from M_{DD} in altitude h as determined before,
- ... the density in altitude h ,
- ... the reference wing area.

The **average relative thickness of the wing** t/c to enter further calculations was calculated from wing tip and wing root relative thickness with Equation (2.13) from **Jenkinson 1999**. In some cases where an average relative thickness of the wing was given in the literature this value was taken for further calculations.

The **wing sweep at 25% chord** ϕ_{25} was given or could easily be determined.

4.2 Calculation, Optimization and Results

The equations can be split in two parts (compare with Table 4.1):

- equations with fixed parameters
- equations with parameters that are free for optimization.

Equations with fixed parameters are equations which are ready to calculate relative thickness. All factors and parameters are given. **Equations with free parameters** are equations that include parameters either unknown or free for adaption. These parameters may be fitted to given aircraft data. In this way the output value for t/c may be optimized.

In any of these two cases the result of the calculation given in Appendix D is the **Standard Error of Estimate SEE** . This value tells us how far off our estimate of the relative thickness (calculated with one of the equations) is, when compared with actual aircraft data.

$$\text{Standard Error of Estimate} = \sqrt{\frac{\sum (y_{estimate} - y)^2}{n}} \quad (4.1)$$

In this equation $y_{estimate}$ is the value (here the relative thickness, t/c) that was calculated, y is the given value from the aircraft, n is the number of test calculations (here $n = 29$).

For each aircraft and each equation we get an $error^2$ that is $(y_{estimate} - y)^2$. Summing up all the $error^2$ calculated with one equation for all $n = 29$ aircraft should be as low as possible.

$\frac{\sum (y_{estimate} - y)^2}{n}$ is the average $error^2$. Taking the square root yields the average error known as the Standard Error of Estimate (SEE). Note that the SEE shows an absolute error. In case of the relative thickness we deal with relative values (in %). Nevertheless the SEE is absolute with respect to the results of t/c . This can be made clear using an example. An aircraft has a relative thickness of 10% the SEE was calculated to be 1%. This means that on average we expect t/c values from our equation that are off by an absolute 1%, i.e. we may expect results like $t/c = 9%$ or $t/c = 11%$.

The **optimization** of the equation means to determine optimized values of the free parameters. This leads to a minimum Standard Error of Estimate. Thus the results obtained are the best results possible with the equation in question and are quite close to the real values of the relative thickness. The best fit is achieved with EXCEL and the modified Newton method of the "Solver". The "Solver" drives the SEE to a minimum.

Torenbeek's equation can be considered an equation with fixed parameters. Nevertheless all its parameters have been questioned and opened up for optimization.

Following Chapter 3.12 two cases can be further distinguished: with consideration of sweep in the calculation of C_L and without the contribution of sweep. It turned out that these two variants produce only small differences in the results. The version taking the lift coefficient

straight into the equation without considering sweep effects on lift produced slightly better results.

The parameters in Torenbeek's equation that could be opened for optimization are:

- k_M Excel notation for the Torenbeek M^* factor
- k_T Excel notation for the Torenbeek constant from the equation originally being 0.3
- e Excel notation for the exponent originally being $2/3$.

Torenbeek's equation with

- ... its parameters in standard form (as proposed by Torenbeek) produced a *SEE* of 2,88 %
- ... all parameters free for optimization produced a *SEE* of only 0,80 %
- ... only the parameters k_M accounting for the airfoil being free for optimization produced a *SEE* of 2,49 %
- ... only the parameters k_T and e free for optimization produced a *SEE* of only 0,89 %
- ... only the parameter k_T free for optimization with $e = 1,094$ as calculated from **Riegels 1958** (see Chapter 3.12) produced a *SEE* of 4,50 %
- ... all parameters free for optimization with $e = 1,094$ as calculated from **Riegels 1958** produced a *SEE* of 2,29 %

One problem with opening up parameters for optimization is that parameters are driven to values that do not have physical meaning in the end. If $k_M = M^*$ can be seen as the local maximum Mach number on the surface (of an unswept wing) when the aircraft flies with a speed of M_{DD} (see Chapter 3.12), then a value of $k_M = 4,7$ for a supercritical wing does not make much sense. On the other hand we need to except parameters without physical meaning if we want to benefit from an optimized fit of parameters to aircraft data.

Appendix E shows the results of a graphical method published by **Schaufele 2000**. This method is similar to the method presented by **Kroo 2001** (see Chapter 3.4). An *SEE* was calculated for Schaufele's method manually by reading values from his charts. It was found out that his results are often far off. The calculated *SEE* is at best 3,3 %. It was concluded that there are better methods around and that a lengthy process to automate this method is not justified in light of the results that can be expected.

The **other equations** are handled straight forward. In each case the Standard Error of Estimate was calculated in order to show how good the equation in question was able to reproduce the relative thickness from the 29 aircraft selected. The Standard Error of Estimate for the relative

thickness of all equations – after having determined optimum parameters – are summarized in Table 4.1.

As it was expected, the best **results** were obtained by the optimized methods. The best result overall was achieved by the equation applying nonlinear regression. This is a method that applies no prior knowledge of aerodynamics but offers a mathematical form that allows for much flexibility to adapt to given parameters. Among the other equations which had not been optimized the equation from Jenkinson gave best results.

Table 4.1 Comparison of different equations used to calculate the relative thickness of a wing based on the Standard Errors of Estimate

Ranking	Method	SEE	optimized	remark
1	t/c from multiple nonlinear regression	0,75%	yes	
2	t/c from TORENBEEK	0,80%	yes	with term "C _L "
3	t/c from multiple linear regression	1,18%	yes	
4	t/c from similarity with sweep	2,43%	yes	
5	t/c from HOWE	3,67%	yes	
6	t/c from similarity without sweep	3,71%	yes	
7	t/c from WEISSHAAR	3,95%	yes	
8	t/c from JENKINSON	4,23%	no	
9	t/c from BÖTTGER	4,32%	no	
10	t/c from RAYMER	4,54%	no	
11	t/c from KROO	4,59%	no	
12	t/c from SHEVELL	8,06%	no	
average SEE		3,25%		

5 Conclusions

The report starts with an introduction to transonic flow around wings and the particular effects which characterize this type of flow. For a better understanding of this type of flow not only the characteristic parameters were presented but also their dependencies on one another.

The aim of this project was to search and develop equations that relate the parameters Mach number, relative thickness, sweep and lift coefficient to one another. 12 equations were found in the literature. The equations were taken from diverse sources. Some equations draw strongly from aerodynamic theory but other equations are purely based on statistical considerations and data regression. In a few cases the starting point in the determination of the equations were diagrams that first needed to be converted into formulas. In many situations this conversion started with intuition, followed by curve fitting techniques supported by EXCEL.

For a better understanding of these equations and the steps that followed, a detailed presentation of each equation was prepared and presented in Chapter 3.

For the calculations done with these 12 equations, 29 transport aircraft were used. The aircraft chosen cover a range of different values of sweep (from 0° to 35°), different Drag Divergence Mach numbers (from 0,65 to 0,88), different average relative wing thickness (from 9% to 13,4%), cruise lift coefficient (from 0,22 to 0,73), and type of airfoil (conventional, peaky, older transonic, and modern transonic airfoils). The investigated aircraft data is presented in form of tables and illustrated in graphical form if deemed necessary.

The equations that had been found in literature are improved by modifying their parameters. The accuracy of these equations was improved by adaptation of the free parameters with respect to the data base of 29 aircraft. For those equations with fixed parameters just the accuracy was calculated.

The best results were achieved by the optimized methods – as expected. The equation based on nonlinear regression can be recommended. Torenbeek's equation will probably be preferred by those that like to see an equation that is based on aerodynamic considerations. From the equations which had not been optimized, Jenkinson's equation gave the best results.

6 Recommendations

This project like every other task can be undertaken as a more detailed study. Always something can be improved. Excellent ideas based on plausible statements are always welcome. All equations can be studied in more detail. The influence of each free parameter could be investigated more profoundly. Maybe another better equation not only with a statistical meaning but also with the scientific meaning could be developed. For a better validity of the optimized parameters the calculations could be made using a larger number of planes.

After an interesting presentation of all equations that could be found at this moment, there are most probably many more equations in the literature that I have not been able to discover. These equations are just waiting for another person to follow in my foot steps to bring them to light.

List of References

- AGARD 1980** AGARD: *Multilingual Aeronautical Dictionary*. Neuilly sur Seine, France : Advisory Group for Aerospace Research and Development (AGARD/NATO), 1980. –
URL: <http://www.rta.nato.int/Search/FTSearch.asp> (2001-11-21)
- Airbus 1987** AIRBUS INDUSTRIE: *Data Base for Design (DBD) : A330-200*. Blagnac : Airbus, 1987
- Airbus 1991** AIRBUS INDUSTRIE: *Data Base for Design (DBD) : A330-300*. Version 300X, Edition 3, 25.6, Blagnac : Airbus, 1991
- Airbus 1992** AIRBUS INDUSTRIE: *Data Base for Design (DBD) : A321-100*. Issue 2.1, Blagnac : Airbus, 1992
- Airbus 2005** URL: http://www.airbus.com/product/a310_specifications.asp (2005-03-07)
- Airliners 2005** URL: <http://www.airliners.net> (2005-02-27)
- Anderson 1989** ANDERSON, J. D.: *Introduction to Flight*. New York : McGraw-Hill, 1989
- Anderson 1990** ANDERSON, J. D.: *Modern Compressible Flow : with historical perspective*. New York : McGraw-Hill, 1990
- Anderson 1991** ANDERSON, J. D.: *Fundamentals of Aerodynamics*. New York : McGraw-Hill, 1991
- BAe 1983** BRITISH AEROSPACE AIRCRAFT GROUP: *Drawing W6J-2, Geometry A320*. Weybridge : BAe, 1983
- Bechtermünz 1998** BECHTERMÜNZ: *Flugzeugtypen der Welt : Modelle, Technik, Daten*. Augsburg : Bechtermünz, 1998
- Beriev 2005** URL: <http://www.beriev.com> (2005-03-04)
- Boeing 2005** URL: <http://www.boeing.com/commercial/767family/technical.html> (2005-03-04)

- Böttger 1993** BÖTTGER, Ole: *Entwurf einer Flugzeugfamilie als Konkurrenz zur Boeing 747-400 und Boeing 777-300*. Hamburg, Fachhochschule Hamburg, Diplomarbeit, 1993. – Supervisor: Marckwardt, K. (FH Hamburg); Hempel, J. (Deutsche Aerospace Airbus)
- Bombardier 2005** URL: <http://www.bombardier.com> (2005-03-04)
- CS-25 2003** EASA: *Certification Specifications for Large Aeroplanes CS-25*. Brussels : European Aviation Safety Agency, 2003. -
URL: http://www.easa.eu.int/doc/Agency_Mesures/Certification_Spec/decision_ED_2003_02_RM.pdf (2005-02-27)
- Dailey 2003** DAILEY, John R.; et al.: *Centennial of Flight : Transonic Flow*. 2003. –
URL: http://www.centennialofflight.gov/essay/Theories_of_Flight/Transonic_Flow/TH19.htm (2005-01-31)
- Ebert 1973** EBERT, Hans J. (Ed.): *Messerschmitt Bölkow Blohm : 111 MBB Flugzeuge 1913-1973*. Stuttgart : Motorbuch, 1973
- Escalona 2005** ESCALONA, E.: *Airplane 3-View Drawings*, 2005. -
URL: <http://www.fortunecity.com/marina/manatee/272/> (2005-02-27)
- Flugzeugtypen 2005** URL: <http://www.flugzeugtypen.net> (2005-02-27)
- Fox 1985** FOX, Robert W.; McDONALD, Alan T.: *Introduction to Fluid Mechanics*. New York : John Wiley, 1985
- Hepperle 2003** HEPERLE, Martin; HEINZE, Wolfgang: *Future Global Range Transport Aircraft*. (RTO-Symposium on Unconventional Vehicles and Emerging Technologies, Bruxelles, 2003). -
URL: http://www.mh-aerotools.de/company/paper_9/global_transport_aircraft.htm (2005-05-28)
- HFB 2005** URL: <http://www.hfb320.de> (2005-02-27)
- Howe 2000** HOWE, D.: *Aircraft Conceptual Design Synthesis*. London : Professional Publishing, 2000

- Janes 1982** TALOR, John W. R.. (Ed.): "Jane's all the World's Aircraft". London : Jane's, 1982. - Jane's Publishing Company, 238 City Road, London, EC1V 2PU, UK
- Janes 1996** JACKSON, Paul (Ed.): *Jane's all the World's Aircraft*. Couldsdon : Jane's, 1996. - Jane's Information Group, 163 Brighton Road, Couldsdon, Surrey CR5 2NH, UK
- Janes 2000** JACKSON, Paul (Ed.): *Jane's all the World's Aircraft*. Couldsdon : Jane's, 2000. - Jane's Information Group, 163 Brighton Road, Couldsdon, Surrey CR5 2NH, UK
- Jenkinson 1999** JENKINSON, Loyd R., SIMPKIN P, RHODES D.: *Civil Jet Aircraft Design*. London : Arnold, 1999
- Jenkinson 2001** JENKINSON, Lloyd; SIMPKIN, Paul; RHODES, Darren: *Civil Jet Aircraft Design : Data Sets*. London : Butterworth-Heinemann, 2001. - URL: <http://www.bh.com/companions/034074152X/appendices/data-a/default.htm> (2005-02-27)
- Jetsite 2005** URL: <http://www.jetsite.com.br> (2005-02-27)
- Kroo 2001** KROO, Ilan: *Aircraft Design : Synthesis and Analysis*. Stanford, CA : Desktop Aeronautics, 2001. – URL: <http://www.desktopaero.com> (2002-06-30)
- Lednicer 2004** LEDNICER, David: *The Incomplete Guide to Airfoil Usage*, 2004. – URL: <http://www.aae.uiuc.edu/m-selig/ads/aircraft.html> (2005-02-27)
- Matulsky 2003** MATULSKY, Harvey; CHRISTOPOULOS, Arthur: *Fitting Models to Biological Data using Linear and Nonlinear Regression : A practical Guide to Curve Fitting*. GraphPad Software : San Diego, CA, 2003. – URL: <http://www.curvefit.com> (2005-02-25)
- Menascé 1995** MENASCE, Daniel A.; et al.: *Defence Aquisition University : DAU Stat Refresher*. Fairfax, Virginia, George Mason University, Center for the New Engineer, Interactive Tutorial, 1995. – URL: <http://cne.gmu.edu/modules/dau/stat> (2005-02-02)
- Obert 1997** OBERT, E.: *Aircraft Design and Aircraft Operation*. Linköping, Linköping Institute of Technology, Short Course Notes, 1997

- Phillips 2005** PHILLIPS, James R.: *ZunZun.com Interactive 2-Dimensional and 3-Dimensional Data Modeling*. – URL: <http://zunzun.com> (2005-02-25)
- Raymer 1992** RAYMER, D.P.: *Aircraft Design: A Conceptual Approach*, AIAA Education Series, Washington D.C. : AIAA, 1992
- Raytheon 2005** URL:
http://www.raytheonaircraft.com/hawker/800xp/hawker_800xp.shtml
(2005-03-04)
- Riegels 1958** RIEGELS, Friedrich W.: *Aerodynamische Profile*. München : Oldenbourg, 1958
- Roskan 1989** ROSKAM, J.: *Airplane Design. Vol. 2 : Preliminary Configuration Design and Integration of the Propulsion System*. Ottawa, Kansas, 1989. – Distribution: Analysis and Research Corporation, 120 East Ninth Street, Suite 2, Lawrence, Kansas, 66044, USA
- Schaufele 2000** SCHAUFELE, Roger D.: *The Elements of Aircraft Preliminary Design*. Santa Ana, CA : Aries Publications, 2000. -
URL: <http://www.aries-publications.com> (2005-02-27)
- Scholz 2005** SCHOLZ, Dieter: *Flugzeugentwurf*. Hamburg, Hochschule für Angewandte Wissenschaften, Fachbereich Fahrzeugtechnik und Flugzeugbau, Vorlesungsskript, 2005
- Shevell 1980** SHEVELL, Richard S.; BAYAN, Fawzi, P.: *Development of a method for predicting the drag divergence Mach number and the drag due to compressibility for conventional and supercritical wings*. Stanford, CA, Stanford University, Department of Aeronautics and Astronautics, Research Report SUDAAR 522, 1980. –
URL: <http://dlib.stanford.edu:6520/text1/dd-ill/drag-divergence.pdf>
(2005-02-25)
- Shevell 1989** SHEVELL, Richard S.: *Fundamentals of Flight*. Englewood Cliffs, New Jersey : Prentice Hall, 1989
- Staufenbiel ca. 1992** STAUFENBIEL, R.: *Luftfahrzeugbau I + II*, RWTH Aachen, Lehrstuhl und Institut für Luft- und Raumfahrt, Skript zur Vorlesung, ca. 1992

- Thorbeck 2001** THORBECK, Jürgen: *Flugzeugentwurf I und II*. Berlin, Technische Universität Berlin, Institut für Luft- und Raumfahrt, Fachgebiet Luftfahr-zeugbau/Leichtbau, Skript, 2001
- Torenbeek 1988** TORENBEEK, Egbert.: *Synthesis of Subsonic Airplane Design*. Delft : University Press, 1988
- USAF 2004a** US AIRFORCE: *Fact Sheets : C-141 STARLIFTER*, 2004. –
URL: <http://www.af.mil/factsheets/factsheet.asp?fsID=93>
(2005-02-27)
- USAF 2004a** US AIRFORCE: *Fact Sheets : C-5 GALAXY*, 2004. –
URL: <http://www.af.mil/factsheets/factsheet.asp?fsID=84>
(2005-03-04)
- VFW 2004** URL: <http://www.vfw614.de> (2005-02-27)
- Weisshaar 2000** WEISSHAAR, T.A.: *Weight and drag estimation : AAE 451 Aircraft Design*, 2000. –
URL: <http://roger.ecn.purdue.edu/~weisshaa/aae451/lectures.htm>
(2004-11-11)

Appendix A

Three-View Drawings

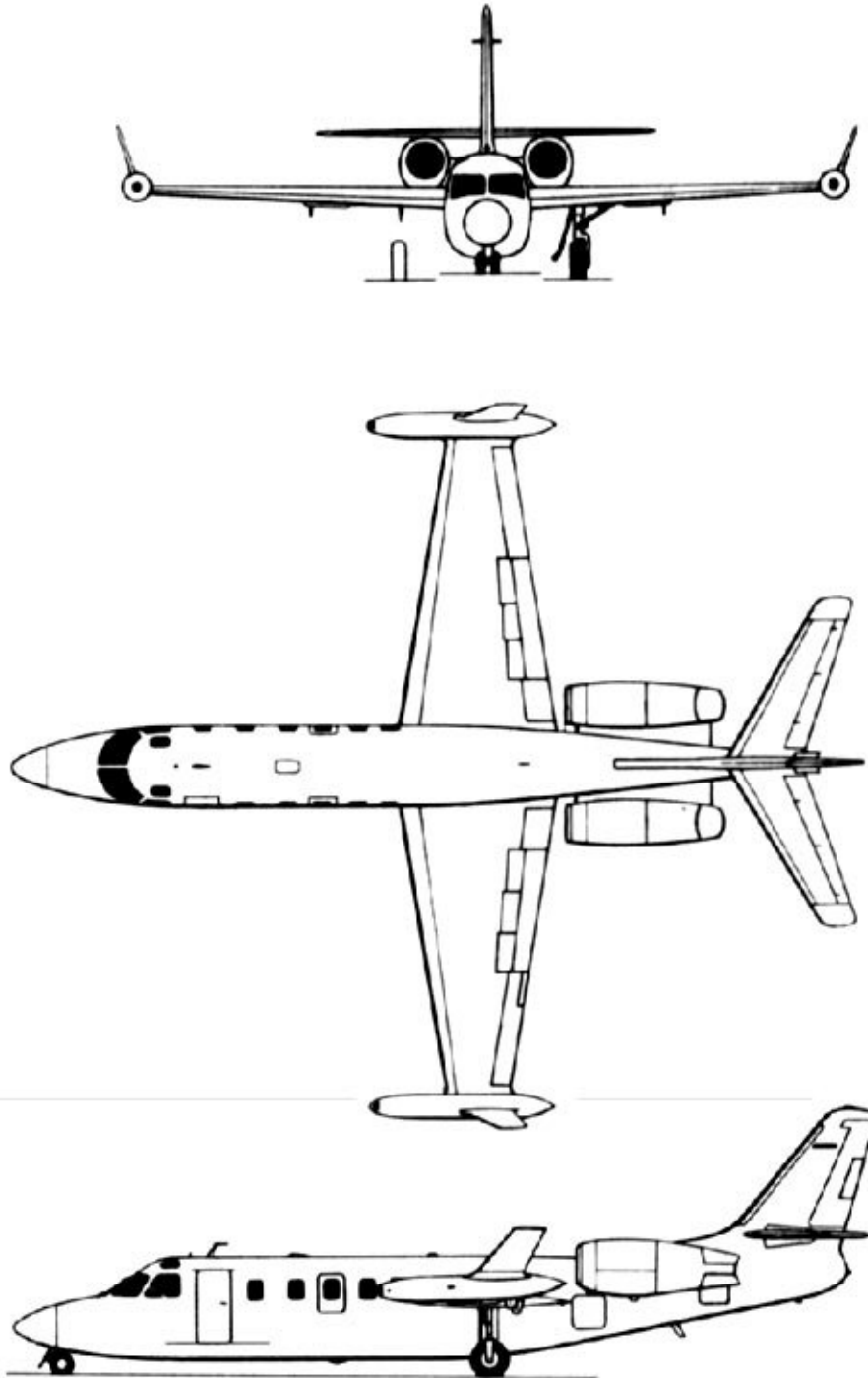


Figure A.1 Three-view drawing: IAI 1124A Westwind

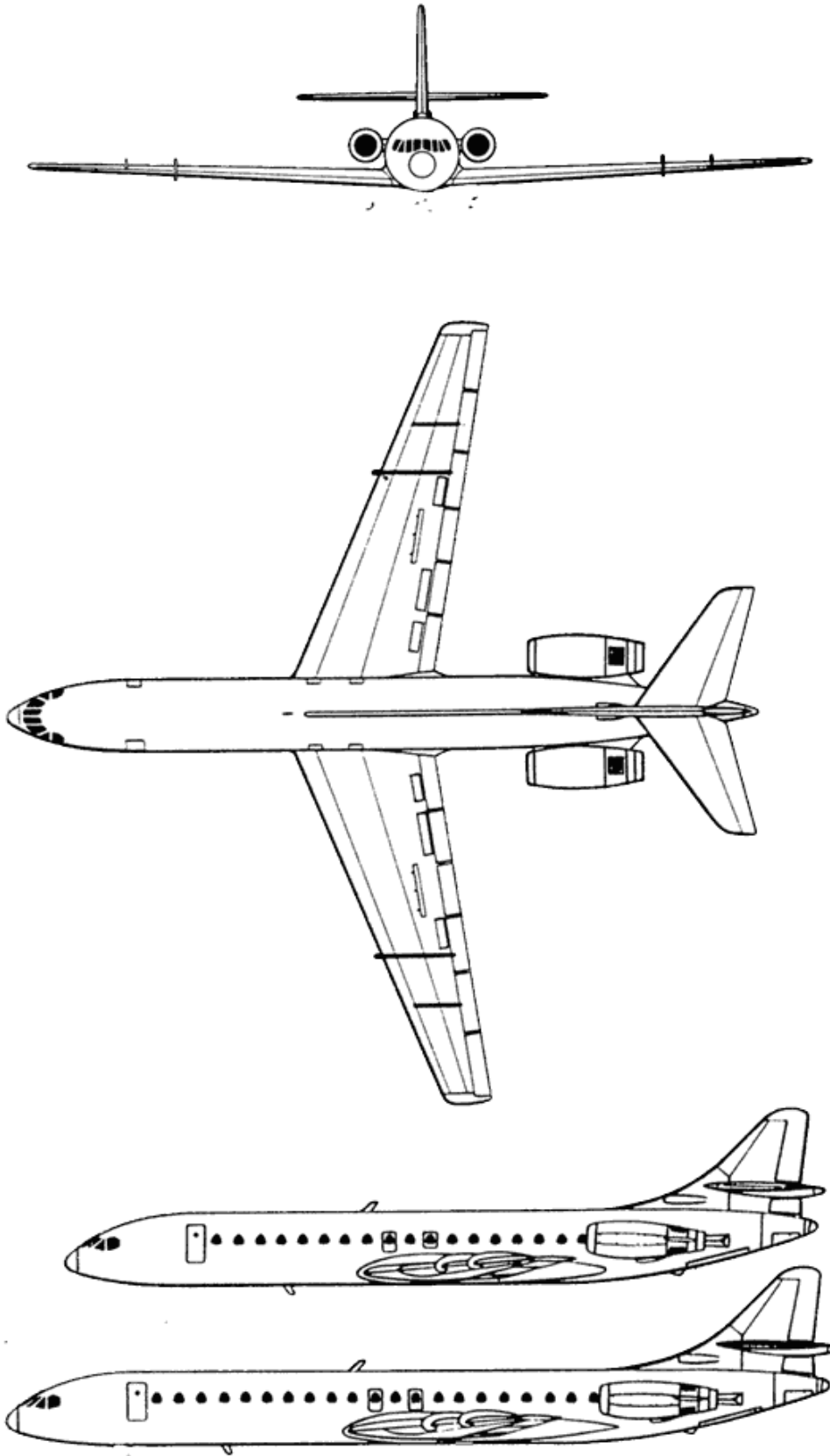


Figure A.2 Three-view drawing: Caravelle

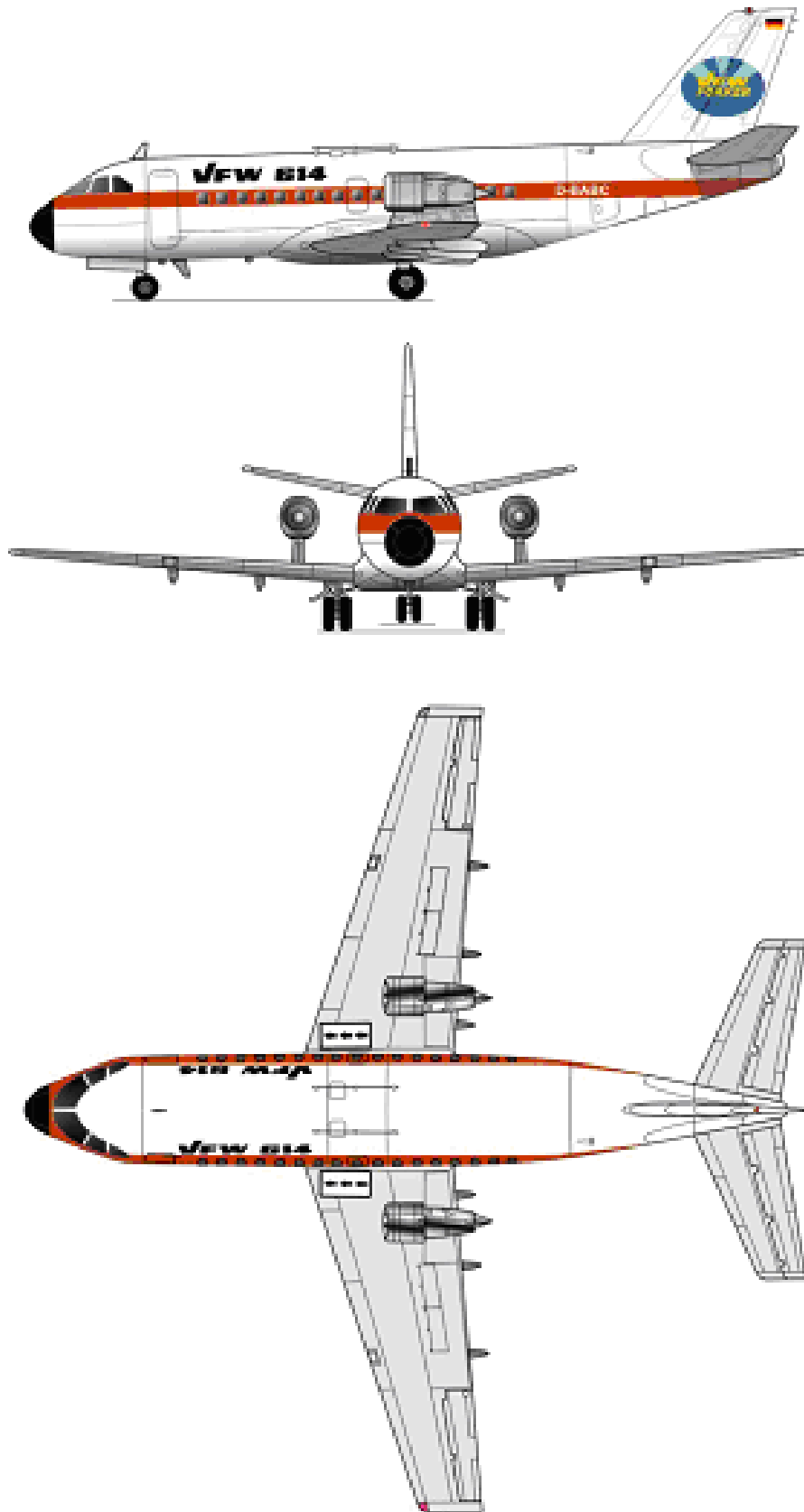


Figure A.3 Three-view drawing: VFW 614

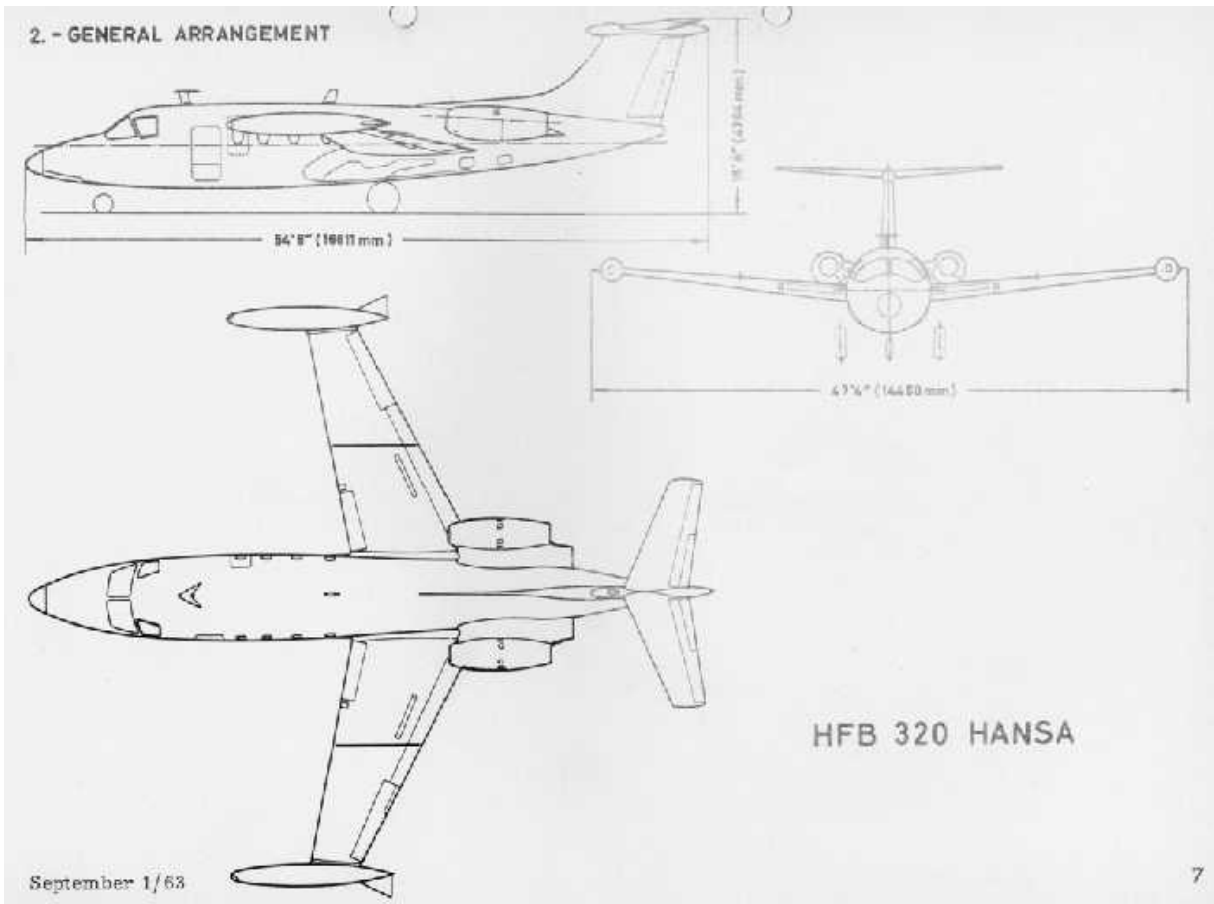


Figure A.4 Three-view drawing: HFB 320

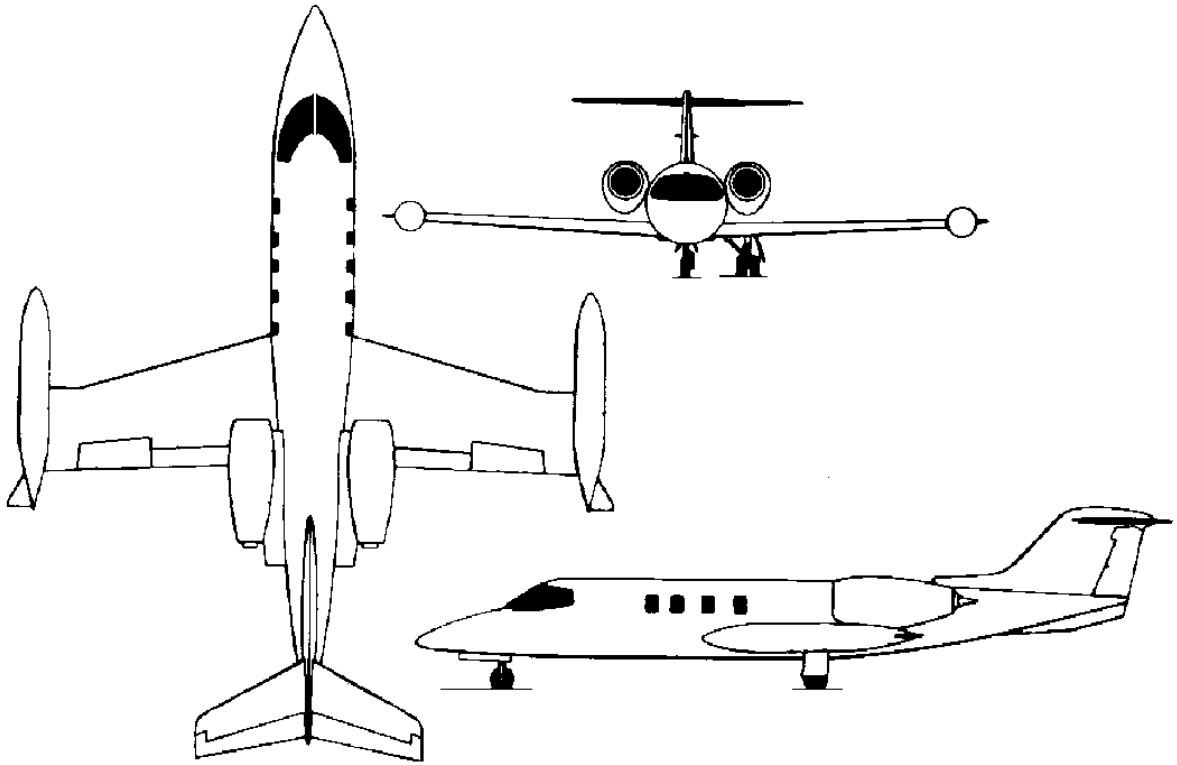


Figure A.5 Three-view drawing: Lear Jet Model 23

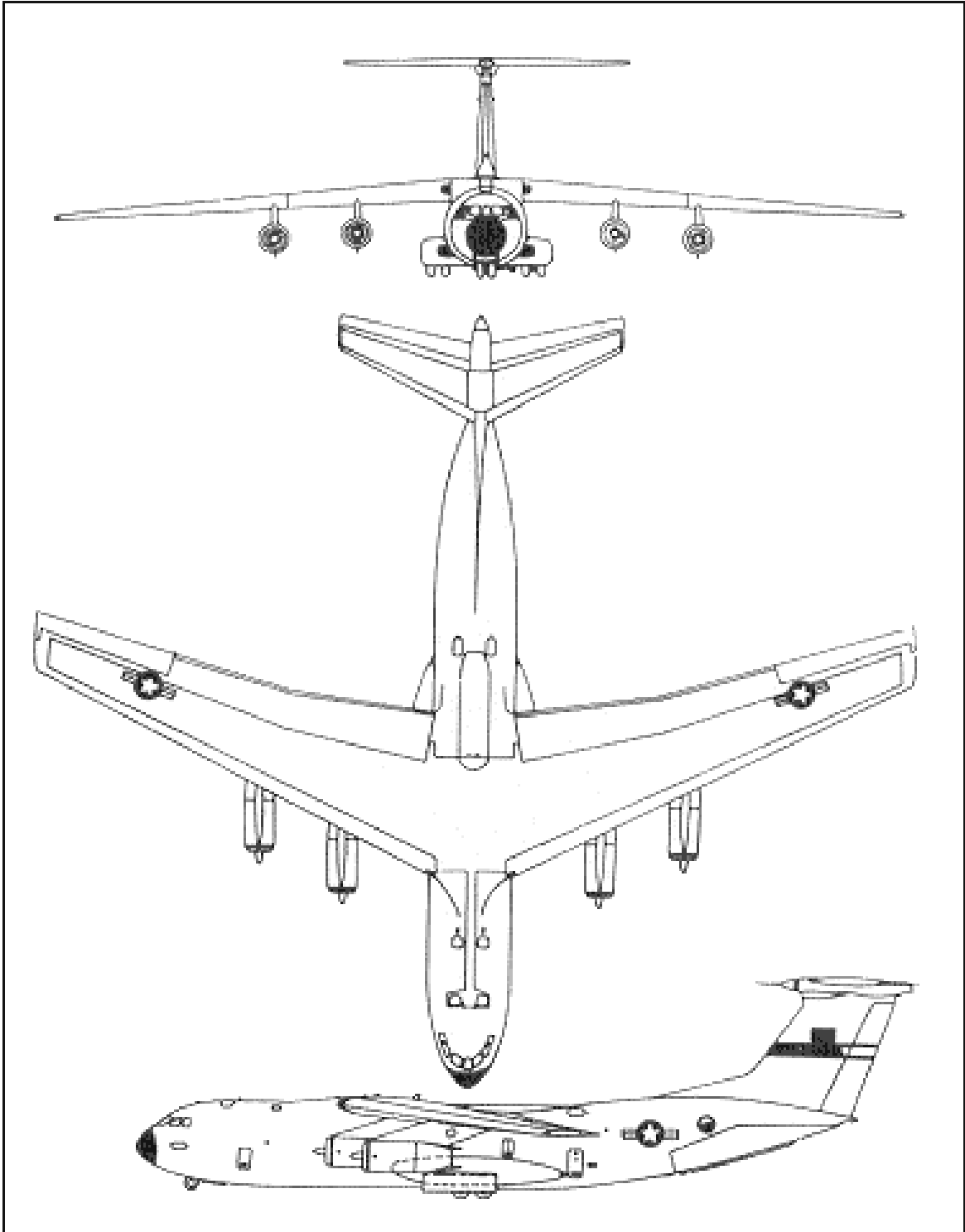


Figure A.6 Three-view drawing: Lockheed C-141 Starlifter

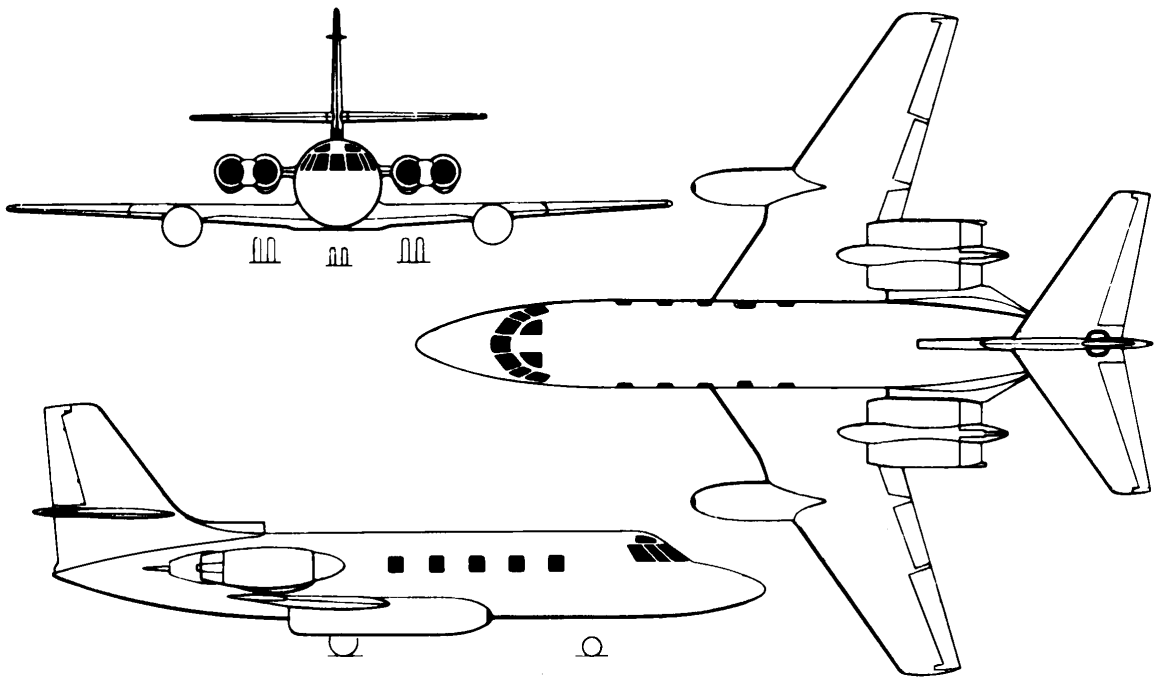


Figure A.7 Three-view drawing: Lockheed Jetstar II

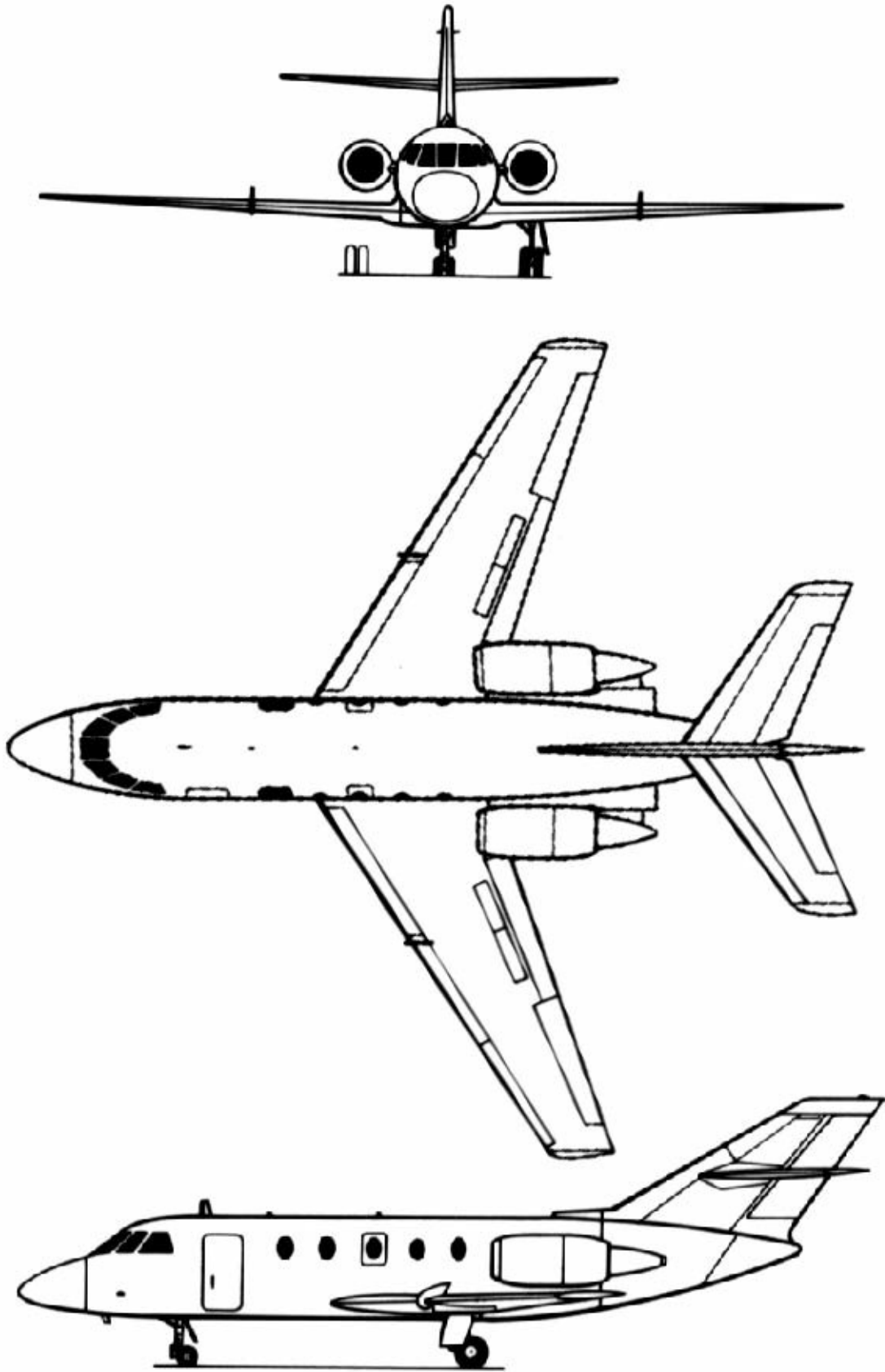


Figure A.8 Three-view drawing: Dassault Falcon 20

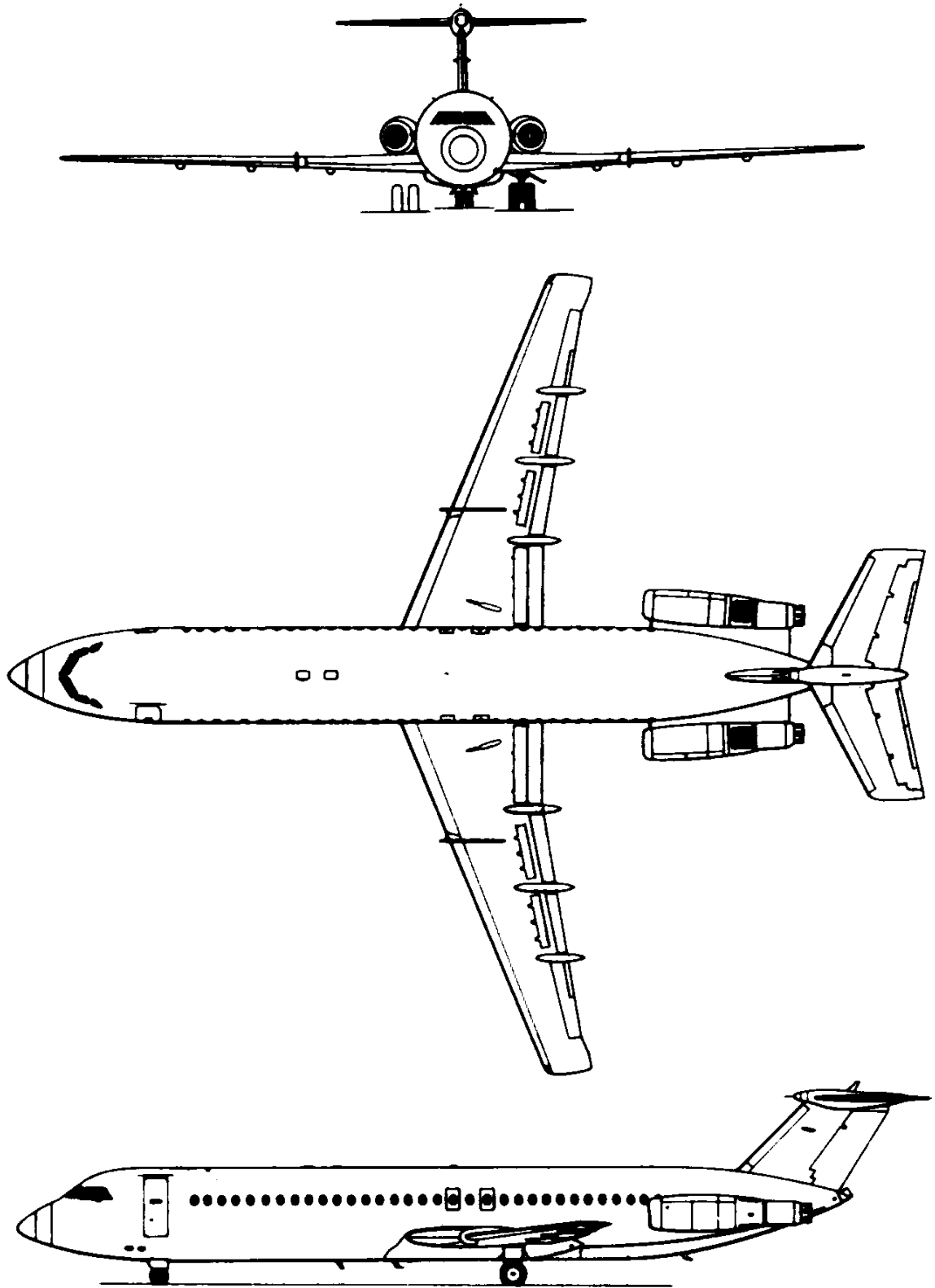


Figure A.9 Three-view drawing: BAC One –Eleven Series 500

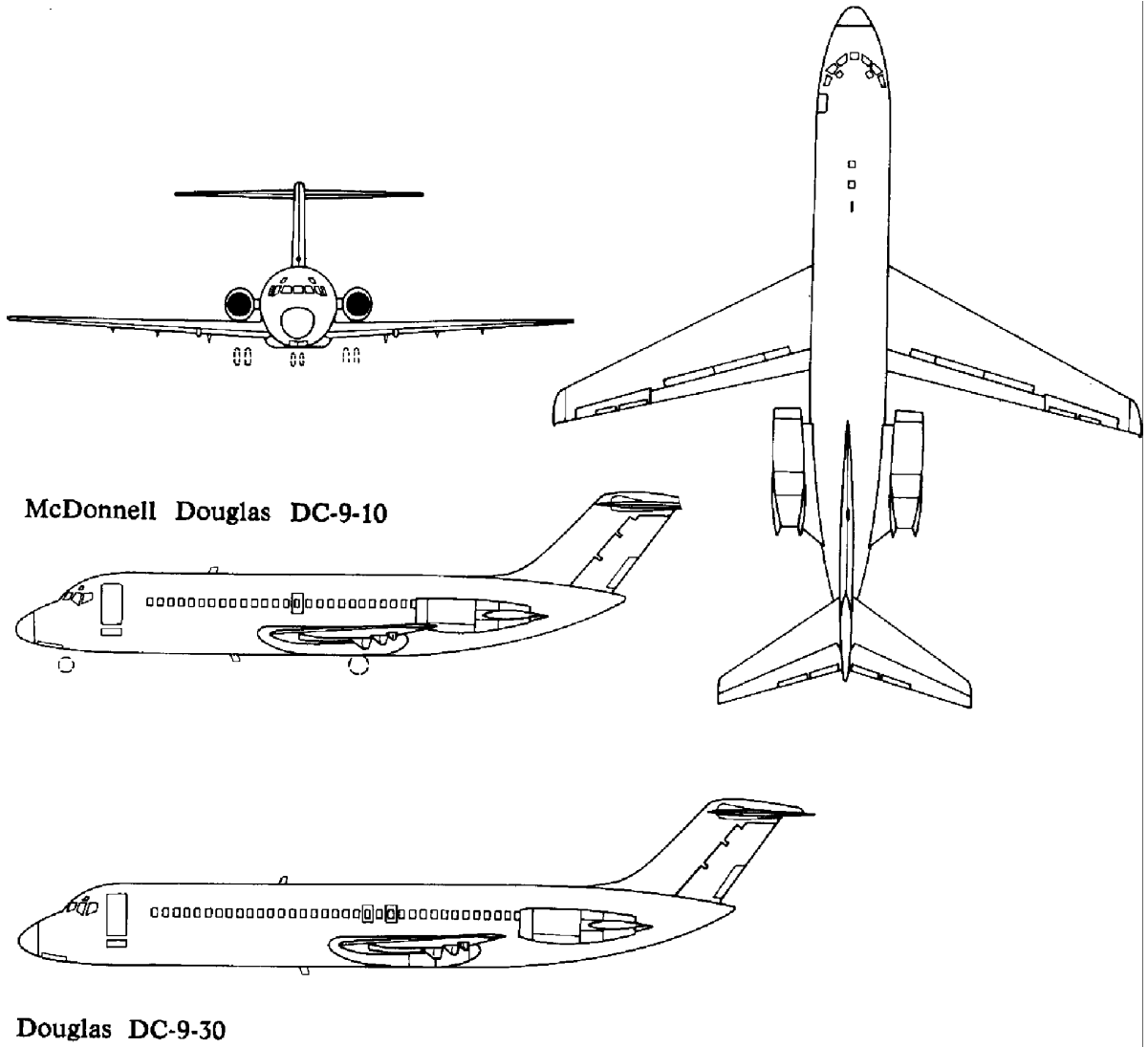


Figure A.10 Three-view drawing: McDonnell Douglas DC-9 Series 30

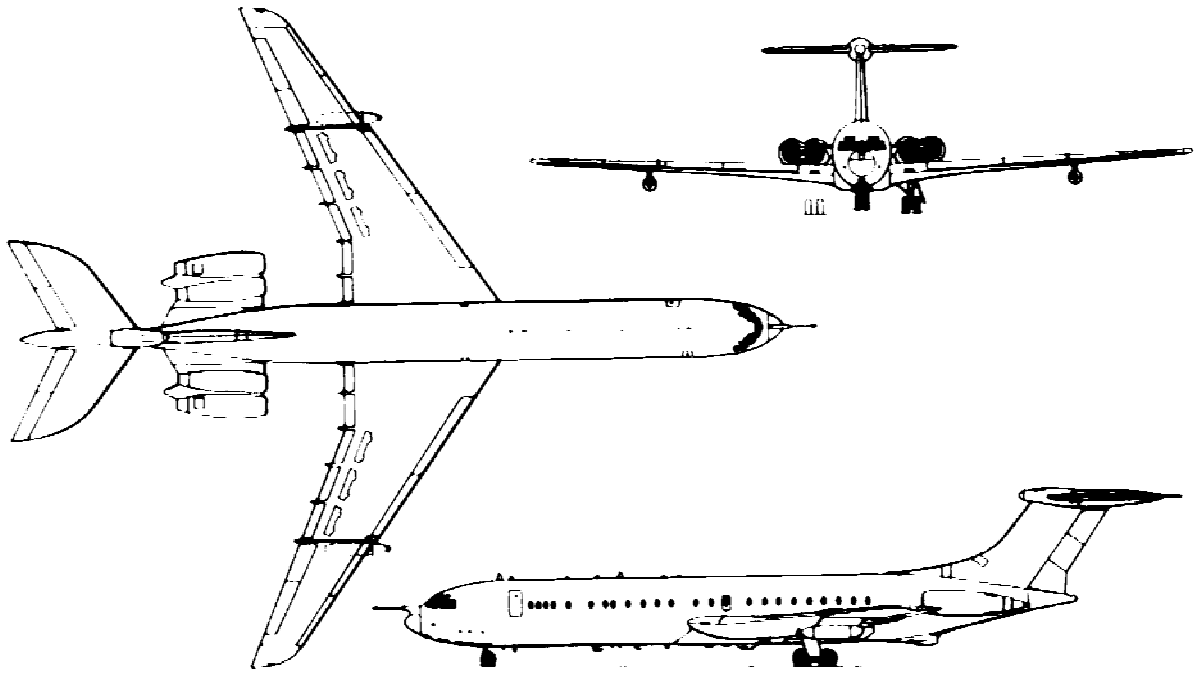


Figure A.11 Three-view drawing: Vickers Super VC10

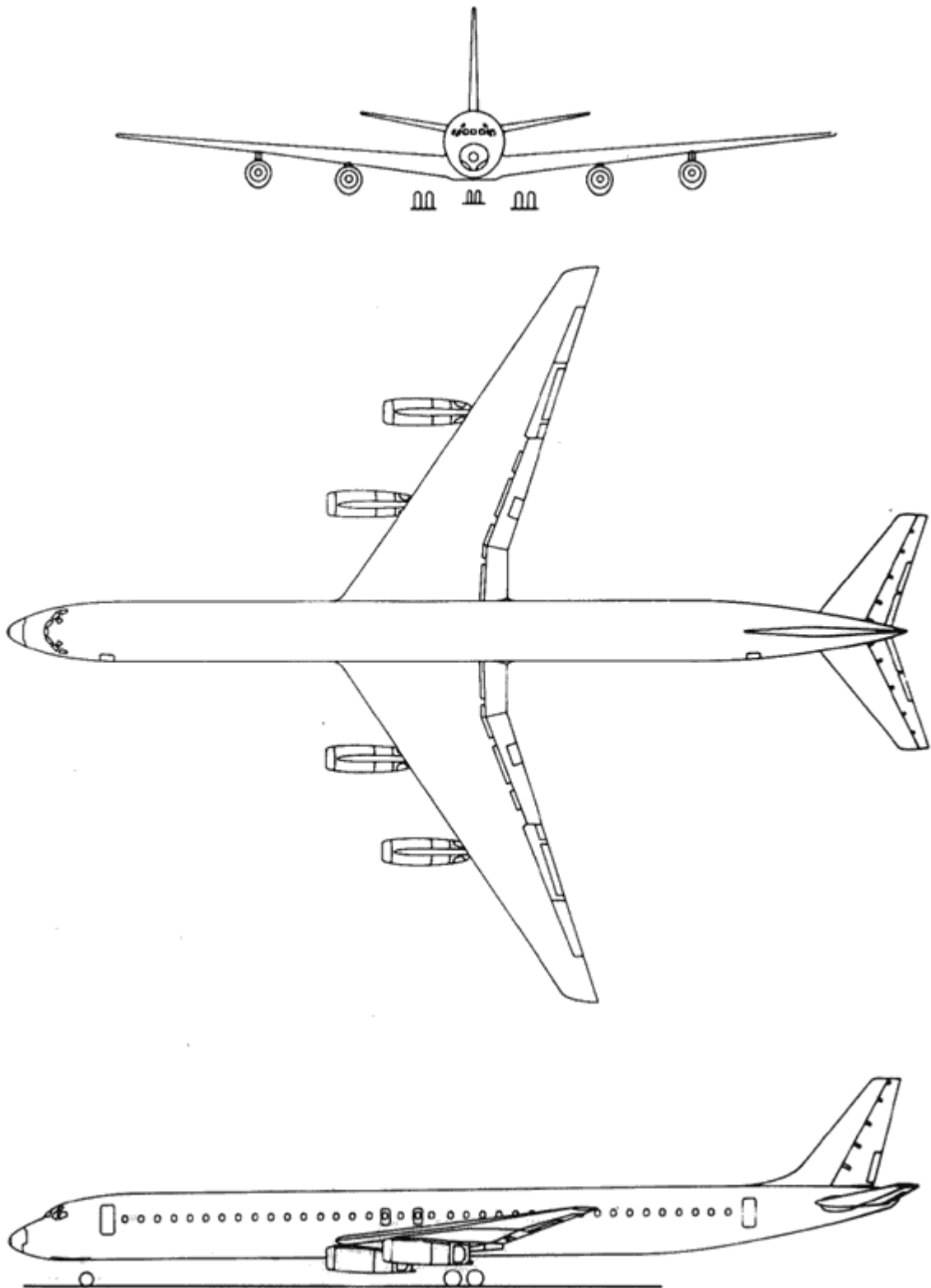


Figure A.12 Three-view drawing: McDonnell Douglas DC-8 Series 63

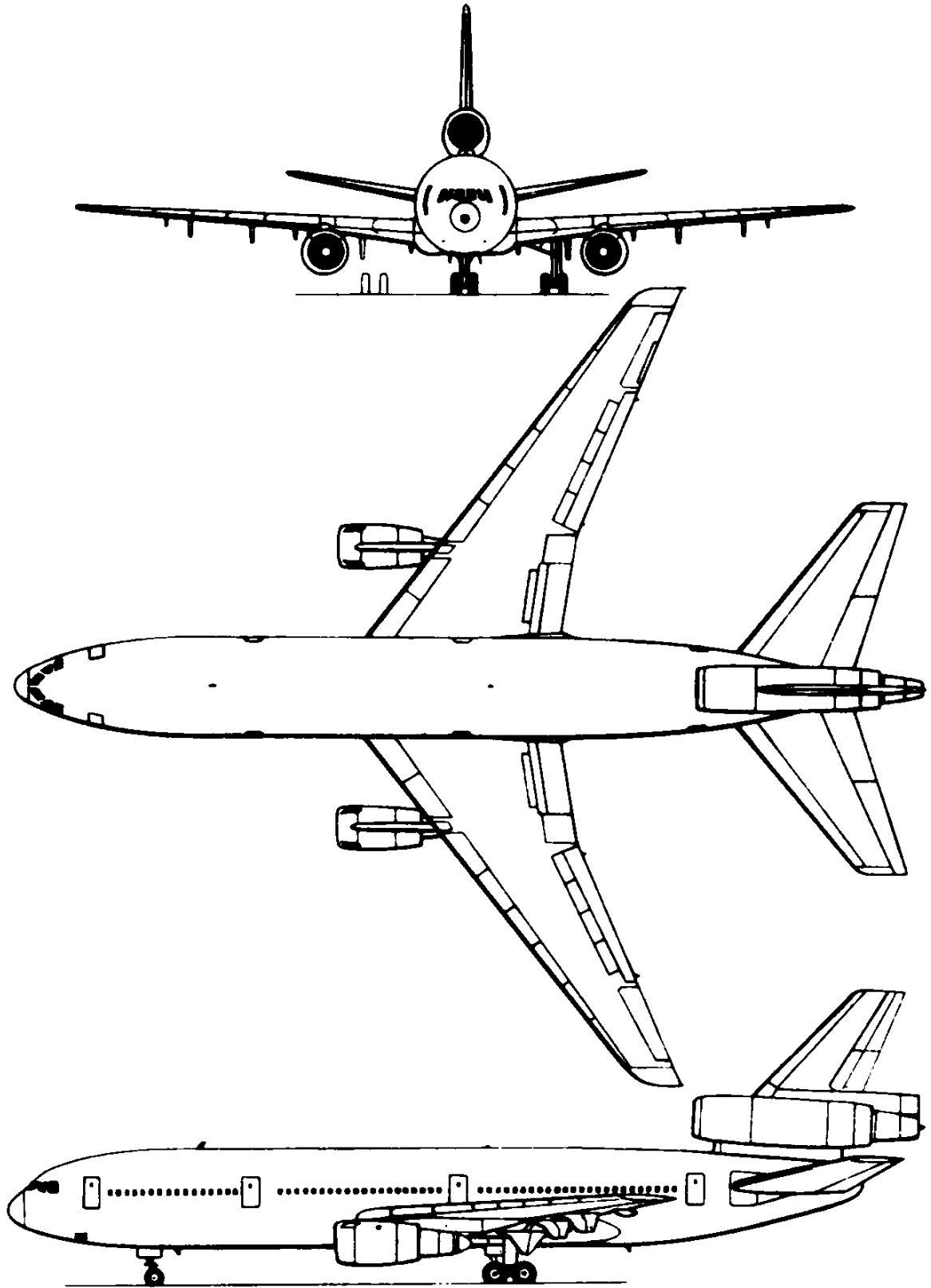


Figure A.13 Three-view drawing: McDonnell Douglas DC-10 Series 10

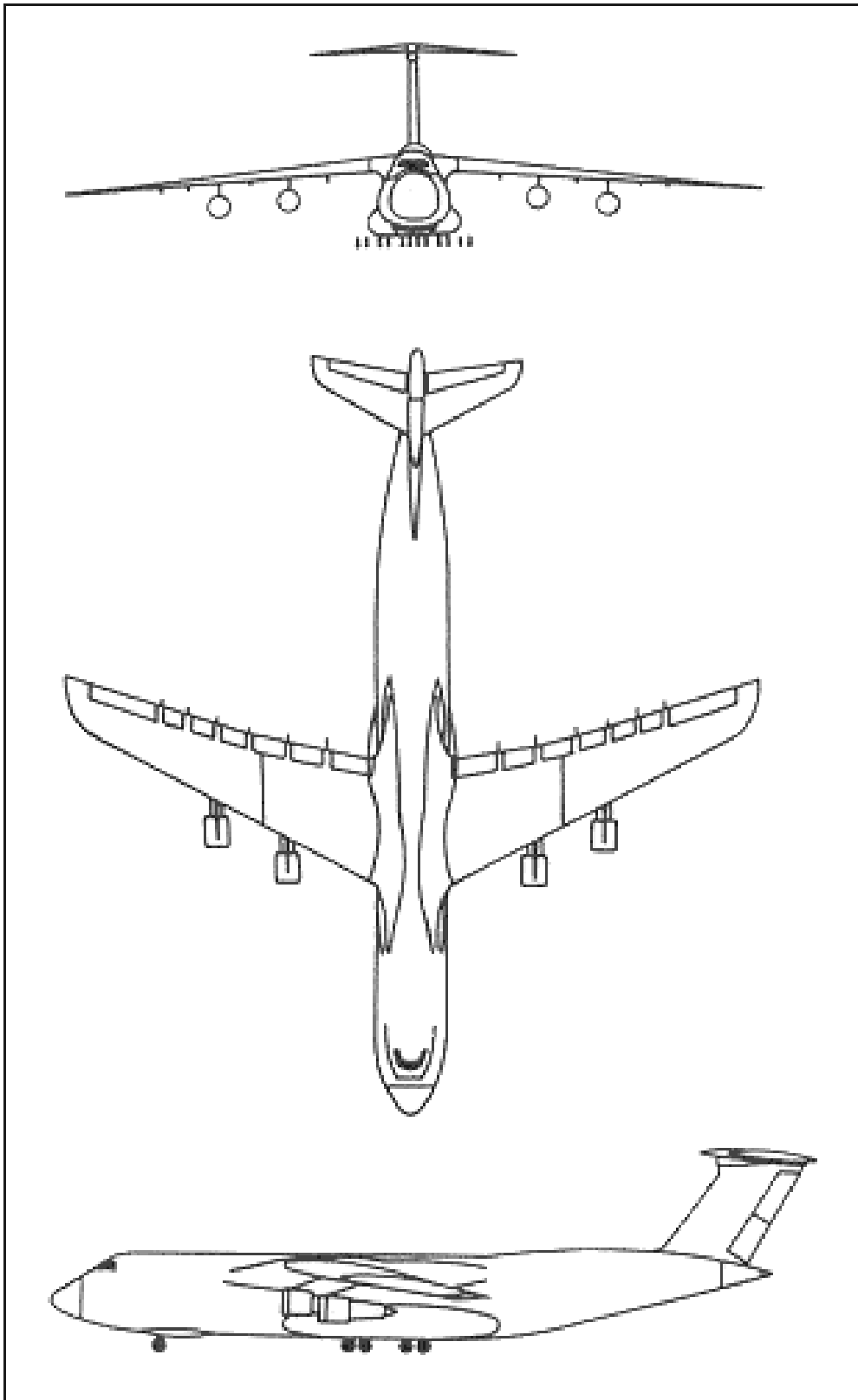


Figure A.14 Three-view drawing: Lockheed C-5A

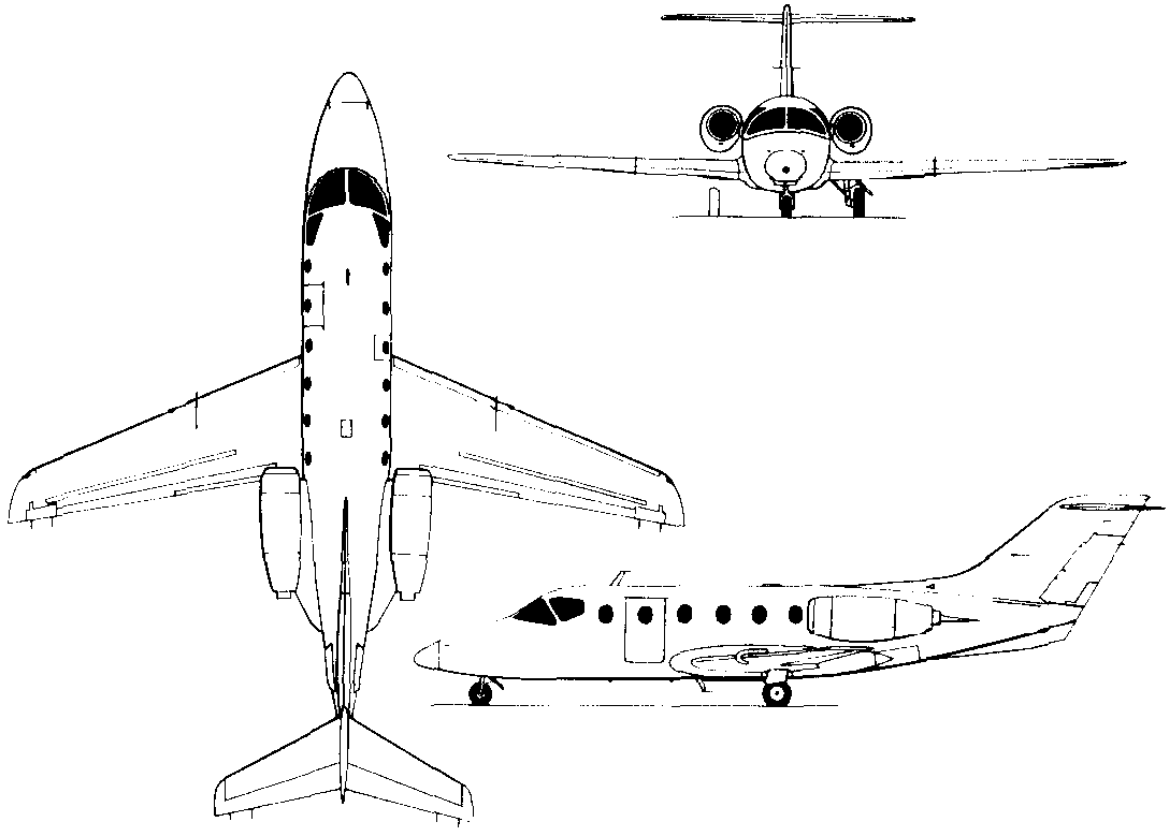


Figure A.15 Three-view drawing: Mitsubishi Diamond I

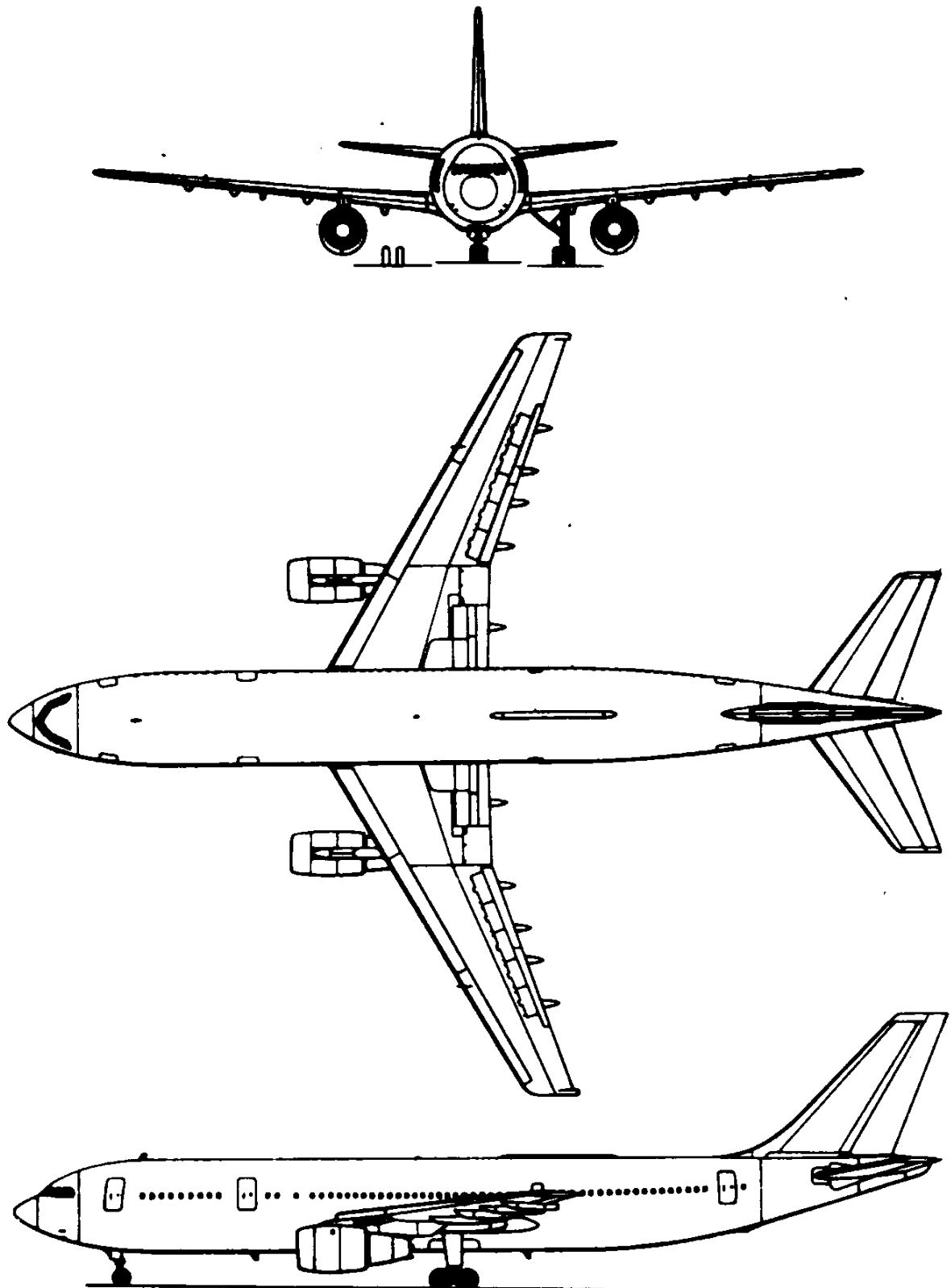


Figure A.16 Three-view drawing: Airbus A300-600

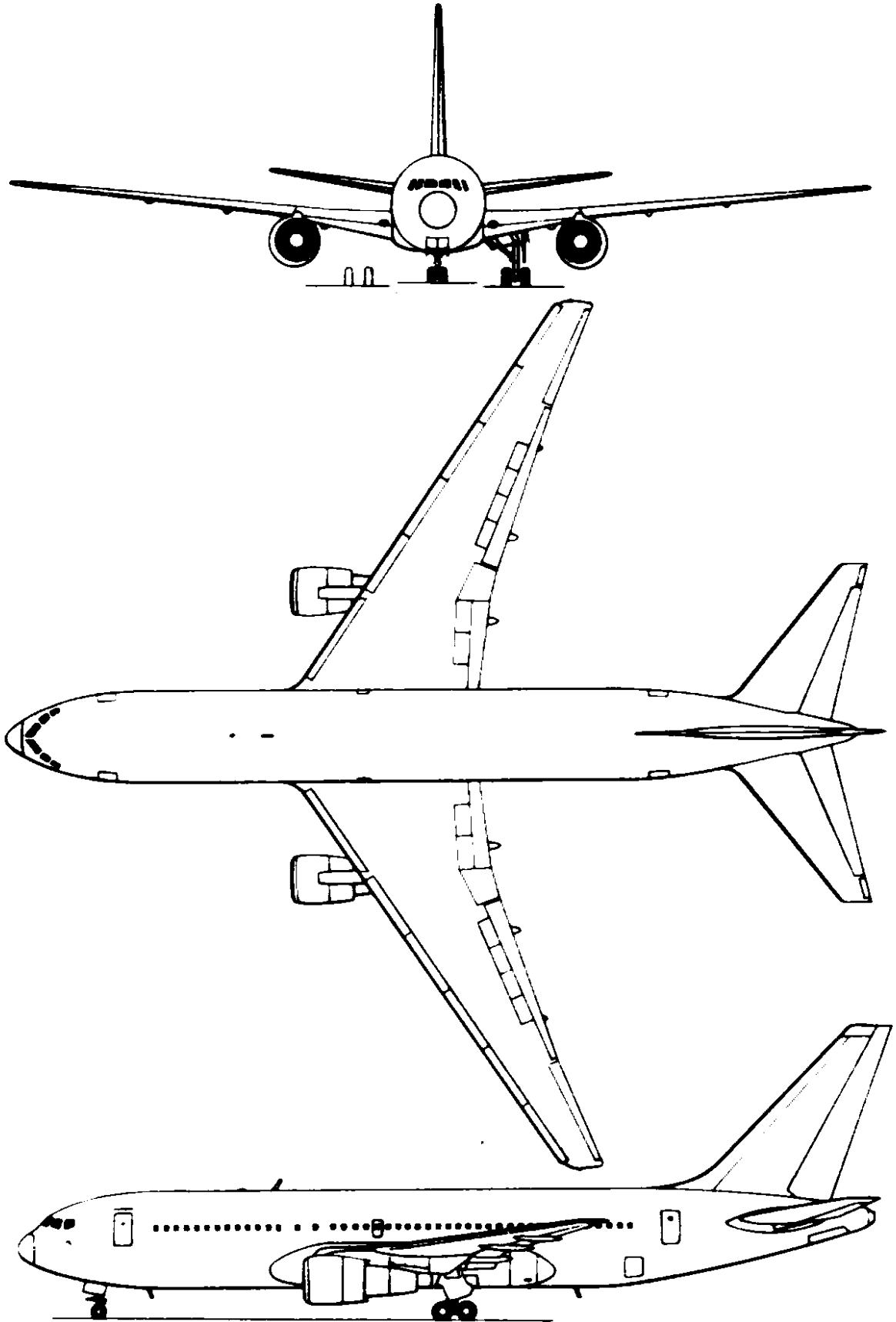


Figure A.17 Three-view drawing: Boeing 767-200

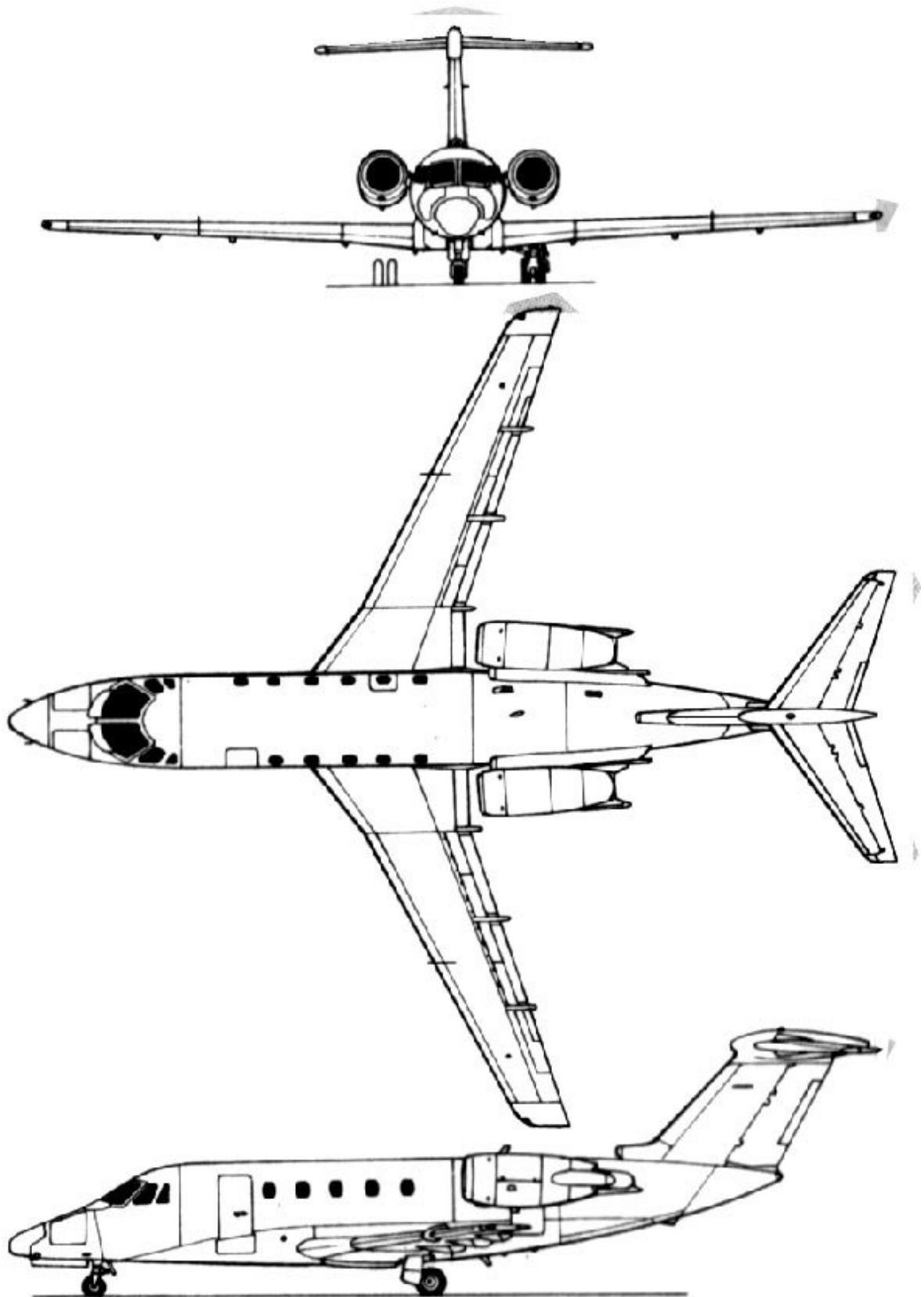


Figure A.18 Three-view drawing: Cessna 650 Citation VI

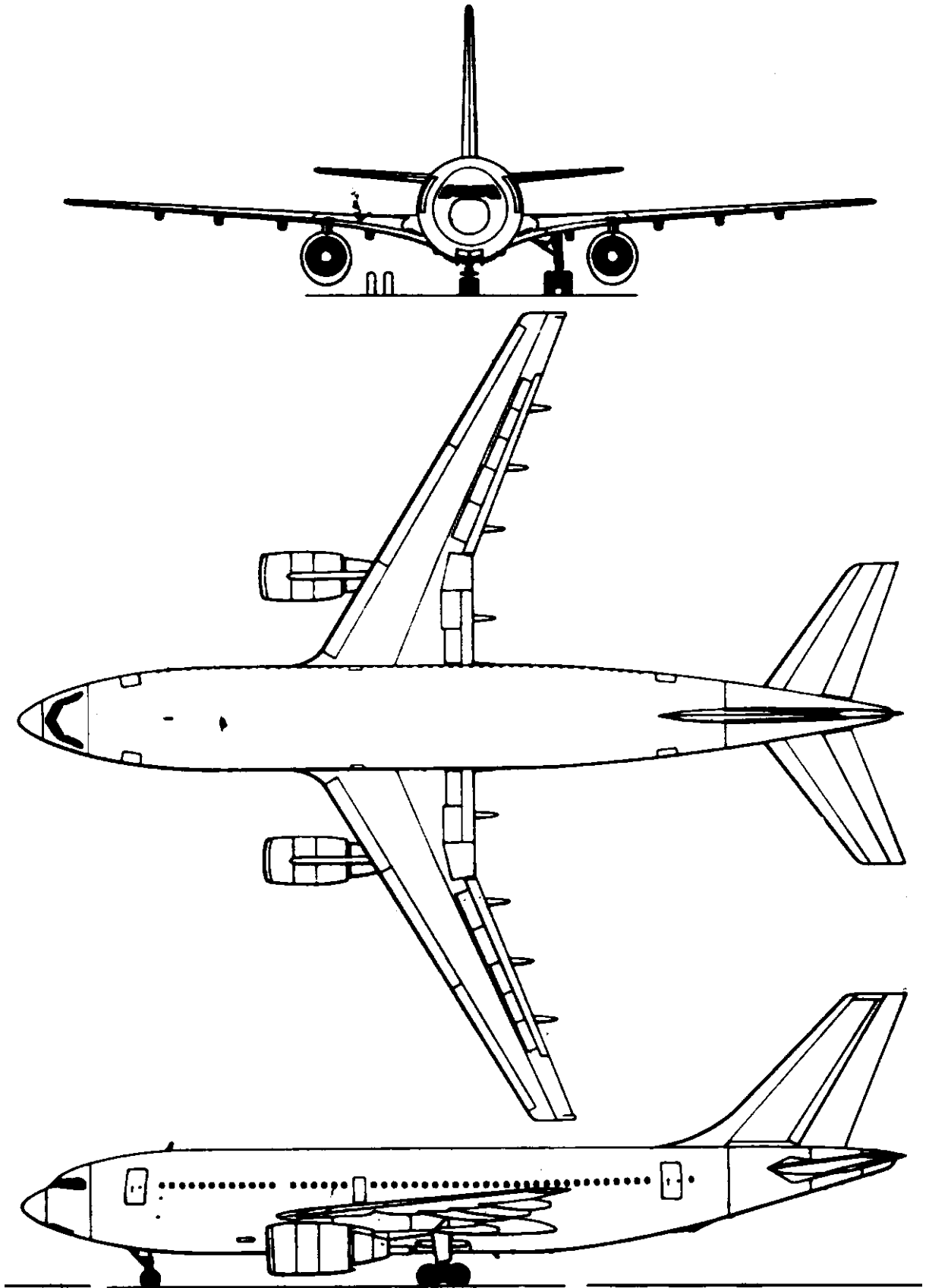


Figure A.19 Three-view drawing: Airbus A310-300

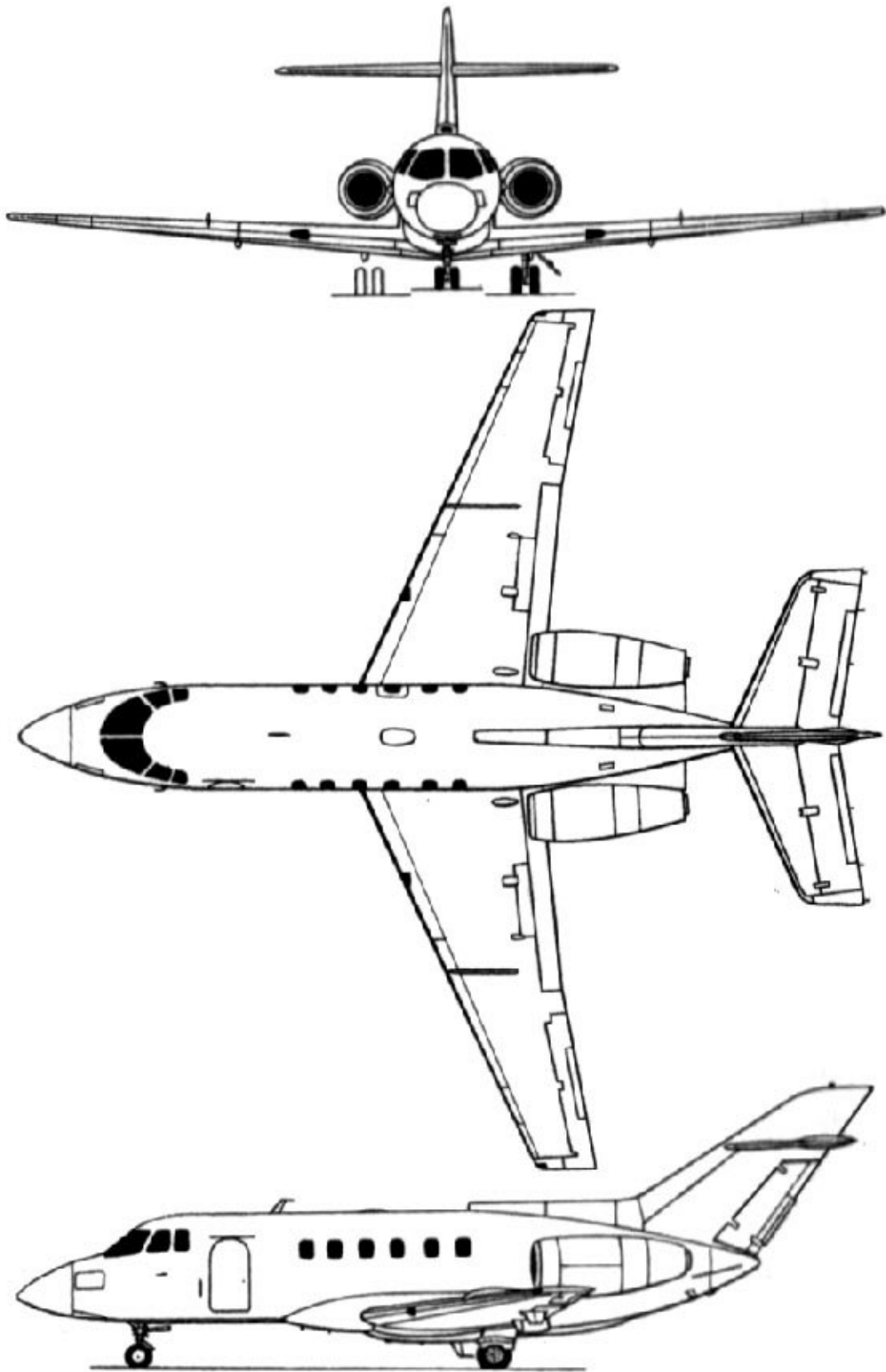


Figure A.20 Three-view drawing: Raytheon Hawker 800XP

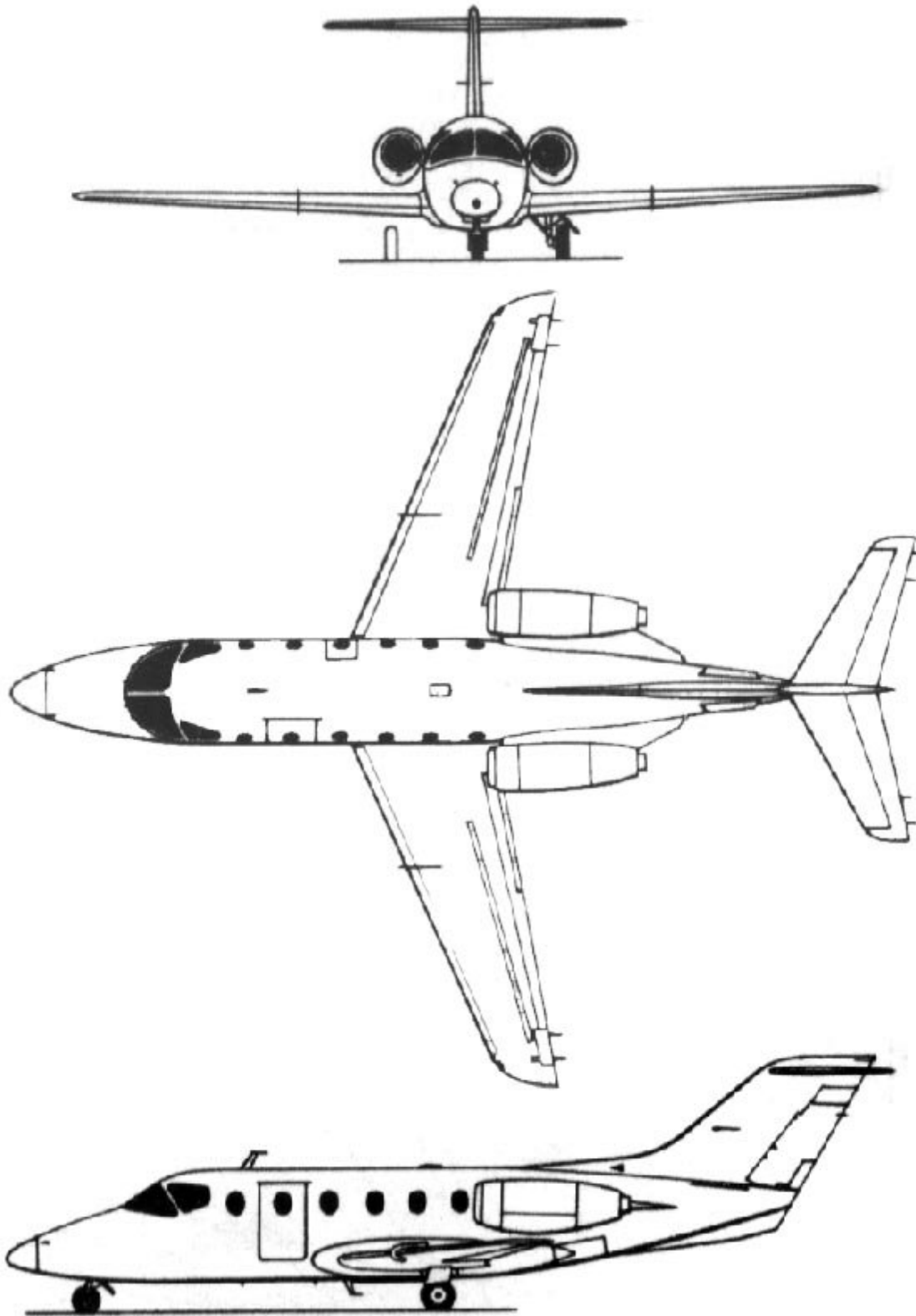


Figure A.21 Three-view drawing: Raytheon Beechjet 400A

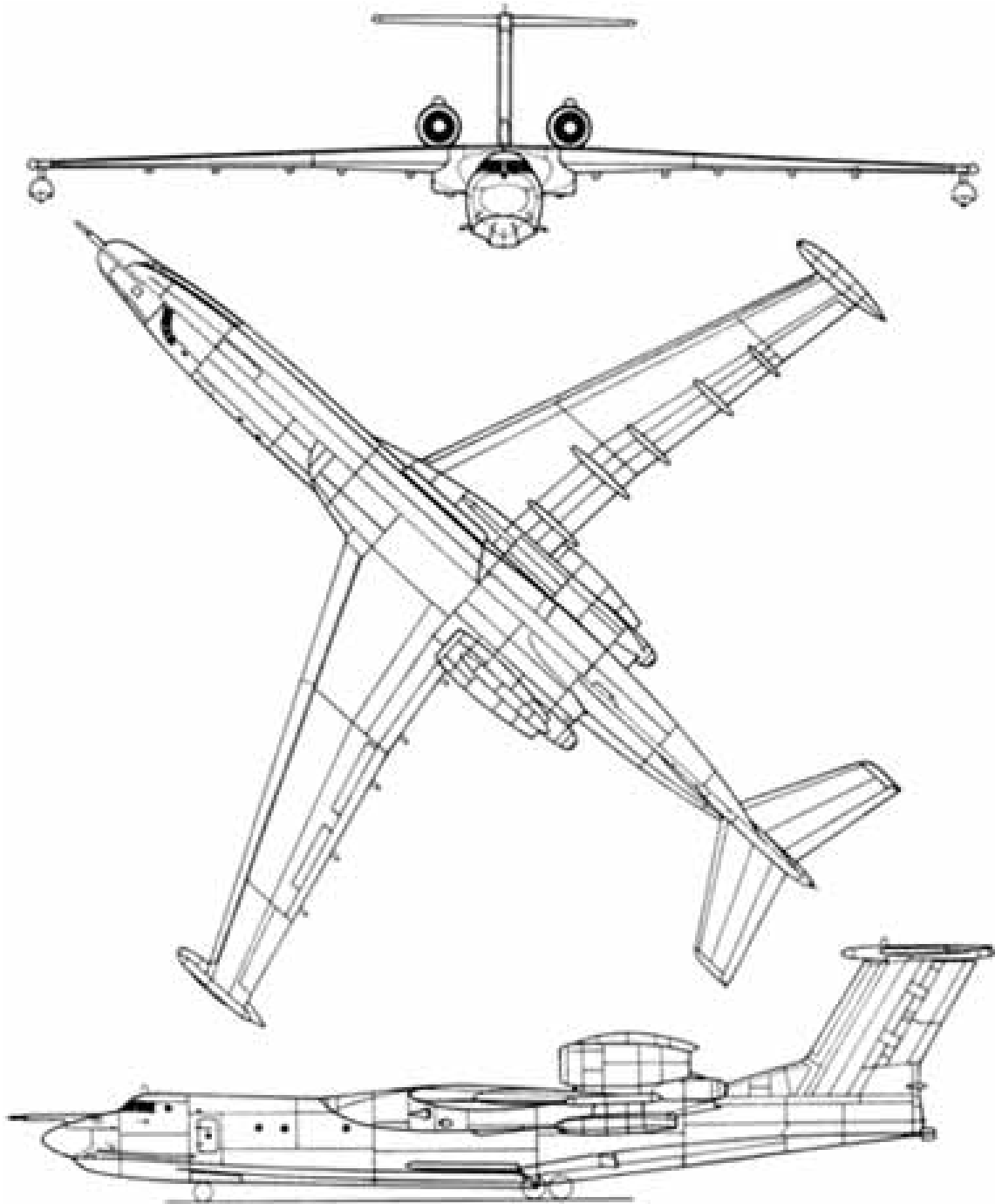


Figure A.22 Three-view drawing: Beriev Be-40

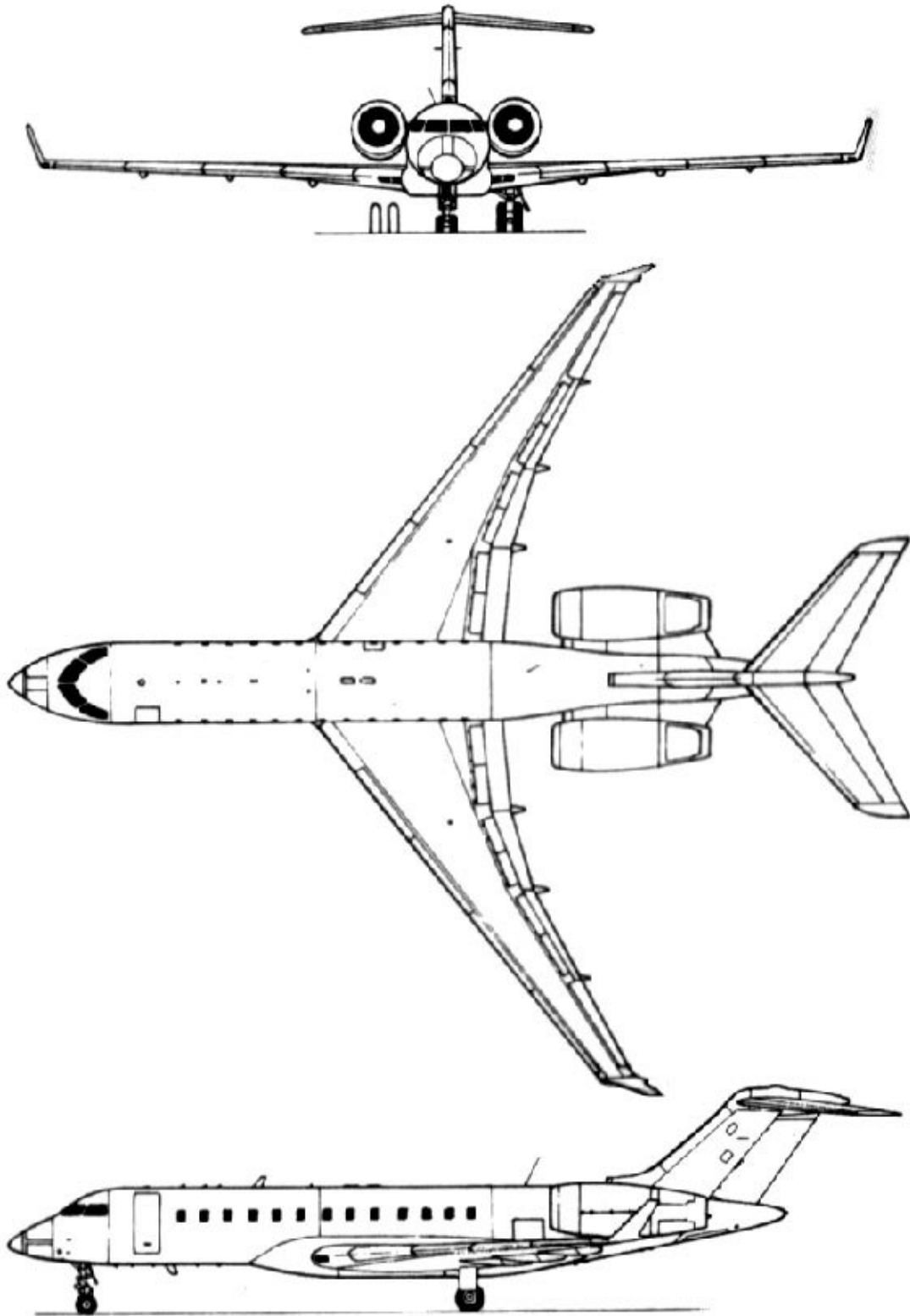


Figure A.23 Three-view drawing: Bombardier Global Express

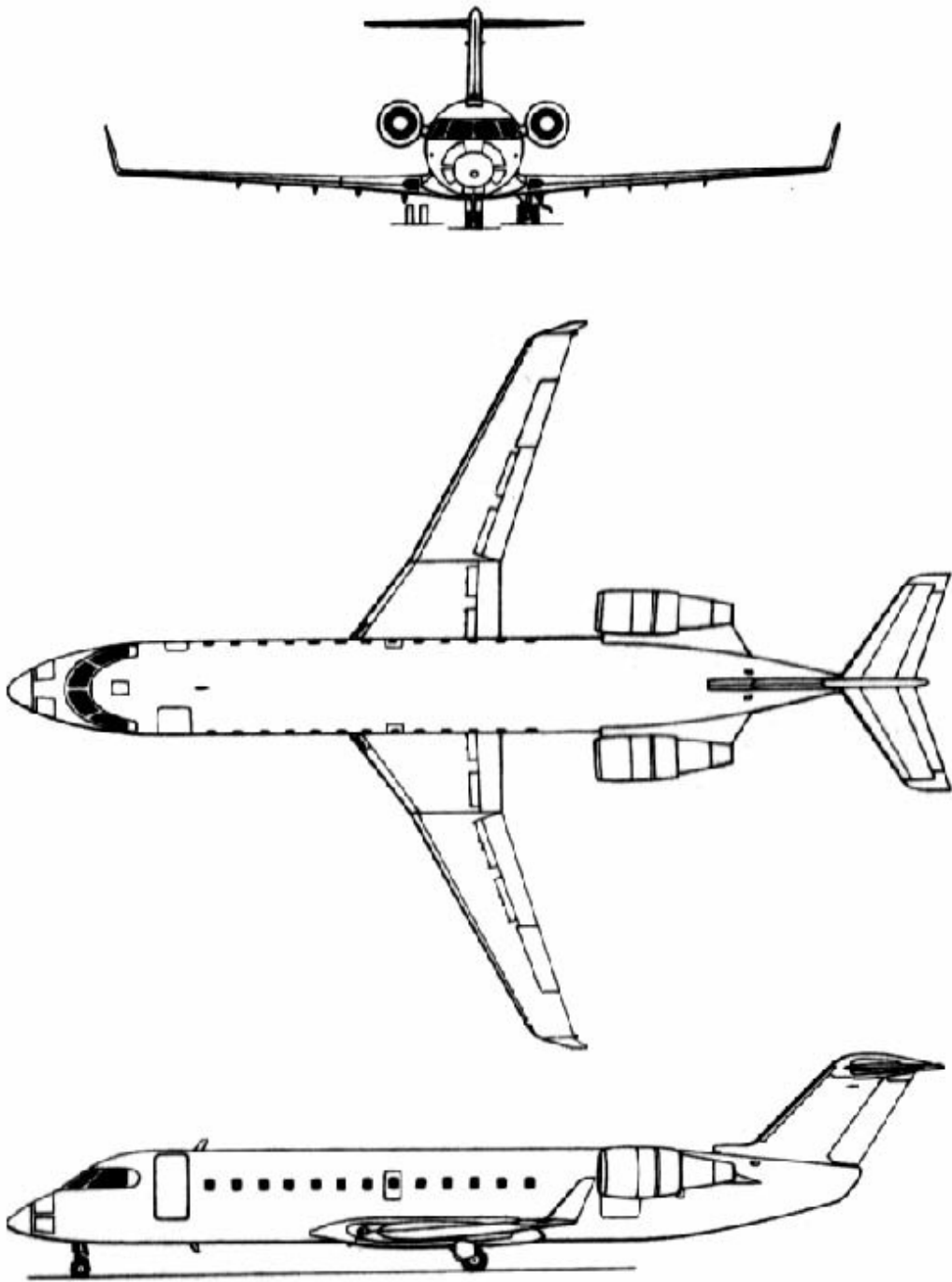


Figure A.24 Three-view drawing: Bombardier Challenger CRJ 200 LR

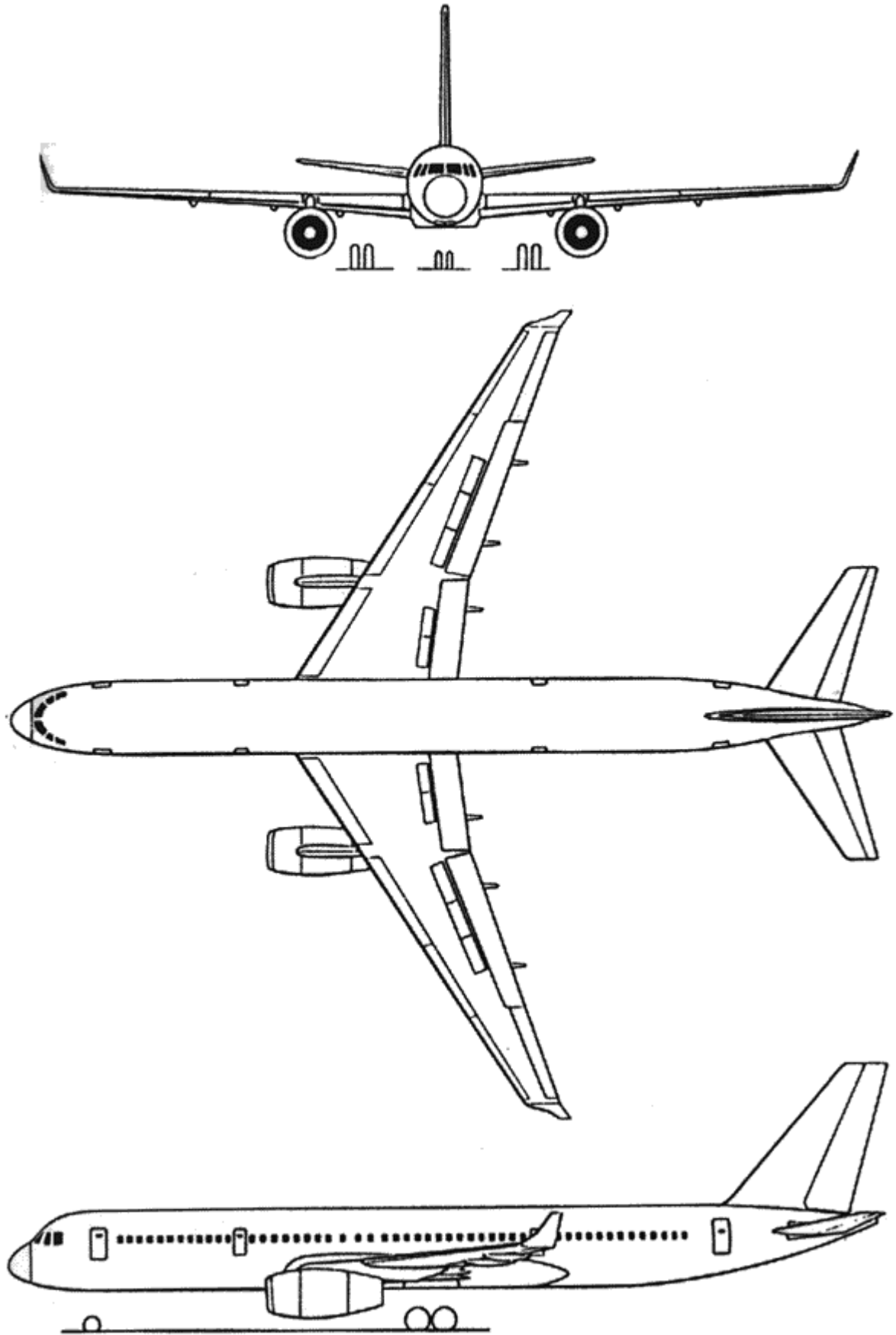


Figure A.25 Three-view drawing: Tupolev Tu-204-300

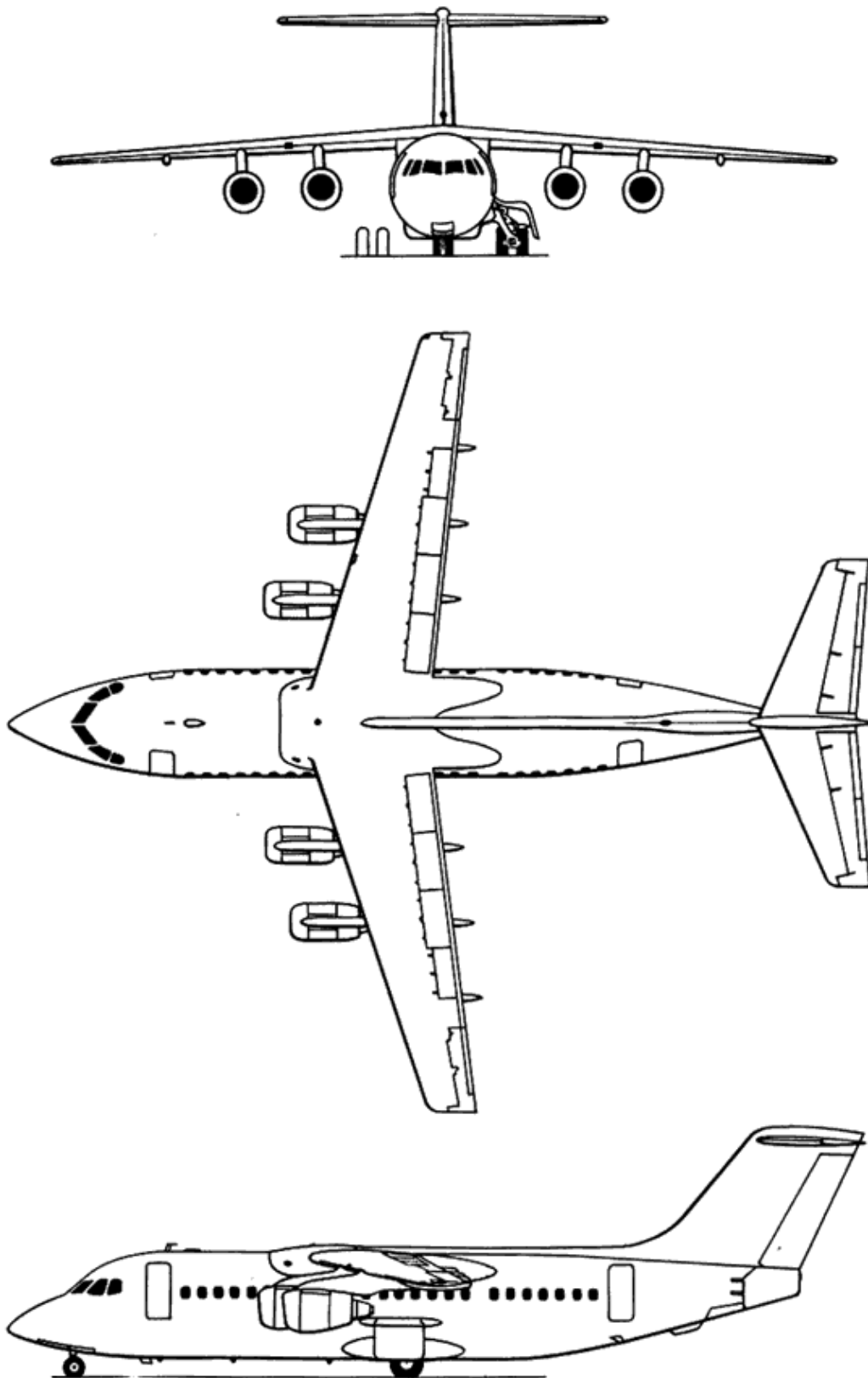


Figure A.26 Three-view drawing: BAe RJ85

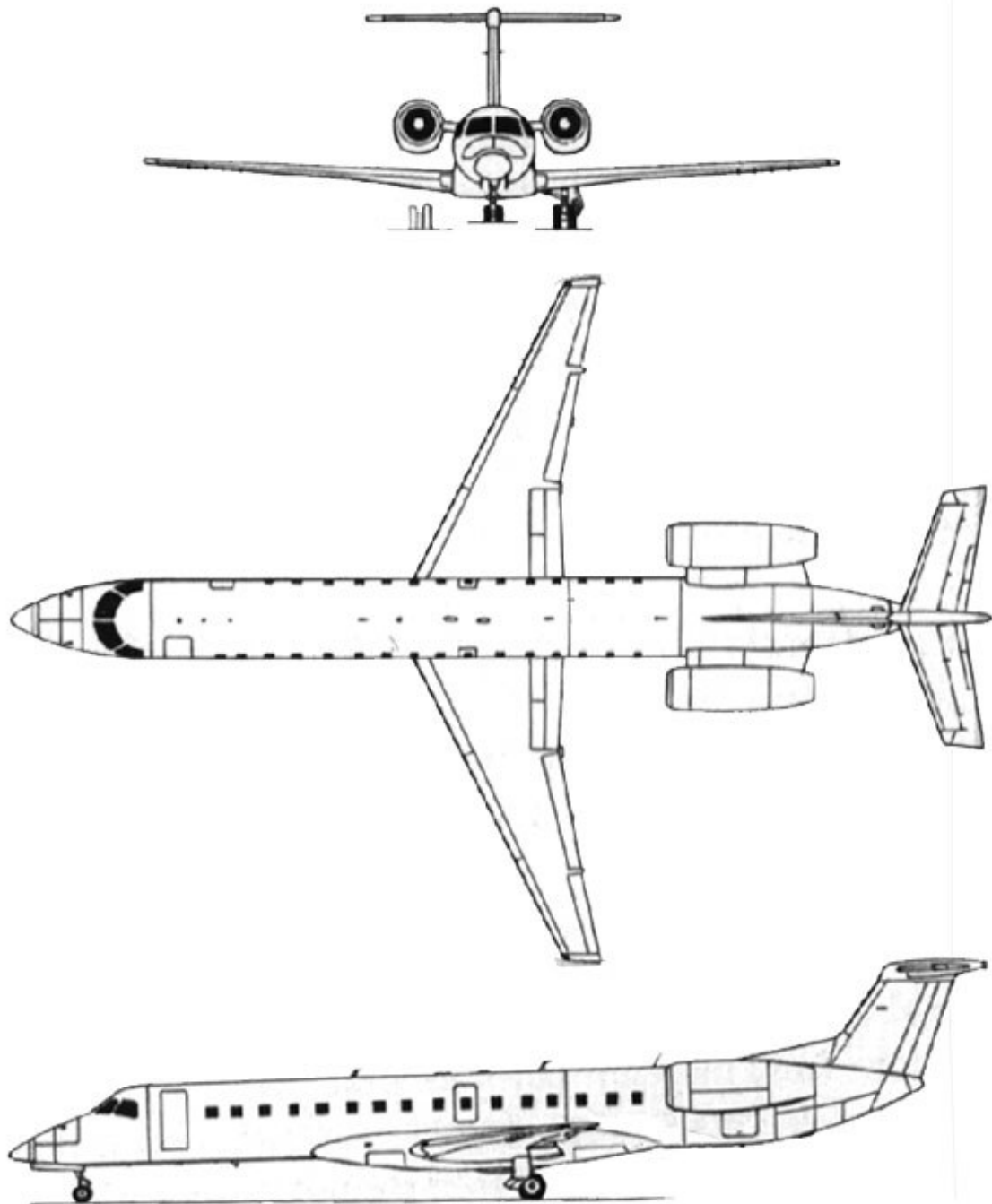


Figure A.27 Three-view drawing: Embraer EMB-145

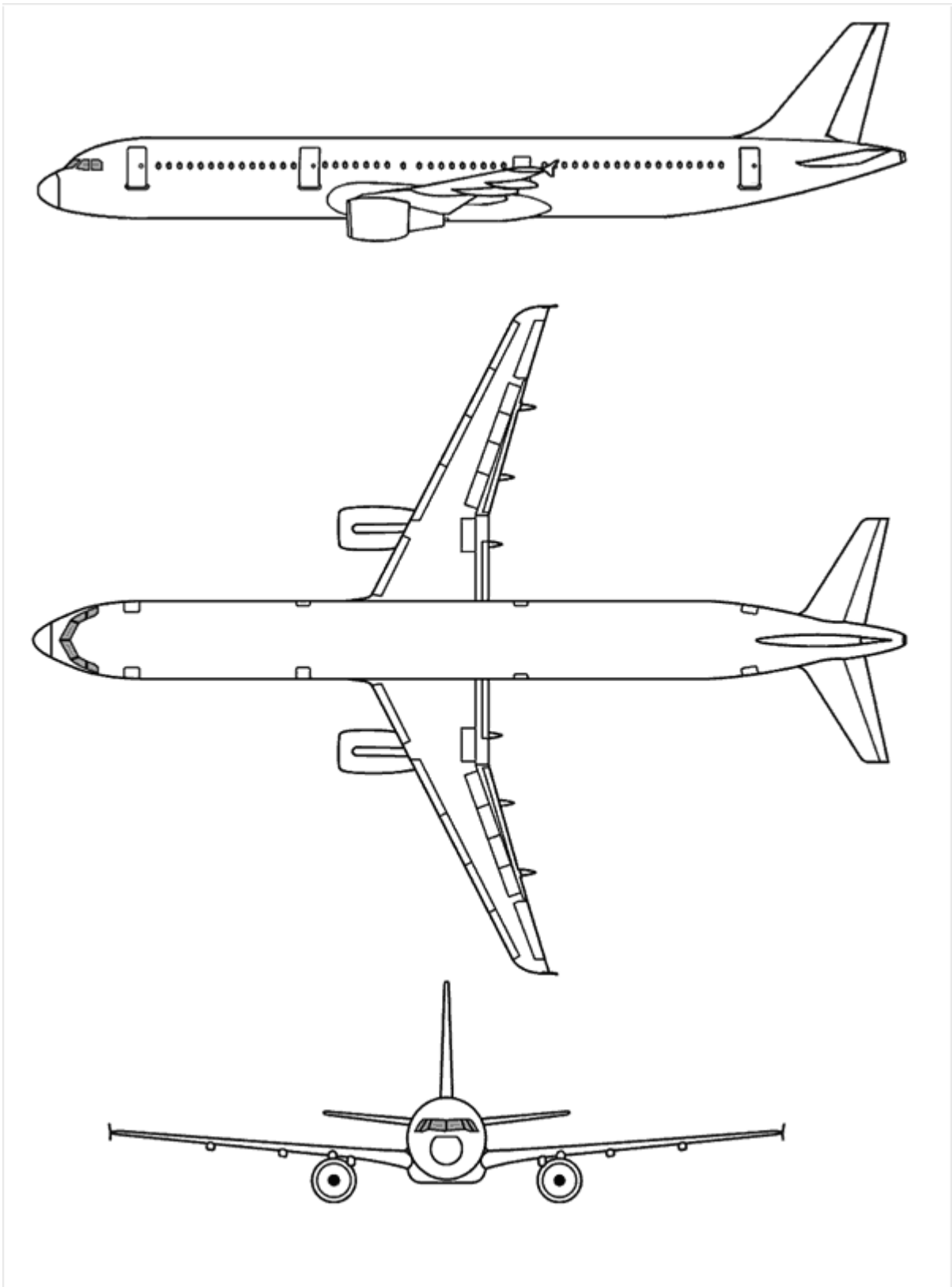


Figure A.28 Three-view drawing: Airbus A321-200

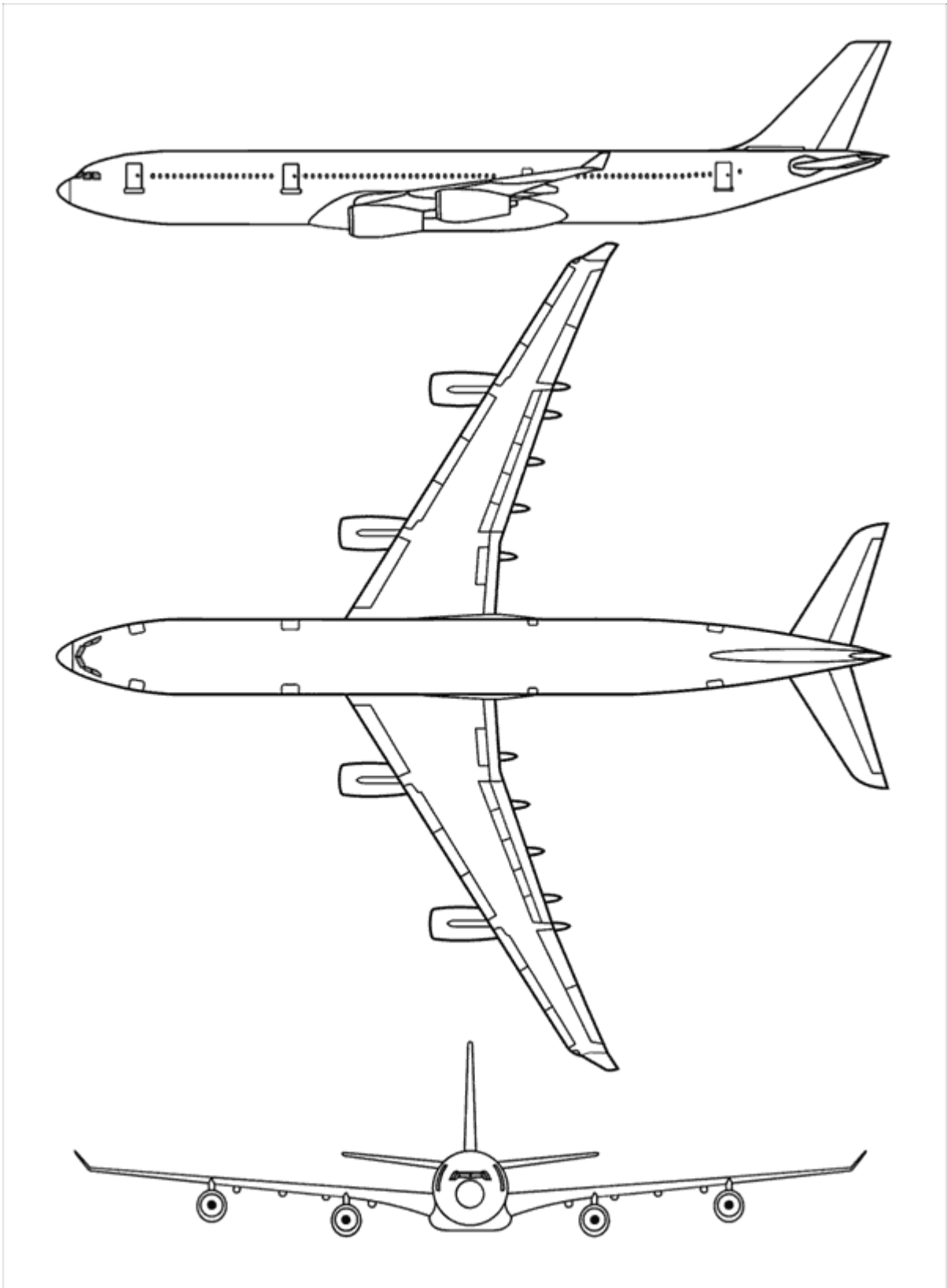


Figure A.29 Three-view drawing: Airbus A340-300

Appendix B

Investigation of Aircraft Parameters from Different Sources

Table B.1 IAI 1124A - Investigation of aircraft parameters from different sources

manufacturer type modell	IAI 1124A Westwind 2	selected	Janes 1982	Lednicer 2004	Jetside 2005
source		for calculation			
page					
wing area, S	m ²	28,64	28,64		
sweep, 1/4 chord, α	deg	4,45	4,45		
max cruise speed, V_{MO}	kt	468,7			468,7
in altitude, h	ft	19400	19400		
max. take-off mass, m_{MTO}	kg	10660	10660		10660
max op. Mach number, M_{MO}	-				
first flight	-	1963			1963
type of airfoil	-	conventional			
root airfoil	-			IAI 54-12 (Sigma 1)	
tip airfoil	-			IAI 54-12 (Sigma 1)	
t/c root	-	12,0%	12,0%		
t/c tip	-	12,0%	12,0%		
average t/c calculated from Jenkinson	-	12,0%			
average t/c given	-				
density, ρ	kg/m ³	0,666			
temperature, T	K	249,7			
speed of sound, a	m/s	316,8			
max cruise Mach number, $M_{CR,max}$	-	0,76			
cruise Mach number, M_{CR}	-	0,76			
drag divergence Mach number, M_{DD}	-	0,76			
mass cruise, m_{CR}	kg	10660			
cruise speed V_{CR}	m/s	241,1			
lift coefficient, C_L	-	0,19			
3 view drawing from					X
		Main data for further calculation			

Table B.2 Sud Aviation Caravelle - Investigation of aircraft parameters from different sources

manufacturer type modell	Sud Aviation Caravelle	selected	Torenbeek 1988	Airliners 2005	Bechtermünz 1998	Jetside 2005	Obert 1997	CS-25 2003	Remark
source		for calculation	220		20		298	25.1441	
wing area, S	m ²	146,7		146,7	146,7				
sweep, 1/4 chord, α_{25}	deg	20	20				20		
max cruise speed, V_{MO}	kt	445,5			445,5				
in altitude, h	ft	18000 *							40000 Caravelle does' t use oxygen equipment
max. take-off mass, m_{MTO}	kg	56000		56000	58000	56000			Therefore cruise altitude is limited to
max op. Mach number, M_{MO}	-	0,81	0,81			0,82			40000 ft following CS-25.1441.
first flight	-	1955	1955		1955	1955			
type of airfoil	-	conventional							
root airfoil	-		NACA 65-212				NACA 64-212		
tip airfoil	-		NACA 65-212				NACA 64-212		
t/c root	-	12,0%							
t/c tip	-	12,0%							
average t/c calculated from Jenkinson	-	12,0%							
average t/c given	-								
density, ρ	kg/m ³	0,698							
temperature, T	K	252,5							
speed of sound, a	m/s	318,5							
max cruise Mach number, $M_{CR,max}$	-	0,72							
cruise Mach number, M_{CR}	-	0,72							
drag divergence Mach number, M_{DD}	-	0,72							
mass cruise, m_{CR}	kg	56000							
cruise speed V_{CR}	m/s	229,2							
lift coefficient, C_L	-	0,20					0,20		
3 view drawing from									X
			Main data for further calculation						
remark			* cruise altitude chosen to fit C_L from Obert 1997						

Table B.3 VFW 614 - Investigation of aircraft parameters from different sources

manufacturer type modell	VFW 614	selected	VFW 2004	Torenbeek 1988	Lednicer 2004
source		for calculation		220	
page					
wing area, S	m ²	64	64		
sweep, 1/4 chord, α_s	deg	15		15	
max cruise speed, V_{MO}	kt	421,2	421,2		
in altitude, h	ft	21000	21000		
max. take-off mass, m_{MTO}	kg	19950	19950		
max op. Mach number, M_{MO}	-	0,65		0,65	
first flight	-	1971	1971	1971	
type of airfoil	-	conventional			
root airfoil	-			NACA 63 ₂ A015	NACA 63A015
tip airfoil	-			NACA 65 ₁ A012	NACA 65A012
t/c root	-	15,0%			
t/c tip	-	12,0%			
average t/c calculated from Jenkinson	-	12,8%			
average t/c given	-				
density, ρ	kg/m ³	0,631			
temperature, T	K	246,5			
speed of sound, a	m/s	314,8			
max cruise Mach number, $M_{CR,max}$	-	0,69			
cruise Mach number, M_{CR}	-	0,65			
drag divergence Mach number, M_{DD}	-	0,65			
mass cruise, m_{CR}	kg	19950			
cruise speed V_{CR}	m/s	204,6			
lift coefficient, C_L	-	0,23			

3 view drawing from

X

Main data for further calculation

Table B.4 HFB 320 - Investigation of aircraft parameters from different sources

manufacturer type modell	HFB 320	selected for calculation	Flugzeugtypen 2005	Torenbeek 1988	Lednicer 2004	Ebert 1973	HFB 2005
source page				220			
wing area, S	m ²	30,1	30,1				30,14
sweep, 1/4 chord, α_s	deg	15		-15			-15
max cruise speed, V_{MO}	kt	445,5	459,0				445,5
in altitude, h	ft	37402	38058			37402	
max. take-off mass, m_{MTO}	kg	9200	8500			9200	9200
max op. Mach number, M_{MO}	-						
first flight	-	1964		1964		1964	
type of airfoil	-	conventional					
root airfoil	-			NACA 65A-1,5-13	NACA 65A(1.5)13		
tip airfoil	-			NACA 63A-1,8-11	NACA 63A(1.8)11		
t/c root	-	13,0%					
t/c tip	-	11,0%					
average t/c calculated from Jenkinson	-	11,5%					
average t/c given	-						
density, ρ	kg/m ³	0,342					
temperature, T	K	216,7					
speed of sound, a	m/s	295,1					
max cruise Mach number, $M_{CR,max}$	-	0,78					
cruise Mach number, M_{CR}	-	0,78					
drag divergence Mach number, M_{DD}	-	0,78					
mass cruise, m_{CR}	kg	9200					
cruise speed V_{CR}	m/s	229,2					
lift coefficient, C_L	-	0,33					

3 view drawing from

Main data for further calculation

X

Table B.5 Gates Lear Jet Model 23 - Investigation of aircraft parameters from different sources

manufacturer	Gates		selected	Bechtermünz 1998	Torenbeek 1988	Lednicer 2004	Escalona 2005
type	Lear Jet		for calculation				
modell	Model 23						
source							
page				559	220		
wing area, S	m ²		21,46	21,46			
sweep, 1/4 chord, α_s	deg		13		13		
max cruise speed, V_{MO}	kt		488	488			
in altitude, h	ft		23999	23999			
max. take-off mass, m_{MTO}	kg		5670	5670			
max op. Mach number, M_{MO}	-		0,765		0,765		
first flight	-		1963	1963	1969		
type of airfoil	-		conventional				
root airfoil	-				NACA 64A 109	NACA 64A109	
tip airfoil	-				NACA 64A 109	NACA 64A109 mod	
t/c root	-		9,0%				
t/c tip	-		9,0%				
average t/c calculated from Jenkinson	-		9,0%				
average t/c given	-						
density, ρ	kg/m ³		0,569				
temperature, T	K		240,6				
speed of sound, a	m/s		311,0				
max cruise Mach number, $M_{CR,max}$	-		0,81				
cruise Mach number, M_{CR}	-		0,765				
drag divergence Mach number, M_{DD}	-		0,765				
mass cruise, m_{CR}	kg		5670				
cruise speed V_{CR}	m/s		237,9				
lift coefficient, C_L	-		0,16				

3 view drawing from

Main data for further calculation

X

Table B.6 Lockheed C-141 Starlifter - Investigation of aircraft parameters from different sources

manufacturer type modell	Lockheed C-141 Starlifter	selected	Bechtermünz 1998	Torenbeek 1988	Lednicer 2004	Flugzeugtypen 2005	USAF 2004a	Escalona 2005
source page		for calculation	575	220				
wing area, S	m ²	299,88	299,88			299,8		
sweep, 1/4 chord, α_s	deg	25		25				
max cruise speed, V_{MO}	kt	497	491			496,8		
in altitude, h	ft	26247				26247		
max. take-off mass, m_{MTO}	kg	143610	155582			143610	146863	
max op. Mach number, M_{MO}	-	0,74					0,74	
first flight	-	1963		1963			1964	
type of airfoil	-	conventional						
root airfoil	-			NACA 0013 mod	NACA 0013 mod			
tip airfoil	-			NACA 0010 mod	NACA 0011 mod			
t/c root	-	13,0%						
t/c tip	-	11,0%						
average t/c calculated from Jenkinson	-	11,5%						
average t/c given	-							
density, ρ	kg/m ³	0,525						
temperature, T	K	236,2						
speed of sound, a	m/s	308,1						
max cruise Mach number, $M_{CR,max}$	-	0,83						
cruise Mach number, M_{CR}	-	0,74						
drag divergence Mach number, M_{DD}	-	0,74						
mass cruise, m_{CR}	kg	143610						
cruise speed V_{CR}	m/s	228,0						
lift coefficient, C_L	-	0,34						

3 view drawing from



Main data for further calculation

X

Table B.7 Lockheed Jetstar II - Investigation of aircraft parameters from different sources

manufacturer	Lockheed				
type	Jetstar				
modell	II				
source		selected	Bechtermünz 1998	Torenbeek 1988	Lednicer 2004 Escalona 2005
page		for calculation	581	220	
wing area, S	m ²	50,4	50,4		
sweep, 1/4 chord, α_s	deg	30		30	
max cruise speed, V_{MO}	kt	475	475		
in altitude, h	ft	30003	30003		
max. take-off mass, m_{MTO}	kg	20185	20185		
max op. Mach number, M_{MO}	-			0,87	
first flight	-	1957	1957	1957	
type of airfoil	-	conventional			
root airfoil	-			NACA 63A112	NACA 63A112
tip airfoil	-			NACA 63A309	NACA 63A309
t/c root	-	13,0%			
t/c tip	-	11,0%			
average t/c calculated from Jenkinson	-	11,5%			
average t/c given	-				
density, ρ	kg/m ³	0,458			
temperature, T	K	228,7			
speed of sound, a	m/s	303,2			
max cruise Mach number, $M_{CR,max}$	-	0,81			
cruise Mach number, M_{CR}	-	0,81			
drag divergence Mach number, M_{DD}	-	0,81			
mass cruise, m_{CR}	kg	20185			
cruise speed V_{CR}	m/s	244,4			
lift coefficient, C_L	-	0,29			

3 view drawing from

Main data for further calculation

X

Table B.8 Dassault Falcon 20 - Investigation of aircraft parameters from different sources

manufacturer type modell	Dassault Falcon 20	follow on model:				
		Falcon 200	Falcon 200	Falcon 20	Falcon 20F	Falcon 20
source		selected	Janes 1982	Lednicer 2004	Bechtermünz 1998	Jetsite 2005
page		for calculation	67		306	
wing area, S	m ²	41	41		41	
sweep, 1/4 chord, α_s	deg	30	30			
max cruise speed, V_{MO}	kt	466	460		466	466
in altitude, h	ft	25000	33000		25000	
max. take-off mass, m_{MTO}	kg	13000	13900		13000	13000
max op. Mach number, M_{MO}	-		0,80			
first flight	-	1963	1983		1963	1963
type of airfoil	-	conventional				
root airfoil	-			NACA 64A010 ?	Falcon 200 got	
tip airfoil	-			NACA 64A108 mod ?	new wing tips	
t/c root	-	10,5%	10,5%	10,0%		
t/c tip	-	8,0%	8,0%	8,0%		
average t/c calculated from Jenkinson	-	9,9%		9,5%		
average t/c given	-					
density, ρ	kg/m ³	0,549				
temperature, T	K	238,6				
speed of sound, a	m/s	309,7				
max cruise Mach number, $M_{CR,max}$	-	0,77				
cruise Mach number, M_{CR}	-	0,77				
drag divergence Mach number, M_{DD}	-	0,77				
mass cruise, m_{CR}	kg	13000				
cruise speed V_{CR}	m/s	239,7				
lift coefficient, C_L	-	0,20				

3 view drawing from


Main data for further calculation

X

Table B.9 BAC One-Eleven Series 500 - Investigation of aircraft parameters from different sources

manufacturer type modell	BAC One-Eleven Series 500	selected for calculation	Janes 1982	Lednicer 2004	Torenbeek 1988	Bechtermünz 1998	Escalona 2005
source			173		220		91
page							
wing area, S	m ²	95,78	95,78				95,78
sweep, 1/4 chord, α_{25}	deg	20	20		20		
max cruise speed, V_{MO}	kt	470	470		352,1	470	
in altitude, h	ft	20997	20997			20997	
max. take-off mass, m_{MTO}	kg	47400	47400		10660	47400	
max op. Mach number, M_{MO}	-	0,78			0,78		
first flight	-	1963	1963		1963	1963	
type of airfoil	-	peaky			peaky		
root airfoil	-			NACA 0012 mod			
tip airfoil	-			NACA 64A310.7 mod			
t/c root	-	12,5%	12,5%	12,0%	12,5%		
t/c tip	-	11,0%	11,0%	10,7%	11,0%		
average t/c calculated from Jenkinson	-	11,4%					
average t/c given	-						
density, ρ	kg/m ³	0,631					
temperature, T	K	246,6					
speed of sound, a	m/s	314,8					
max cruise Mach number, $M_{CR,max}$	-	0,77					
cruise Mach number, M_{CR}	-	0,78					
drag divergence Mach number, M_{DD}	-	0,78					
mass cruise, m_{CR}	kg	47400					
cruise speed V_{CR}	m/s	245,5					
lift coefficient, C_L	-	0,26					

3 view drawing from

 main data for further calculation

X

Table B.10 McDonnell Douglas DC-9 Series 30 - Investigation of aircraft parameters from different sources

manufacturer	McDonnell Douglas										
type	DC-9										
modell	Series 30										
source		selected	Janes 1982	Lednicer 2004	Torenbeek 1988	Bechtermünz 1998	Escalona 2005	Shevell 1980	Obert 1997		
page		for calculation	418		220	611		3	322		
wing area, S	m ²	92,97	92,97			92,97					
sweep, 1/4 chord, δ_{25}	deg	24	24		24						
max cruise speed, V_{MO}	kt	490	490		340,2	485					
in altitude, h	ft	25000	25000		0						
max. take-off mass, m_{MTO}	kg	54885	54885		54885	54885					
max op. Mach number, M_{MO}	-	0,84			0,84					0,84	
first flight	-	1966	1966		1966	1965					
type of airfoil	-	peaky			peaky			peaky			
root airfoil	-			DSMA-433A/-434A							
tip airfoil	-			DSMA-435A/-436A							
t/c root	-	13,65%			13,65%						
t/c tip	-	9,60%			9,60%						
average t/c calculated from Jenkinson	-	10,61%			10,61%						
average t/c given	-		11,00%		11,60%			10,66%			
density, ρ	kg/m ³	0,549									
temperature, T	K	238,6									
speed of sound, a	m/s	309,7									
max cruise Mach number, $M_{CR,max}$	-	0,81									
cruise Mach number, M_{CR}	-	0,84									
drag divergence Mach number, M_{DD}	-	0,84									
mass cruise, m_{CR}	kg	54885									
cruise speed V_{CR}	m/s	260,1									
lift coefficient, C_L	-	0,31									
3 view drawing from										X	
			main data for further calculation								

Table B.11 Vickers Super VC10 - Investigation of aircraft parameters from different sources

manufacturer type modell	Vickers VC10 Super VC10	selected for calculation	Lednicer 2004	Torenbeek 1988 220	Bechtermünz 1998 91	Escalona 2005	Flugzeugtypen 2005	Jetsite 2005
source page								
wing area, S	m ²	268,2					268,2	
sweep, 1/4 chord, α_{25}	deg	32,5		32,5				
max cruise speed, V_{MO}	kt	505		303,5	505			513,0
in altitude, h	ft	31004		0	31004			
max. take-off mass, m_{MTO}	kg	151953			151953		152000	151950
max op. Mach number, M_{MO}	-	0,86		0,86				
first flight	-	1962/1964		1962/1964				1962
type of airfoil	-	peaky		peaky				
root airfoil	-		Pearcey 13%					
tip airfoil	-		Pearcey 9.75%					
t/c root	-	13,00%	13,00%	12,50%				
t/c tip	-	9,75%	9,75%	9,75%				
average t/c calculated from Jenkinson	-	10,44%						
average t/c given	-							
density, ρ	kg/m ³	0,442						
temperature, T	K	226,7						
speed of sound, a	m/s	301,9						
max cruise Mach number, $M_{CR,max}$	-	0,86						
cruise Mach number, M_{CR}	-	0,86						
drag divergence Mach number, M_{DD}	-	0,86						
mass cruise, m_{CR}	kg	151953						
cruise speed V_{CR}	m/s	259,6						
lift coefficient, C_L	-	0,37						
3 view drawing from								X
remark								


main data for further calculation

data of VC-10 listed in Janes 1970/1971

Table B.12 McDonnell Douglas DC-8 Series 63 - Investigation of aircraft parameters from different sources

manufacturer	McDonnell Douglas									
type	DC-8									
modell	Series 63									
source		selected	Janes 1982	Torenbeek 1988	Lednicer 2004	Bechtermünz 1998	Shevell 1980	Jetsite 2005	Airliners 2005	Obert 1997
page		for calculation	418	220		362	3			321-333
wing area, S	m ²	271,92	Super 73:			271,92				271,9
sweep, 1/4 chord, α_{25}	deg	30,5		30			30,5			
max cruise speed, V_{MO}	kt	521,6	521,0	340,2		521,6		504,9		479
in altitude, h	ft	30000	35000	0		30000				?
max. take-off mass, m_{MTO}	kg	158757	158755			158757		147148		158760
max op. Mach number, M_{MO}	-	0,88	0,80	0,88				0,88		0,88
first flight	-	1967		1966/1967		1967				
type of airfoil	-	peaky					peaky			
root airfoil	-				DSMA-277/-280					
tip airfoil	-				DSMA-281					
t/c root	-	12,00%		12,00%						12,00%
t/c tip	-	10,16%		10,16%						10,20%
average t/c calculated from Jenkinson	-	10,62%		10,62%						
average t/c given	-			11,10%			10,80%			
density, ρ	kg/m ³	0,458								
temperature, T	K	228,7								
speed of sound, a	m/s	303,2								
max cruise Mach number, $M_{CR,max}$	-	0,89								
cruise Mach number, M_{CR}	-	0,88								
drag divergence Mach number, M_{DD}	-	0,88								
mass cruise, m_{CR}	kg	158757								
cruise speed V_{CR}	m/s	266,8								
lift coefficient, C_L	-	0,35								

3 view drawing from


 main data for further calculation

X

Table B.13 McDonnell Douglas DC-10 Series 10 - Investigation of aircraft parameters from different sources

manufacturer type modell	McDonnell Douglas										
	DC-10 Series 10	selected for calculation	Janes 1982	Torenbeek 1988	Lednicer 2004	Bechtermünz 1998	Schaufele 2000	Escalona 2005	Jenkinson 2001	Airliners 2005	
source			421	220		612	97				
page											
wing area, S	m ²	367,7	367,7			367,7			367,7	367,7	
sweep, 1/4 chord, α	deg	35	35	35					35		
max cruise speed, V_{MO}	kt	490,0	490,0			490,3			475,0		
in altitude, h	ft	30000	30000			30000			31000		
max. take-off mass, m_{MTO}	kg	263085	263085			263084			190854	263085	
max op. Mach number, M_{MO}	-	0,88	0,88	0,88					0,88		
first flight	-	1972	1972	1970		1970					
type of airfoil	-	peaky					peaky				
root airfoil	-				DSMA-496/-521/-522						
tip airfoil	-				DSMA-519/-520						
t/c root	-	12,50%		12,50%							
t/c tip	-	10,00%		10,00%							
average t/c calculated from Jenkinson	-	10,63%									
average t/c given	-	11,00%		11,00%					11,00%		
density, ρ	kg/m ³	0,458									
temperature, T	K	228,7									
speed of sound, a	m/s	303,2									
max cruise Mach number, $M_{CR,max}$	-	0,83									
cruise Mach number, M_{CR}	-	0,88									
drag divergence Mach number, M_{DD}	-	0,88									
mass cruise, m_{CR}	kg	263085									
cruise speed V_{CR}	m/s	266,8									
lift coefficient, C_L	-	0,43									

3 view drawing from

 main data for further calculation

X

Table B.14 Lockheed C-5A, L500 Galaxy- Investigation of aircraft parameters from different sources

manufacturer type modell	Lockheed C-5A, L500 Galaxy									
source		selected	Torenbeek 1988	Lednicer 2004	Bechtermünz 1998	Schaufele 2000	Escalona 2005	Jetsite 2005	Flugzeugtypen 2005	USAF 2004b
page		for calculation	220		574	97				
wing area, S	m ²	575,98			575,98				576	
sweep, 1/4 chord, α_{25}	deg	25	25							
max cruise speed, V_{MO}	kt	450,3	349,9		450,3			496,2	496,8	450,0
in altitude, h	ft	24893	24893 *		?			?	?	?
max. take-off mass, m_{MTO}	kg	348813			348813			379657	371000	348818
max op. Mach number, M_{MO}	-	0,825	0,825							0,77
first flight	-	1968	1968		1968			1968		
type of airfoil	-	peaky				peaky				
root airfoil	-			NACA 0012.41 mod						
tip airfoil	-			NACA 0011 mod						
t/c root	-	12,00%	12,50%	12,00%						
t/c tip	-	11,00%	9,70%	11,00%						
average t/c calculated from Jenkinson	-	11,25%	10,40%	11,25%						
average t/c given	-	11,50%	11,50%							
density, ρ	kg/m ³	0,551								
temperature, T	K	238,8								
speed of sound, a	m/s	309,8								
max cruise Mach number, $M_{CR,max}$	-	0,75								
cruise Mach number, M_{CR}	-	0,83								
drag divergence Mach number, M_{DD}	-	0,83								
mass cruise, m_{CR}	kg	348813								
cruise speed V_{CR}	m/s	255,6								
lift coefficient, C_L	-	0,33								
3 view drawing from										X
remark										

data of C-5A listed in Janes 1970/1971

* altitude for max curise speed calculated from data given in **Torenbeek 1988** (see separate calculation)


Table B.15 Mitsubishi Diamond I - Investigation of aircraft parameters from different sources

manufacturer type modell	Mitsubishi Diamond I	selected for calculation	Janes 1982 426	Lednicer 2004	Bechtermünz 1998 657
source page					
wing area, S	m ²	22,43	22,43		22,43
sweep, 1/4 chord, α_{25}	deg	20	20		
max cruise speed, V_{MO}	kt	405	405 *		400
in altitude, h	ft	39000	39000 *		39009
max. take-off mass, m_{MTO}	kg	6636	6636		6636
max op. Mach number, M_{MO}	-		0,785		
first flight	-	1978	1978		
type of airfoil	-	supercritical			
root airfoil	-			MAC510 (13.2%)	
tip airfoil	-			MAC510 (11.3%)	
t/c root	-	13,2%	13,2%	13,2%	
t/c tip	-	11,3%	11,3%	11,3%	
average t/c calculated from Jenkinson	-	11,8%			
average t/c given	-				
density, ρ	kg/m ³	0,316			
temperature, T	K	216,7			
speed of sound, a	m/s	295,1			
max cruise Mach number, $M_{CR,max}$	-	0,71			
cruise Mach number, M_{CR}	-	0,71			
drag divergence Mach number, M_{DD}	-	0,71			
mass cruise, m_{CR}	kg	6636			
cruise speed V_{CR}	m/s	208,4			
lift coefficient, C_L	-	0,42			
3 view drawing from					X
remark			Main data for further calculation		
		* typical speed			

Table B.16 Airbus A 300-600 - Investigation of aircraft parameters from different sources

manufacturer type modell	Airbus A 300 - 600			B?	600-R	600-R	600		
source		selected	Janes 1982	Lednicer 2004	Torenbeek 1988	Bechtermünz 1998	Jenkinson 2001	HAW 1999	Escalona 2005
page		for calculation	100		220	35			
wing area, S	m ²	260	260			260	260	260	
sweep, 1/4 chord, α_{25}	deg	28	28		28		28	28	
max cruise speed, V_{MO}	kt	480	492		360,7	481	480	335	
in altitude, h	ft	31000	25000		0	25000	31000	?	
max. take-off mass, m_{MTO}	kg	165000	142000			165000	170500	165000	
max op. Mach number, M_{MO}	-	0,82			0,84		0,82	0,82	
first flight	-	1972	1972		1972	1972			
type of airfoil	-	supercritical							
root airfoil	-			?					
tip airfoil	-			?					
t/c root	-			15,0%	15,0%				
t/c tip	-			?	?				
average t/c calculated from Jenkinson	-						10,5%		
average t/c given	-	10,5%	10,5%		13,5%			10,5%	
density, ρ	kg/m ³	0,442							
temperature, T	K	226,7							
speed of sound, a	m/s	301,9							
max cruise Mach number, $M_{CR,max}$	-	0,82							
cruise Mach number, M_{CR}	-	0,82							
drag divergence Mach number, M_{DD}	-	0,82							
mass cruise, m_{CR}	kg	165000							
cruise speed V_{CR}	m/s	246,9							
lift coefficient, C_L	-	0,46							

3 view drawing from


 Main data for further calculation

X

Table B.17 Boeing 767-200 - Investigation of aircraft parameters from different sources

manufacturer	Boeing							
type	767							
modell	200	200ER						
source		selected	Janes 1982	Lednicer 2004	Boeing 2005	Bechtermünz 1998	Jenkinson 2001	Escalona 2005
page		for calculation				173		
wing area, S	m ²	283,3	283,3			283,35	283,3	
sweep, 1/4 chord, α_{25}	deg	31,3	31,3					
max cruise speed, V_{MO}	kt	488	488		459,5		488	
in altitude, h	ft	39000	39000		35000		39000	
max. take-off mass, m_{MTO}	kg	136080	136080		179170	136078	136078	
max op. Mach number, M_{MO}	-				0,80	0,80		
first flight	-		1982			1981	1982	
type of airfoil	-	supercritical						
root airfoil	-							
tip airfoil	-							
t/c root	-	15,1%		15,1%				
t/c tip	-	10,3%		10,3%				
average t/c calculated from Jenkinson	-	11,5%					11,5%	
average t/c given	-							
density, ρ	kg/m ³	0,316						
temperature, T	K	216,7						
speed of sound, a	m/s	295,1						
max cruise Mach number, $M_{CR,max}$	-	0,85						
cruise Mach number, M_{CR}	-	0,85						
drag divergence Mach number, M_{DD}	-	0,85						
mass cruise, m_{CR}	kg	136080						
cruise speed V_{CR}	m/s	251,0						
lift coefficient, C_L	-	0,47						

3 view drawing from

 Main data for further calculation

X


Table B.18 Cessna 650 Citation VI - Investigation of aircraft parameters from different sources

manufacturer type modell	Cessna 650 Citation VI	based on 650 Citation III				Citation III
source page		selected for calculation	Janes 1993	Lednicer 2004	Obert 1997	Jetsite 2005
wing area, S	m ²	28,99	28,99			
sweep, 1/4 chord, α_{25}	deg	23	23		27,2 (LE)	
max cruise speed, V_{MO}	kt	472	472			486
in altitude, h	ft	35000	35000			
max. take-off mass, m_{MTO}	kg	9979	9979			9980
max op. Mach number, M_{MO}	-	0,851	0,851			
first flight	-	1979	1992			1979
type of airfoil	-	supercritical				
root airfoil	-			Cessna 7001 (16.0%)		
tip airfoil	-			Cessna 7003 (12.5%)		
t/c root	-	16,0%		16,0%	15,40%	
t/c tip	-	12,5%		12,5%	11,00%	
average t/c calculated from Jenkinson	-	13,4%		13,4%	12,1%	
average t/c given	-					
density, ρ	kg/m ³	0,380				
temperature, T	K	218,8				
speed of sound, a	m/s	296,5				
max cruise Mach number, $M_{CR,max}$	-	0,82				
cruise Mach number, M_{CR}	-	0,82				
drag divergence Mach number, M_{DD}	-	0,82				
mass cruise, m_{CR}	kg	9979				
cruise speed V_{CR}	m/s	242,8				
lift coefficient, C_L	-	0,30			0,506	
3 view drawing from						X
			Main data for further calculation			

Table B.19 Airbus A 310-300 - Investigation of aircraft parameters from different sources

manufacturer type modell	Airbus A310 - 300	selected for calculation	Janes 1982 106	Obert 1997 342	HAW 1999	Jenkinson 2001	Airbus 2005	Escalona 2005
source								
page								
wing area, S	m ²	219	219		218,54	219	219	
sweep, 1/4 chord, α_{25}	deg	28	28			28	28	
max cruise speed, V_{MO}	kt	483	483			484		
in altitude, h	ft	30000	30000			35000		
max. take-off mass, m_{MTO}	kg	150000	138600		150000	150000	150000	
max op. Mach number, M_{MO}	-	0,84	0,82		0,84	0,84	0,84	
first flight	-		1983					
type of airfoil	-	supercritical						
root airfoil	-							
tip airfoil	-							
t/c root	-	15,2%		15,2%	15,2%			
t/c tip	-	10,8%		10,8%	10,8%			
average t/c calculated from Jenkinson	-	11,9%		11,9%	11,9%	11,80%		
average t/c given	-		11,80%					
density, ρ	kg/m ³	0,458						
temperature, T	K	228,7						
speed of sound, a	m/s	303,2						
max cruise Mach number, $M_{CR,max}$	-	0,82						
cruise Mach number, M_{CR}	-	0,82						
drag divergence Mach number, M_{DD}	-	0,82						
mass cruise, m_{CR}	kg	150000						
cruise speed V_{CR}	m/s	248,5						
lift coefficient, C_L	-	0,47						

3 view drawing from

 Main data for further calculation

X

Table B.20 Raytheon Hawker 800XP - Investigation of aircraft parameters from different sources

manufacturer type modell	Raytheon Hawker 800XP	derived from Bae HS 125	Janes 1996	BAe HS 125 -700 Bechtermünz 1998	Raytheon 2005	Jetsite 2005
source page	selected for calculation		714	210		
wing area, S	m ²		34,75	34,75	32,79	34,5
sweep, 1/4 chord, α_{25}	deg		20	20		
max cruise speed, V_{MO}	kt		447	456	436	447
in altitude, h	ft		37000	29000	25000	37000
max. take-off mass, m_{MTO}	kg		12700	12701	11567	12700
max op. Mach number, M_{MO}	-		0,8			0,8
first flight	-		1976	1995	1976	1976
type of airfoil	-		supercritical	*		
root airfoil	-					
tip airfoil	-					
t/c root	-		14,00%	14,00%		
t/c tip	-			8,35%		
average t/c calculated from Jenkinson	-		12,59%			
average t/c given	-					
density, ρ	kg/m ³		0,348			
temperature, T	K		216,7			
speed of sound, a	m/s		295,1			
max cruise Mach number, $M_{CR,max}$	-		0,78			
cruise Mach number, M_{CR}	-		0,80			
drag divergence Mach number, M_{DD}	-		0,80			
mass cruise, m_{CR}	kg		12700			
cruise speed V_{CR}	m/s		236,1			
lift coefficient, C_L	-		0,37			

3 view drawing from

X

remark

main data for further calculation


* modified (enlarged) wing for BAe HS 125 series 800 in 1983 (**Bechtermünz 1998**)

apparently: outer t/c reduced from 11% to 8,35% compared to 1962-modell (**Torenbeek 1988**)

Table B.21 Raytheon Beechjet 400A - Investigation of aircraft parameters from different sources

manufacturer type modell	Raytheon Beechjet 400A	selected for calculation	Janes 1996	Lednicer 2004	Bechtermünz 1998	Jetsite 2005
source page					105	
wing area, S	m ²	22,43	22,43		22,43	
sweep, 1/4 chord, α_{25}	deg	20	20			
max cruise speed, V_{MO}	kt	468	468		461	
in altitude, h	ft	27000	27000		29003	
max. take-off mass, m_{MTO}	kg	7303	7303		7303	7303
max op. Mach number, M_{MO}	-					0,78
first flight	-	1978			1978 (Mitsubishi Mu-300)	1978
type of airfoil	-	supercritical		MAC510 (13.2%)		
root airfoil	-			MAC510 (11.3%)		
tip airfoil	-					
t/c root	-	13,2%	13,2%	13,2%		
t/c tip	-	11,3%	11,3%	11,3%		
average t/c calculated from Jenkinson	-	11,8%		11,8%		
average t/c given	-					
density, ρ	kg/m ³	0,511				
temperature, T	K	234,7				
speed of sound, a	m/s	307,1				
max cruise Mach number, $M_{CR,max}$	-	0,78				
cruise Mach number, M_{CR}	-	0,78				
drag divergence Mach number, M_{DD}	-	0,78				
mass cruise, m_{CR}	kg	7303				
cruise speed V_{CR}	m/s	240,8				
lift coefficient, C_L	-	0,22				

3 view drawing from


 main data for further calculation

X

Table B.22 Beriev Be-40 - Investigation of aircraft parameters from different sources

manufacturer type modell	Beriev Be-40	selected for calculation	Janes 1996 353	Lednicer 2004	Bechtermünz 1998 122	Beriev 2005
source page						
wing area, S	m ²	200	200		200	
sweep, 1/4 chord, α_{25}	deg	23	23			
max cruise speed, V_{MO}	kt	432,0	388		410	432,0
in altitude, h	ft	19680	19680		19685	
max. take-off mass, m_{MTO}	kg	86000	86000		86000	86000
max op. Mach number, M_{MO}	-					
first flight	-	1986			1986	
type of airfoil	-	supercritical				
root airfoil	-			TsAGI 14.5%		
tip airfoil	-			TsAGI 11.5%		
t/c root	-	14,5%	14,5%	14,5%		
t/c tip	-	11,3%	11,3%	11,5%		
average t/c calculated from Jenkinson	-	12,1%				
average t/c given	-					
density, ρ	kg/m ³	0,660				
temperature, T	K	249,2				
speed of sound, a	m/s	316,4				
max cruise Mach number, $M_{CR,max}$	-	0,70				
cruise Mach number, M_{CR}	-	0,70				
drag divergence Mach number, M_{DD}	-	0,70				
mass cruise, m_{CR}	kg	86000				
cruise speed V_{CR}	m/s	222,2				
lift coefficient, C_L	-	0,26				

3 view drawing from

 main data for further calculation

X

Table B.23 Bombardier Global Express - Investigation of aircraft parameters from different sources

manufacturer type modell	Bombardier Global Express	XRS				
		selected for calculation	Janes 2000	Jetsite 2005	Bombardier 2005	Lednicer 2004
source page			38			
wing area, S	m ²	94,95	94,95			
sweep, 1/4 chord, α_{25}	deg	35	35			
max cruise speed, V_{MO}	kt	513	528 *		513,0	
in altitude, h	ft	43000	30870		43000	
max. take-off mass, m_{MTO}	kg	44452	43091	42412	44452	
max op. Mach number, M_{MO}	-	0,89	0,89	0,88	0,89	
first flight	-	1996		1996		
type of airfoil	-	supercritical				
root airfoil	-					Canadair 11%
tip airfoil	-					Canadair 11%
t/c root	-	11,0%				11,0%
t/c tip	-	11,0%				11,0%
average t/c calculated from Jenkinson	-	11,00%				
average t/c given	-		11,0%			
density, ρ	kg/m ³	0,261				
temperature, T	K	216,7				
speed of sound, a	m/s	295,1				
max cruise Mach number, $M_{CR,max}$	-	0,89				
cruise Mach number, M_{CR}	-	0,89				
drag divergence Mach number, M_{DD}	-	0,89				
mass cruise, m_{CR}	kg	44452				
cruise speed V_{CR}	m/s	262,6				
lift coefficient, C_L	-	0,51				
3 view drawing from				X		
remark						* IAS converted to TAS

main data for further calculation


Table B.24 Bombardier Challenger CRJ 200 LR - Investigation of aircraft parameters from different sources

manufacturer type modell	Bombardier Challenger CRJ 200 LR	selected for calculation	Janes 2000 43	CRJ 200 Lednicer 2004	Challenger 800 Bombardier 2005	CRJ 200 Jetsite 2005
wing area, S	m ²	54,54	54,54		48,35	
sweep, 1/4 chord, α_{25}	deg	24,54	24,54			
max cruise speed, V_{MO}	kt	454	454		459	424
in altitude, h	ft	37000	37000			
max. take-off mass, m_{MTO}	kg	24040	24040		24040	24040
max op. Mach number, M_{MO}	-				0,8	
first flight	-	1991				1991
type of airfoil	-	supercritical				
root airfoil	-			Canadair 13,2%		
tip airfoil	-			Canadair 10%		
t/c root	-	13,2%	13,2%	13,2%		
t/c tip	-	10,0%	10,0%	10,0%		
average t/c calculated from Jenkinson	-	10,8%	10,8%	10,8%		
average t/c given	-	10,8%				
density, ρ	kg/m ³	0,348				
temperature, T	K	216,7				
speed of sound, a	m/s	295,1				
max cruise Mach number, $M_{CR,max}$	-	0,79				
cruise Mach number, M_{CR}	-	0,79				
drag divergence Mach number, M_{DD}	-	0,79				
mass cruise, m_{CR}	kg	24040				
cruise speed V_{CR}	m/s	233,6				
lift coefficient, C_L	-	0,46				
3 view drawing from					(X)	X
			main data for further calculation			

Table B.25 Tupolev Tu-204-300 - Investigation of aircraft parameters from different sources

manufacturer type modell	Tupolev Tu-204-300	Tu-204-200				
		selected for calculation	Janes 1996 449	Lednicer 2004	Bechtermünz 1998 887	Jenkinson 2001 887
wing area, S	m ²	182,4	182,4		182,4	182,4
sweep, 1/4 chord, α_{25}	deg	28	28			28
max cruise speed, V_{MO}	kt	448	448		459	458
in altitude, h	ft	39700	39700		39370	40000
max. take-off mass, m_{MTO}	kg	110755	110755		110755	110750
max op. Mach number, M_{MO}	-					
first flight	-	1989	1989		1989	
type of airfoil	-	supercritical				
root airfoil	-					
tip airfoil	-					
t/c root	-	14,0%	14,0%	14,0%		
t/c tip	-	10,0%	10,0%	9,0%		
average t/c calculated from Jenkinson	-	11,00%				
average t/c given	-					
density, ρ	kg/m ³	0,306				
temperature, T	K	216,7				
speed of sound, a	m/s	295,1				
max cruise Mach number, $M_{CR,max}$	-	0,78				
cruise Mach number, M_{CR}	-	0,78				
drag divergence Mach number, M_{DD}	-	0,78				
mass cruise, m_{CR}	kg	110755				
cruise speed V_{CR}	m/s	230,5				
lift coefficient, C_L	-	0,73				

3 view drawing from

 main data for further calculation

X

Table B.26 Bae RJ85 - Investigation of aircraft parameters from different sources

manufacturer type modell	Bae RJ85	selected for calculation	Janes 1996	Jenkinson 2001	Jetsite 2005
source					
page			516		
wing area, S	m ²	77,29	77,29		77,3
sweep, 1/4 chord, α_{25}	deg	15	15		15
max cruise speed, V_{MO}	kt	432,0	458,3 *		432,0
in altitude, h	ft	29000			29000
max. take-off mass, m_{MTO}	kg	43998	43998		42184
max op. Mach number, M_{MO}	-	0,73	0,73		0,73
first flight	-	1992	1992		
type of airfoil	-	supercritical			
root airfoil	-				
tip airfoil	-				
t/c root	-	15,3%	15,3%		
t/c tip	-	12,2%	12,2%		
average t/c calculated from Jenkinson	-	13,0%	13,0%		12,98%
average t/c given	-				
density, ρ	kg/m ³	0,475			
temperature, T	K	230,7			
speed of sound, a	m/s	304,5			
max cruise Mach number, $M_{CR,max}$	-	0,73			
cruise Mach number, M_{CR}	-	0,73			
drag divergence Mach number, M_{DD}	-	0,73			
mass cruise, m_{CR}	kg	43998			
cruise speed V_{CR}	m/s	222,2			
lift coefficient, C_L	-	0,48			
3 view drawing from					
remark					

main data for further calculation

* IAS: 300 kt => 458,3 kt at 29000 ft

X

Table B.27 Embraer EMB-125 - Investigation of aircraft parameters from different sources

manufacturer type modell	Embraer EMB-145	selected for calculation	Janes 1996	Jenkinson 2001	Jetsite 2005
source					
page			20		
wing area, S	m ²	51,18	51,18	51,18	
sweep, 1/4 chord, α_{25}	deg	22,73	22,73	22,73	
max cruise speed, V_{MO}	kt	410	410	410,0	
in altitude, h	ft	37000	37000	37000	
max. take-off mass, m_{MTO}	kg	19200	19200	19200	
max op. Mach number, M_{MO}	-	0,75	0,75	0,76	
first flight	-	1995	1995		
type of airfoil	-	supercritical			
root airfoil	-				
tip airfoil	-				
t/c root	-				
t/c tip	-				
average t/c calculated from Jenkinson	-	11,0%		11,0%	
average t/c given	-				
density, ρ	kg/m ³	0,348			
temperature, T	K	216,7			
speed of sound, a	m/s	295,1			
max cruise Mach number, $M_{CR,max}$	-	0,71			
cruise Mach number, M_{CR}	-	0,75			
drag divergence Mach number, M_{DD}	-	0,75			
mass cruise, m_{CR}	kg	19200			
cruise speed V_{CR}	m/s	221,3			
lift coefficient, C_L	-	0,43			
3 view drawing from					X
remark		main data for further calculation * standard: 19200 kg; extended range: 20600 kg			

Table B.28 Airbus A321-200 - Investigation of aircraft parameters from different sources

manufacturer	Airbus							
type	A321					A320		
modell	-200			-100				
source	selected	Janes 1996	HAW 1999	Jenkinson 2001	Airbus 1992	BAe 1983	Jetsite 2005	
page	for calculation	169						
wing area, S	m ²	122,4	122,4 *	122,4	122,4	122,4	122,4	
sweep, 1/4 chord, α_{25}	deg	24,96	25 *	24,967	25	24,96	24,96	
max cruise speed, V_{MO}	kt	487,0		349,9	487,0			
in altitude, h	ft	28000			28000			
max. take-off mass, m_{MTO}	kg	89000	89000 **	83500	89000			
max op. Mach number, M_{MO}	-			0,82	0,82			
first flight	-	1993	1993					
type of airfoil	-	supercritical						
root airfoil	-							
tip airfoil	-							
t/c root	-	15,15%		15,15%			15,1%	
t/c tip	-	10,84%		10,84%			10,8%	
average t/c calculated from Jenkinson	-	11,92%		11,92%				
average t/c given	-							
density, ρ	kg/m ³	0,493						
temperature, T	K	232,7						
speed of sound, a	m/s	305,8						
max cruise Mach number, $M_{CR,max}$	-	0,82						
cruise Mach number, M_{CR}	-	0,82						
drag divergence Mach number, M_{DD}	-	0,82						
mass cruise, m_{CR}	kg	89000						
cruise speed V_{CR}	m/s	250,5						
lift coefficient, C_L	-	0,46						
3 view drawing from							X	
remark		main data for further calculation						
		* taken from A320						
		** standard: 83000 kg; option: 89000 kg						

Table B.29 Airbus A321-200 - Investigation of aircraft parameters from different sources

manufacturer type modell	Airbus A340 300	selected for calculation	Janes 1996 163	HAW 1999	Jenkinson 2001	A330 300 Airbus 1991	A330 200 Airbus 1987	Jetsite 2005
wing area, S	m ²	361,63	363,1	361,63	363,1		361,63	
sweep, 1/4 chord, α_{25}	deg	29,74	30	29,8	29,7	29,735	30	
max cruise speed, V_{MO}	kt	500		349,9	500,0			
in altitude, h	ft	33000			33000			
max. take-off mass, m_{MTO}	kg	271000	271000 *	257000	271000			
max op. Mach number, M_{MO}	-		0,86	0,86	0,86	0,86		
first flight	-	1991	1991					
type of airfoil	-	supercritical						
root airfoil	-							
tip airfoil	-							
t/c root	-	15,3%				15,30%	15,25%	
t/c tip	-	10,6%				10,60%		
average t/c calculated from Jenkinson	-	11,8%				11,8%		
average t/c given	-							
density, ρ	kg/m ³	0,410						
temperature, T	K	222,8						
speed of sound, a	m/s	299,2						
max cruise Mach number, $M_{CR,max}$	-	0,86						
cruise Mach number, M_{CR}	-	0,86						
drag divergence Mach number, M_{DD}	-	0,86						
mass cruise, m_{CR}	kg	271000						
cruise speed V_{CR}	m/s	257,2						
lift coefficient, C_L	-	0,54						
3 view drawing from								X
remark		main data for further calculation						
		** standard: 257000 kg; option: 260000 kg; longer range version: 271000 kg; longer range version option: 275000 kg						

Appendix C

Summary of Aircraft Parameters

Table C.1 Summary of data for aircraft with conventional airfoils

aircraft	phi_25	C_L	M_DD	t/c
IAI	4,5	0,19	0,76	12,0%
Caravelle	20,0	0,20	0,72	12,0%
VFW 614	15,0	0,23	0,65	12,8%
HFB 320	15,0	0,33	0,78	11,5%
Lear Jet	13,0	0,16	0,77	9,0%
Starlifter	25,0	0,34	0,74	11,5%
Jetstar	30,0	0,29	0,81	11,5%
Falcon 20	30,0	0,20	0,77	9,9%

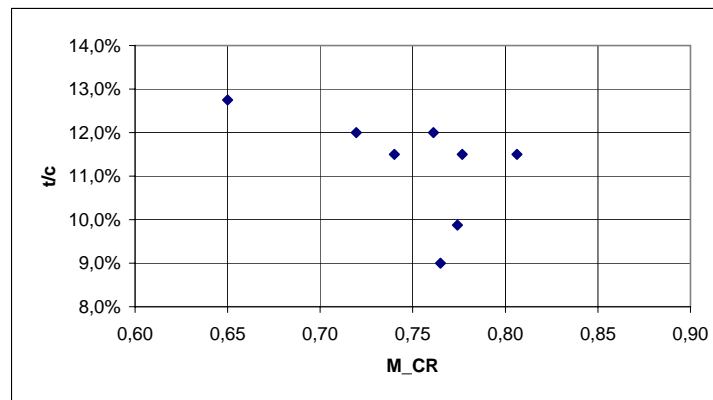
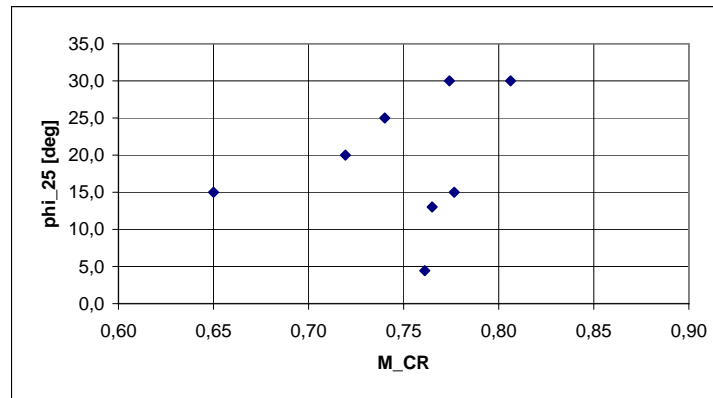
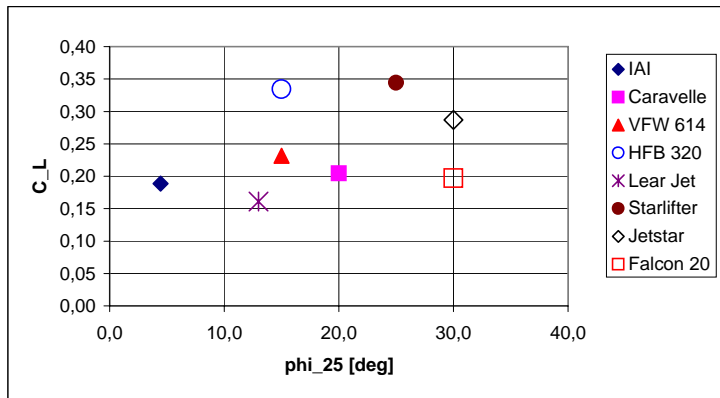


Table C.2 Summary of data for aircraft with peaky airfoils

aircraft	phi_25	C_L	M_DD	t/c
BAC 1-11	20,0	0,26	0,78	11,4%
DC-9	24,0	0,31	0,84	10,6%
VC-10	32,5	0,37	0,86	10,4%
DC-8	30,5	0,35	0,88	10,6%
DC-10	35,0	0,43	0,88	11,0%
C-5A	25,0	0,33	0,83	11,5%

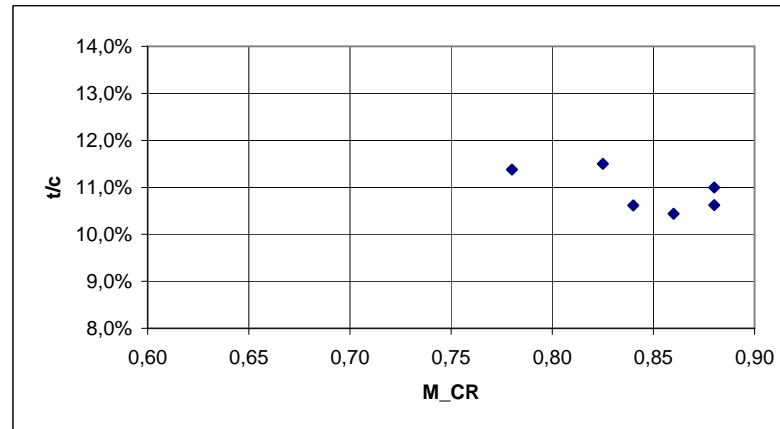
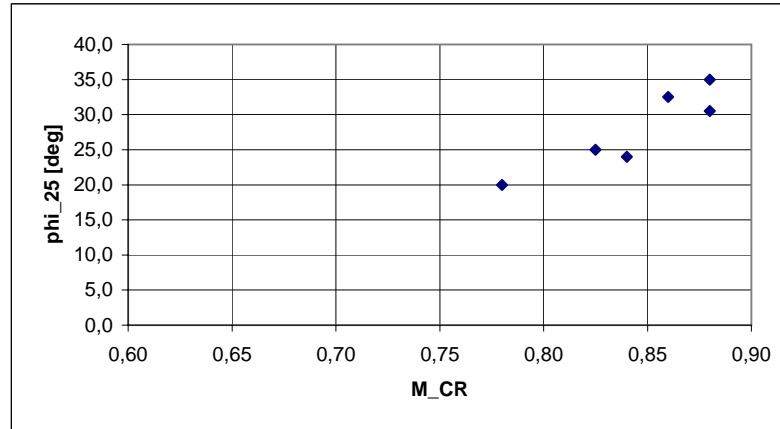
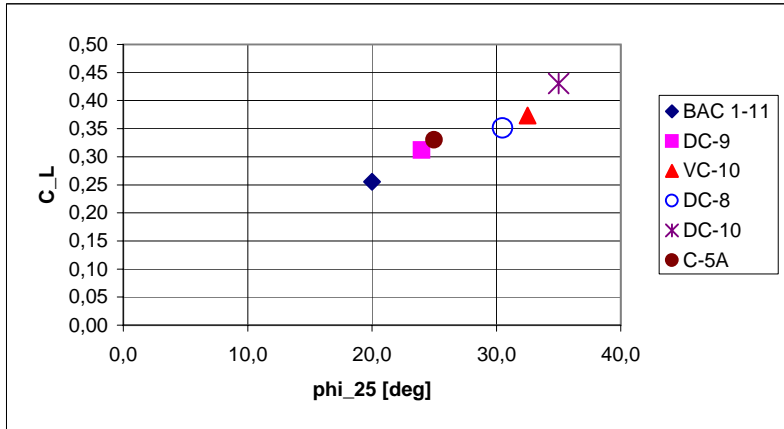


Table C.3 Summary of data for aircraft with older supercritical airfoils

aircraft	phi_25	C L	M_DD	t/c
Mitsubishi Diamond I	20,0	0,42	0,71	11,8%
Airbus A300	28,0	0,46	0,82	10,5%
Boeing 767-200	31,3	0,47	0,85	11,5%
Cessna 650	23,0	0,30	0,82	13,4%
Airbus A 310	28,0	0,47	0,82	11,9%
Hawker 800XP	20,0	0,37	0,80	12,6%
Beechjet 400A	20,0	0,22	0,78	11,8%
Beriev Be-40	23,0	0,26	0,70	12,1%

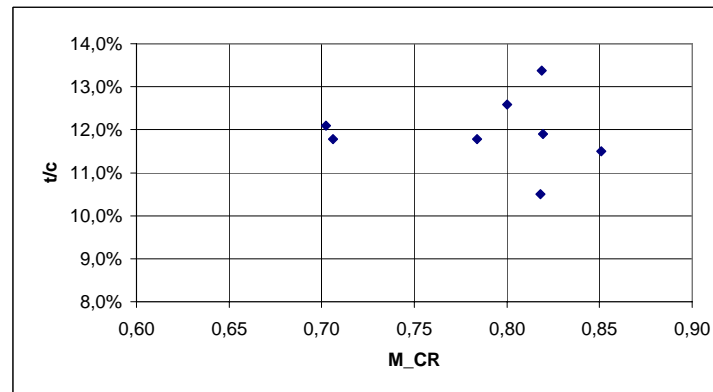
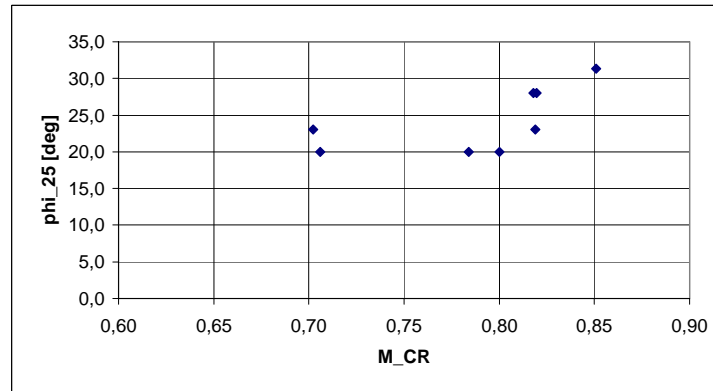
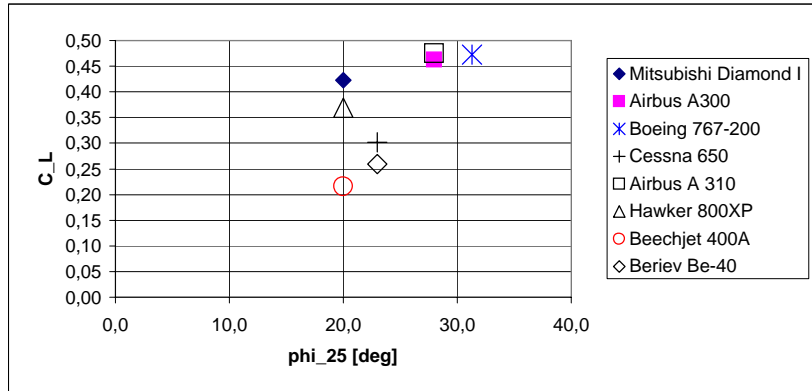
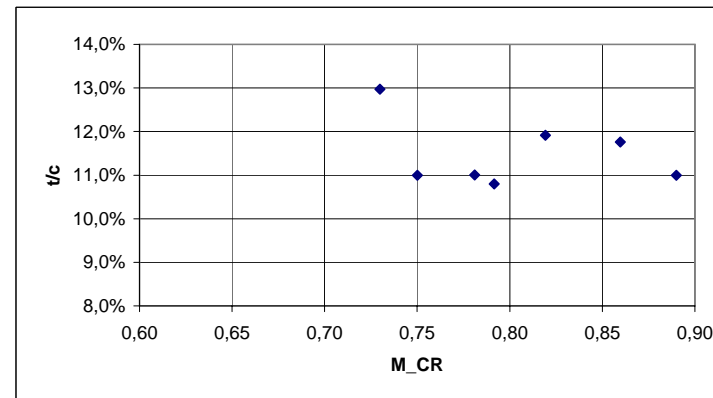
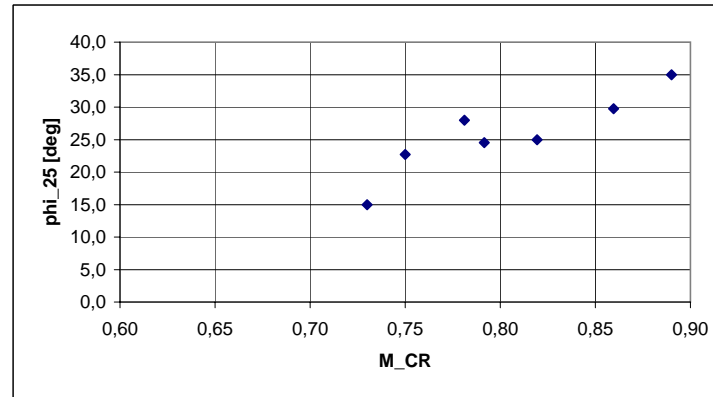
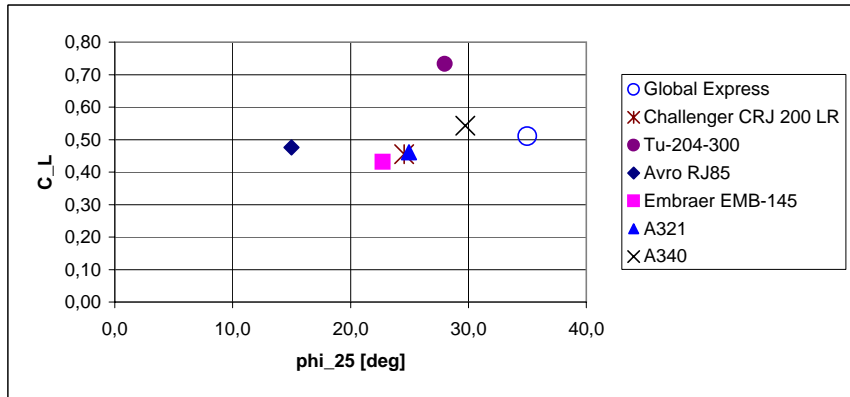


Table C.4 Summary of data for aircraft with modern supercritical airfoils

aircraft	phi_25	C_L	M_DD	t/c
Global Express	35,0	0,51	0,89	11,0%
Challenger CRJ 200 LR	24,5	0,46	0,79	10,8%
Tu-204-300	28,0	0,73	0,78	11,0%
Avro RJ85	15,0	0,48	0,73	13,0%
Embraer EMB-145	22,7	0,43	0,75	11,0%
A321	25,0	0,46	0,82	11,9%
A340	29,7	0,54	0,86	11,8%



Appendix D

Calculation of Relative Thickness / Optimization of Equations

Table D.1 Relative thickness of a wing - aircraft with conventional airfoils (1)

Number of aircraft included in this statistic

29

Manufacturer Type Model	IAI 1124A Westwind 2	Sud Aviation Caravelle	VFW 614	HFB 320	Gates Lear Jet Model 23	Lockheed C-141 Starlifter	Lockheed Jetstar II	Dassault Falcon 20	min	max
sweep, 1/4 chord, ϕ_{25} [deg]	4,45	20,00	15,00	15,00	13,00	25,00	30,00	30,00	4,45	35,00
drag divergence Mach number, M_{DD}	0,76112	0,71943	0,65000	0,77665	0,76500	0,74000	0,80630	0,77412	0,65	0,89
lift coefficient, C_L	0,18859	0,20427	0,23160	0,33422	0,16111	0,34427	0,28697	0,19720	0,16111	0,73316
airfoil	conv.	conv.	conv.	conv.	conv.	conv.	conv.	conv.		
$M_{DD,eff}$	0,76	0,70	0,64	0,76	0,76	0,70	0,75	0,72	0,63883	0,81685
	set	standard	opt. k_M	opt. all	opt. $k_{T,e}$	opt. $k_{T,e}=RIE$	opt. all, $e=RIE$			
$k_{M,conv}$	0,907	1,000	0,991	0,907	1,000	1,000	1,820			
$k_{M,peaky}$	1,209	1,050	1,158	1,209	1,050	1,050	12,480			
$k_{M,super}$	4,703	1,135	1,098	4,703	1,135	1,135	2,376			
$k_{M,super,modern}$	1,735	1,135	1,143	1,735	1,135	1,135	2,594			
k_T	0,130	0,300	0,300	0,130	0,131	0,447	0,119			
e	0,038	0,667	0,667	0,038	0,027	1,094	1,094			
k_M	0,907	0,907	0,907	0,907	0,907	0,907	0,907	0,907		
t/c from TORENBEEK with C_L	11,89%	11,50%	12,03%	11,30%	11,68%	10,95%	10,28%	10,51%	sum:	SEE:
error^2	0,00000	0,00003	0,00005	0,00000	0,00072	0,00003	0,00015	0,00004	0,00187	0,80%
t/c from TORENBEEK with $C_L/\cos\phi_{25}$	11,89%	11,49%	12,03%	11,28%	11,67%	10,92%	10,23%	10,49%	sum:	SEE:
error^2	0,00000	0,00003	0,00005	0,00000	0,00072	0,00003	0,00016	0,00004	0,00189	0,81%
	set	HOWE optimized								
AF_{conv}	0,861	0,80	0,861							
AF_{peaky}	0,935	0,85	0,935							
AF_{super}	0,907	0,90	0,907							
$AF_{super,modern}$	0,926	0,95	0,926							
AF	0,86	0,86	0,86	0,86	0,86	0,86	0,86	0,86		
t/c from HOWE	8,19%	14,29%	19,88%	6,40%	8,95%	12,18%	8,17%	12,06%	sum:	SEE:
error^2	0,00145	0,00053	0,00508	0,00260	0,00000	0,00005	0,00111	0,00048	0,03899	3,67%
t/c from JENKINSON	14,58%	18,57%	22,68%	12,21%	15,13%	15,97%	12,79%	16,27%	sum:	SEE:
error^2	0,00067	0,00431	0,00985	0,00005	0,00375	0,00200	0,00017	0,00409	0,05193	4,23%
K	1,71362									
t/c from similarity without sweep	12,16%	14,94%	19,56%	11,14%	11,91%	13,56%	9,23%	11,31%	sum:	SEE:
error^2	0,00000	0,00086	0,00464	0,00001	0,00085	0,00043	0,00052	0,00021	0,03990	3,71%
Kphi	1,89055									
t/c from similarity with sweep	10,56%	14,16%	17,52%	10,37%	10,84%	13,75%	11,11%	12,83%	sum:	SEE:
error^2	0,00021	0,00047	0,00227	0,00013	0,00034	0,00051	0,00002	0,00088	0,01707	2,43%
a	0,14602									
LINEAR REGRESSION b	-0,00513									
c	0,00257									
t/c= $a*M_{DD,eff} + b*C_L + c*k_m$	11,23%	10,31%	9,44%	11,21%	11,18%	10,34%	11,04%	10,65%	sum:	SEE:
error^2	0,00006	0,00028	0,00109	0,00001	0,00047	0,00013	0,00002	0,00006	0,00405	1,18%
k_t	0,11846									

opt. k_M 2,49% **standard** 2,88% **opt. all** 0,80%

SEE Standard Error of Estimate

$$Standard\ Error\ of\ Estimate = \sqrt{\frac{\sum (y_{estimate} - y)^2}{n}}$$

Table D.2 Relative thickness of a wing - aircraft with conventional airfoils (2)

Number of aircraft included in this statistic

29

Manufacturer Type Model	IAI 1124A Westwind 2	Sud Aviation Caravelle	VFW 614	HFB 320	Gates Lear Jet Model 23	Lockheed C-141 Starlifter	Lockheed Jetstar II	Dassault Falcon 20	min	max
sweep, 1/4 chord, ϕ_{25} [deg]	4,45	20,00	15,00	15,00	13,00	25,00	30,00	30,00	4,45	35,00
drag divergence Mach number, M_{DD}	0,76112	0,71943	0,65000	0,77665	0,76500	0,74000	0,80630	0,77412	0,65	0,89
lift coefficient, C_L	0,18859	0,20427	0,23160	0,33422	0,16111	0,34427	0,28697	0,19720	0,16111	0,73316
airfoil	conv.	conv.	conv.	conv.	conv.	conv.	conv.	conv.		
$M_{DD,eff}$	0,76	0,70	0,64	0,76	0,76	0,70	0,75	0,72	0,63883	0,81685
	set	standard	opt. k_M	opt. all	opt. $k_{T,e}$	opt. $k_{T,e}=RIE$	opt. all, $e=RIE$			
k_t	0,11846									
t	-0,21501									
NONLINEAR REGRESSION										
u	0,54396									
v	0,05128									
w	0,03748									
$t/c=k_t*M_{DD}^{*t}(\cos \phi_{25})^u*c_L^v*k_M^w$	0,11471	11,29%	11,79%	11,56%	11,23%	11,30%	10,72%	10,61%	sum:	SEE:
error ²	0,00003	0,00005	0,00009	0,00000	0,00050	0,00000	0,00006	0,00005	0,00164	0,75%
K_{AA}	0,88717									
t/c from WEISSHAAR	10,90%	17,67%	22,65%	9,77%	12,16%	15,82%	13,04%	16,49%	sum:	SEE:
error ²	0,00012	0,00321	0,00980	0,00030	0,00100	0,00187	0,00024	0,00438	0,04521	3,95%
t/c from RAYMER	9,03%	13,20%	14,53%	6,69%	10,23%	11,72%	8,60%	12,55%	sum:	SEE:
error ²	0,00088	0,00014	0,00032	0,00231	0,00015	0,00001	0,00084	0,00072	0,05982	4,54%
t/c from SHEVELL	13,94%	22,41%	30,10%	11,59%	15,50%	19,07%	15,68%	21,12%	sum:	SEE:
error ²	0,00038	0,01083	0,03011	0,00000	0,00423	0,00574	0,00175	0,01264	0,18854	8,06%
a	-1,147									
b	0,200									
c	0,838									
d	4,057									
t/c from BÖTTGER	0,11649	0,19432	0,24384	0,12955	0,13515	0,18836	0,14200	0,17101	sum:	SEE:
error ²	0,00001	0,00552	0,01353	0,00021	0,00204	0,00538	0,00073	0,00522	0,06288	4,66%
y	0,18973	0,23133	0,24822	0,35822	0,16970	0,41913	0,38262	0,26294		
M_{DIV}	0,74112	0,69943	0,63000	0,75665	0,74500	0,72000	0,78630	0,75412		
ΔM_{DIV}	0,04	0,04	0,04	0,04	0,04	0,04	0,04	0,04		
$M_{DIV_peaky} = M_{DIV} + \Delta M_{DIV}$	0,78112	0,73943	0,67000	0,79665	0,78500	0,76000	0,82630	0,79412		
M_{CC}	0,76188	0,71801	0,65192	0,77516	0,76432	0,73608	0,79780	0,76674		
u	2,83550	2,83550	2,83550	2,83550	2,83550	2,83550	2,83550	2,83550		
v	-1,82634	-1,80861	-1,80141	-1,75453	-1,83488	-1,72857	-1,74413	-1,79514		
w	0,15237	0,22892	0,27054	0,12951	0,17123	0,19896	0,18246	0,23330		
arg in root	1,60737	0,67460	0,17656	1,60948	1,42473	0,73136	0,97252	0,57644		
x	0,09849	0,17409	0,24356	0,08568	0,11308	0,15401	0,13366	0,18267		
t/c from KROO	9,82%	16,36%	23,53%	8,28%	11,02%	13,96%	11,57%	15,82%	sum:	SEE:
error ²	0,00048	0,00190	0,01161	0,00104	0,00041	0,00060	0,00000	0,00353	0,05695	4,59%
ϕ_{25}	4,5	20,0	15,0	15,0	13,0	25,0	30,0	30,0		
C_L	0,19	0,20	0,23	0,33	0,16	0,34	0,29	0,20		
M_{DIV}	0,74112	0,69943	0,63000	0,75665	0,74500	0,72000	0,78630	0,75412		
ΔM_{DIV}	0,08	0,08	0,08	0,08	0,08	0,08	0,08	0,08		
$M_{DIV_supercrit} = M_{DIV} + \Delta M_{DIV}$	0,82	0,78	0,71	0,84	0,83	0,80	0,87	0,83		
t/c from SCHAUFLE (roughly from chart)	7,00%	14,00%	15,00%	7,00%	8,00%	14,00%	10,00%	15,00%	sum:	SEE:
error ²	0,00250	0,00040	0,00051	0,00203	0,00010	0,00063	0,00023	0,00263	0,03182	3,31%

standard 5,49 0,6 auf sc 5,04% 0,6 auf sc&pe: 4,54%

all 4,66% sup. crit. 4,32%

SEE Standard Error of Estimate

Table D.3 Relative thickness of a wing - aircraft with peaky airfoils (1)

Number of aircraft included in this statistic

Manufacturer Type Model	BAC One-Eleven Series 500	McDonnell Douglas DC-9 Series 30	Vickers VC-10 Super VC-10	McDonnell Douglas DC-8 Series 63	McDonnell Douglas DC-10 Series 10	Lockheed C-5A	min	max				
sweep, 1/4 chord, ϕ_{25} [deg]	20,00	24,00	32,50	30,50	35,00	25,00	4,45	35,00				
drag divergence Mach number, M_{DD}	0,78000	0,84000	0,86000	0,88000	0,88000	0,82500	0,65	0,89				
lift coefficient, C_L	0,25531	0,31184	0,37355	0,35114	0,43032	0,33008	0,16111	0,73316				
airfoil	peaky	peaky	peaky	peaky	peaky	peaky						
$M_{DD,eff}$	0,76	0,80	0,79	0,82	0,80	0,79	0,63883	0,81685				
$k_{M,conv}$												
$k_{M,peaky}$												
$k_{M,super}$												
$k_{M,super,modern}$												
k_T												
e												
k_M	1,209	1,209	1,209	1,209	1,209	1,209						
t/c from TORENBEEK with C_L	11,79%	11,31%	10,46%	10,62%	10,13%	11,27%	sum:	SEE:	opt. k_M	standard	opt. all	
error^2	0,00002	0,00005	0,00000	0,00000	0,00008	0,00001	0,00187	0,80%	2,49%	2,88%	0,80%	
t/c from TORENBEEK with $C_L/\cos\phi_{25}$	11,78%	11,30%	10,44%	10,60%	10,10%	11,26%	sum:	SEE:				
error^2	0,00002	0,00005	0,00000	0,00000	0,00008	0,00001	0,00189	0,81%				
AF_{conv}												
AF_{peaky}												
AF_{super}												
$AF_{super,modern}$												
AF	0,93	0,93	0,93	0,93	0,93	0,93						
t/c from HOWE	15,31%	10,06%	10,75%	8,27%	9,52%	11,63%	sum:	SEE:				
error^2	0,00154	0,00003	0,00001	0,00055	0,00022	0,00000	0,03899	3,67%				
t/c from JENKINSON	13,54%	9,03%	8,28%	6,73%	6,62%	10,02%	sum:	SEE:				
error^2	0,00047	0,00025	0,00047	0,00151	0,00192	0,00022	0,05193	4,23%				
K												
t/c from similarity without sweep	10,92%	7,12%	5,92%	4,78%	4,78%	8,05%	sum:	SEE:				
error^2	0,00002	0,00122	0,00204	0,00341	0,00387	0,00119	0,03990	3,71%				
Kphi												
t/c from similarity with sweep	10,78%	8,15%	8,88%	7,38%	8,51%	9,12%	sum:	SEE:				
error^2	0,00004	0,00061	0,00024	0,00105	0,00062	0,00056	0,01707	2,43%				
LINEAR REGRESSION												
t/c= $a*M_{DD,eff} + b*C_L + c*k_m$	11,22%	11,87%	11,65%	12,06%	11,72%	11,61%	sum:	SEE:				
error^2	0,00000	0,00016	0,00015	0,00021	0,00005	0,00000	0,00405	1,18%				

$$Standard\ Error\ of\ Estimate = \sqrt{\frac{\sum (y_{estimate} - y)^2}{n}}$$

Table D.4 Relative thickness of a wing - aircraft with peaky airfoils (2)

Number of aircraft included in this statistic

Manufacturer Type Model	BAC One-Eleven Series 500	McDonnell Douglas DC-9 Series 30	Vickers VC-10 Super VC-10	McDonnell Douglas DC-8 Series 63	McDonnell Douglas DC-10 Series 10	Lockheed C-5A	min	max
sweep, 1/4 chord, ϕ_{25} [deg]	20,00	24,00	32,50	30,50	35,00	25,00	4,45	35,00
drag divergence Mach number, M_{DD}	0,78000	0,84000	0,86000	0,88000	0,88000	0,82500	0,65	0,89
lift coefficient, C_L	0,25531	0,31184	0,37355	0,35114	0,43032	0,33008	0,16111	0,73316
airfoil	peaky	peaky	peaky	peaky	peaky	peaky		
$M_{DD,eff}$	0,76	0,80	0,79	0,82	0,80	0,79	0,63883	0,81685
NONLINEAR REGRESSION								
k_t								
t								
u								
v								
w								
$t/c = k_t * M_{DD}^{t^*} * (\cos \phi_{25})^{u^*} * c_L^{v^*} * k_M^{w^*}$	11,34%	11,11%	10,68%	10,72%	10,54%	11,14%	sum:	SEE:
error ²	0,00000	0,00002	0,00001	0,00000	0,00002	0,00001	0,00164	0,75%
K_AA								
t/c from WEISSHAAR	11,77%	7,53%	9,22%	7,03%	8,37%	9,00%	sum:	SEE:
error ²	0,00002	0,00095	0,00015	0,00129	0,00069	0,00063	0,04521	3,95%
t/c from RAYMER	14,63%	6,81%	6,40%	4,83%	5,01%	8,17%	sum:	SEE:
error ²	0,00106	0,00145	0,00163	0,00335	0,00359	0,00111	0,05982	4,54%
t/c from SHEVELL	14,36%	9,29%	10,24%	8,18%	8,64%	10,60%	sum:	SEE:
error ²	0,00089	0,00018	0,00000	0,00060	0,00055	0,00008	0,18854	8,06%
a								
b								
c								
d								
t/c from BÖTTGER	0,13979	0,09602	0,09935	0,07653	0,08601	0,11200	sum:	SEE:
error ²	0,00068	0,00010	0,00003	0,00088	0,00058	0,00001	0,06288	4,66%
y	0,28913	0,37365	0,52516	0,47298	0,64130	0,40186		
M_{DIV}	0,76000	0,82000	0,84000	0,86000	0,86000	0,80500		
ΔM_{DIV}	0,00	0,00	0,00	0,00	0,00	0,00		
$M_{DIV_peaky} = M_{DIV} + \Delta M_{DIV}$	0,76000	0,82000	0,84000	0,86000	0,86000	0,80500		
M_{CC}	0,73799	0,79464	0,80962	0,83006	0,82735	0,77966		
u	2,83550	2,83550	2,83550	2,83550	2,83550	2,83550		
v	-1,78397	-1,74795	-1,68338	-1,70562	-1,63388	-1,73593		
w	0,19859	0,14923	0,16205	0,14010	0,14392	0,16291		
arg in root	0,93015	1,36274	0,99584	1,32011	1,03725	1,16569		
x	0,14451	0,10238	0,12087	0,09816	0,10852	0,11572		
t/c from KROO	13,58%	9,35%	10,19%	8,46%	8,89%	10,49%	sum:	SEE:
error ²	0,00049	0,00016	0,00001	0,00047	0,00045	0,00010	0,05695	4,59%
ϕ_{25}	20,0	24,0	32,5	30,5	35,0	25,0		
C_L	0,26	0,31	0,37	0,35	0,43	0,33		
M_{DIV}	0,76000	0,82000	0,84000	0,86000	0,86000	0,80500		
ΔM_{DIV}	0,04	0,04	0,04	0,04	0,04	0,04		
$M_{DIV_supercrit} = M_{DIV} + \Delta M_{DIV}$	0,80	0,86	0,88	0,90	0,90	0,85		
t/c from SCHAUFLE (roughly from chart)	12,50%	8,50%	9,50%	6,50%	7,00%	8,00%	sum:	SEE:
error ²	0,00013	0,00045	0,00009	0,00170	0,00160	0,00123	0,03182	3,31%

standard 5,49 0,6 auf sc 5,04% 0,6 auf sc&pe: 4,54%

all 4,66% sup. crit. 4,32%

Table D.5 Relative thickness of a wing - aircraft with supercritical airfoils (1)

Number of aircraft included in this statistic

Manufacturer Type Model	Mitsubishi Diamond I	Airbus A300 -600	Boeing 767 200	Cessna 650 Citation VI	Airbus A310 -300	Raytheon Hawker 800XP	Raytheon Beechjet 400A	Beriev Be-40	min	max
sweep, 1/4 chord, ϕ_{25} [deg]	20,00	28,00	31,30	23,00	28,00	20,00	20,00	23,00	4,45	35,00
drag divergence Mach number, M_{DD}	0,70611	0,81805	0,85081	0,81885	0,81959	0,80000	0,78401	0,70227	0,65	0,89
lift coefficient, C_L	0,42264	0,46235	0,47262	0,30176	0,47491	0,36945	0,21559	0,25893	0,16111	0,73316
airfoil	super crit.	super crit.	super crit.	super crit.	super crit.	super crit.	super crit.	super crit.		
$M_{DD,eff}$	0,68	0,77	0,79	0,79	0,77	0,78	0,76	0,67	0,63883	0,81685

$k_{M,conv}$															
$k_{M,peaky}$															
$k_{M,super}$															
$k_{M,super,modern}$															
k_T															
e															
k_M	4,703	4,703	4,703	4,703	4,703	4,703	4,703	4,703							
t/c from TORENBEEK with C_L	12,40%	11,49%	11,09%	11,95%	11,49%	12,22%	12,25%	12,17%	sum:	SEE:	opt. k_M	standard	opt. all		
error^2	0,00004	0,00010	0,00002	0,00020	0,00002	0,00001	0,00002	0,00000	0,00187	0,80%	2,49%	2,88%	0,80%		
t/c from TORENBEEK with $C_L/\cos\phi_{25}$	12,40%	11,49%	11,09%	11,95%	11,49%	12,22%	12,25%	12,17%	sum:	SEE:					
error^2	0,00004	0,00010	0,00002	0,00020	0,00002	0,00001	0,00002	0,00000	0,00189	0,81%					
AF_{conv}															
AF_{peaky}															
AF_{super}															
$AF_{super,modern}$															
AF	0,91	0,91	0,91	0,91	0,91	0,91	0,91	0,91							
t/c from HOWE	18,05%	9,23%	7,35%	9,14%	8,96%	9,48%	12,56%	20,75%	sum:	SEE:					
error^2	0,00393	0,00016	0,00172	0,00179	0,00087	0,00097	0,00006	0,00749	0,03899	3,67%					
t/c from JENKINSON	16,70%	9,30%	7,41%	10,54%	9,03%	10,62%	13,77%	19,50%	sum:	SEE:					
error^2	0,00242	0,00014	0,00167	0,00081	0,00082	0,00039	0,00040	0,00547	0,05193	4,23%					
K															
t/c from similarity without sweep	15,83%	8,48%	6,47%	8,43%	8,38%	9,63%	10,66%	16,08%	sum:	SEE:					
error^2	0,00164	0,00041	0,00253	0,00244	0,00124	0,00088	0,00012	0,00159	0,03990	3,71%					
K_{phi}															
t/c from similarity with sweep	14,91%	10,07%	9,06%	9,11%	9,99%	9,68%	10,56%	15,52%	sum:	SEE:					
error^2	0,00098	0,00002	0,00059	0,00182	0,00037	0,00085	0,00015	0,00117	0,01707	2,43%					
LINEAR REGRESSION															
a															
b															
c															
t/c= $a*M_{DD,eff} + b*C_L + c*k_m$	10,99%	12,20%	12,45%	12,53%	12,21%	12,34%	12,20%	10,92%	sum:	SEE:					
error^2	0,00006	0,00029	0,00009	0,00007	0,00001	0,00001	0,00002	0,00014	0,00405	1,18%					
k_t															

$$Standard\ Error\ of\ Estimate = \sqrt{\frac{\sum (x_{estimate} - y)^2}{n}}$$

Table D.6 Relative thickness of a wing - aircraft with supercritical airfoils (2)

Number of aircraft included in this statistic

Manufacturer Type Model	Mitsubishi Diamond I	Airbus A300 -600	Boeing 767 200	Cessna 650 Citation VI	Airbus A310 -300	Raytheon Hawker 800XP	Raytheon Beechjet 400A	Beriev Be-40	min	max
sweep, 1/4 chord, ϕ_{25} [deg]	20,00	28,00	31,30	23,00	28,00	20,00	20,00	23,00	4,45	35,00
drag divergence Mach number, M_{DD}	0,70611	0,81805	0,85081	0,81885	0,81959	0,80000	0,78401	0,70227	0,65	0,89
lift coefficient, C_L	0,42264	0,46235	0,47262	0,30176	0,47491	0,36945	0,21559	0,25893	0,16111	0,73316
airfoil	super crit.	super crit.	super crit.	super crit.	super crit.	super crit.	super crit.	super crit.		
$M_{DD,eff}$	0,68	0,77	0,79	0,79	0,77	0,78	0,76	0,67	0,63883	0,81685
NONLINEAR REGRESSION										
$t/c = k_t \cdot M_{DD}^t \cdot (\cos \phi_{25})^u \cdot c_L^v \cdot k_M^w$	12,51%	11,77%	11,48%	11,78%	11,79%	12,10%	11,82%	12,08%	sum:	SEE:
error ²	0,00005	0,00016	0,00000	0,00025	0,00000	0,00002	0,00000	0,00000	0,00164	0,75%
K_AA										
t/c from WEISSHAAR	16,52%	9,32%	8,16%	9,00%	9,06%	8,79%	11,84%	19,35%	sum:	SEE:
error ²	0,00225	0,00014	0,00112	0,00191	0,00081	0,00144	0,00000	0,00525	0,04521	3,95%
t/c from RAYMER	19,55%	8,14%	6,12%	8,60%	7,87%	9,03%	15,05%	22,87%	sum:	SEE:
error ²	0,00604	0,00056	0,00290	0,00228	0,00162	0,00127	0,00107	0,01161	0,05982	4,54%
t/c from SHEVELL	28,42%	15,78%	13,68%	16,89%	15,32%	16,42%	21,58%	34,20%	sum:	SEE:
error ²	0,02771	0,00279	0,00047	0,00124	0,00117	0,00147	0,00961	0,04883	0,18854	8,06%
a										
b										
c										
d										
t/c from BÖTTGER	0,20398	0,12176	0,10006	0,11251	0,11943	0,12103	0,13619	0,21752	sum:	SEE:
error ²	0,00743	0,00028	0,00022	0,00045	0,00000	0,00002	0,00034	0,00932	0,06288	4,66%
y	0,47863	0,59306	0,64733	0,35613	0,60918	0,41839	0,24415	0,30558		
M_DIV	0,68611	0,79805	0,83081	0,79885	0,79959	0,78000	0,76401	0,68227		
ΔM_{DIV}	-0,04	-0,04	-0,04	-0,04	-0,04	-0,04	-0,04	-0,04		
M_DIV_peaky = M_DIV + ΔM_{DIV}	0,64611	0,75805	0,79081	0,75885	0,75959	0,74000	0,72401	0,64227		
M_CC	0,62739	0,73286	0,76286	0,73578	0,73435	0,71857	0,70304	0,62274		
u	2,83550	2,83550	2,83550	2,83550	2,83550	2,83550	2,83550	2,83550		
v	-1,70321	-1,65444	-1,63131	-1,75542	-1,64757	-1,72888	-1,80314	-1,77696		
w	0,26462	0,18421	0,16860	0,20139	0,17967	0,19099	0,24043	0,31555		
arg in root	-0,10037	0,64786	0,74888	0,79733	0,67664	0,82285	0,52442	-0,42136		
x	#ZAHL!	0,14980	0,13506	0,15209	0,14547	0,14491	0,19026	#ZAHL!		
t/c from KROO	#ZAHL!	13,23%	11,54%	14,00%	12,84%	13,62%	17,88%	#ZAHL!	sum:	SEE:
error ²		0,00074	0,00000	0,00004	0,00009	0,00011	0,00373		0,05695	4,59%
ϕ_{25}	20,0	28,0	31,3	23,0	28,0	20,0	20,0	23,0		
C_L	0,42	0,46	0,47	0,30	0,47	0,37	0,22	0,26		
M_DIV	0,68611	0,79805	0,83081	0,79885	0,79959	0,78000	0,76401	0,68227		
ΔM_{DIV}	0,00	0,00	0,00	0,00	0,00	0,00	0,00	0,00		
M_DIV_supercrit = M_DIV + ΔM_{DIV}	0,69	0,80	0,83	0,80	0,80	0,78	0,76	0,68		
t/c from SCHAUFLE (roughly from chart)	18,00%	9,50%	11,50%	13,00%	9,00%	12,00%	16,00%	20,00%	sum:	SEE:
error ²	0,00388	0,00010	0,00000	0,00001	0,00084	0,00003	0,00179	0,00624	0,03182	3,31%

standard 5,49 0,6 auf sc 5,04% 0,6 auf sc&pe: 4,54%

all 4,66% sup. crit. 4,32%

Table D.7 Relative thickness of a wing - aircraft with modern supercritical airfoils (1)

Number of aircraft included in this statistic

Manufacturer Type Model	Bombardier Global Express	Bombardier Challenger CRJ 200 LR	Tupolev Tu-204-300	BAe RJ85	Embraer EMB-145	Airbus A321 -200	Airbus A340 -300	min	max
sweep, 1/4 chord, ϕ_{25} [deg]	35,00	24,54	28,00	15,00	22,73	24,96	29,74	4,45	35,00
drag divergence Mach number, M_{DD}	0,89000	0,79154	0,78107	0,72989	0,75000	0,81931	0,85968	0,65	0,89
lift coefficient, C_L	0,51020	0,45516	0,73316	0,47562	0,43148	0,46096	0,54237	0,16111	0,73316
airfoil	modern super crit.	modern super crit.	modern super crit.	modern super crit.	modern super crit.	modern super crit.	modern super crit.		
$M_{DD,eff}$	0,81	0,75	0,73	0,72	0,72	0,78	0,80	0,63883	0,81685
$k_{M,conv}$									
$k_{M,peaky}$									
$k_{M,super}$									
$k_{M,super,modern}$									
k_T									
e									
k_M	1,735	1,735	1,735	1,735	1,735	1,735	1,735		
t/c from TORENBEEK with C_L	10,42%	11,69%	11,37%	12,50%	11,93%	11,60%	11,05%	sum:	SEE:
error^2	0,00003	0,00008	0,00001	0,00002	0,00009	0,00001	0,00005	0,00187	0,80%
t/c from TORENBEEK with $C_L/\cos\phi_{25}$	10,41%	11,69%	11,36%	12,49%	11,93%	11,59%	11,05%	sum:	SEE:
error^2	0,00003	0,00008	0,00001	0,00002	0,00009	0,00001	0,00005	0,00189	0,81%
AF_{conv}									
AF_{peaky}									
AF_{super}									
$AF_{super,modern}$									
AF	0,93	0,93	0,93	0,93	0,93	0,93	0,93		
t/c from HOWE	6,90%	12,51%	11,83%	16,06%	16,21%	9,93%	7,02%	sum:	SEE:
error^2	0,00168	0,00029	0,00007	0,00095	0,00271	0,00039	0,00225	0,03899	3,67%
t/c from JENKINSON	4,86%	10,74%	8,45%	13,75%	13,78%	8,73%	5,57%	sum:	SEE:
error^2	0,00377	0,00000	0,00065	0,00006	0,00077	0,00102	0,00383	0,05193	4,23%
K									
t/c from similarity without sweep	4,23%	10,17%	10,85%	14,24%	12,90%	8,40%	5,94%	sum:	SEE:
error^2	0,00459	0,00004	0,00000	0,00016	0,00036	0,00124	0,00339	0,03990	3,71%
Kphi									
t/c from similarity with sweep	8,00%	10,85%	12,05%	13,01%	12,84%	9,42%	8,25%	sum:	SEE:
error^2	0,00090	0,00000	0,00011	0,00000	0,00034	0,00062	0,00123	0,01707	2,43%
a									
LINEAR									
REGRESSION									
t/c= $a*M_{DD,eff} + b*C_L + c*k_m$	11,95%	11,24%	10,79%	10,68%	10,74%	11,60%	11,87%	sum:	SEE:
error^2	0,00009	0,00002	0,00000	0,00053	0,00001	0,00001	0,00000	0,00405	1,18%

opt. k_M
2,49%

Table D.8 Relative thickness of a wing - aircraft with modern supercritical airfoils (2)

Number of aircraft included in this statistic

Manufacturer Type Model	Bombardier Global Express	Bombardier Challenger CRJ 200 LR	Tupolev Tu-204-300	BAe RJ85	Embraer EMB-145	Airbus A321 -200	Airbus A340 -300	min	max
sweep, 1/4 chord, ϕ_{25} [deg]	35,00	24,54	28,00	15,00	22,73	24,96	29,74	4,45	35,00
drag divergence Mach number, M_{DD}	0,89000	0,79154	0,78107	0,72989	0,75000	0,81931	0,85968	0,65	0,89
lift coefficient, C_L	0,51020	0,45516	0,73316	0,47562	0,43148	0,46096	0,54237	0,16111	0,73316
airfoil	modern super crit.	modern super crit.	modern super crit.	modern super crit.	modern super crit.	modern super crit.	modern super crit.		
$M_{DD,eff}$	0,81	0,75	0,73	0,72	0,72	0,78	0,80	0,63883	0,81685
NONLINEAR REGRESSION									
k_t									
$t/c = k_t \cdot M_{DD}^t \cdot (\cos \phi_{25})^u \cdot c_L^v \cdot k_M^w$	10,75%	11,60%	11,73%	12,22%	11,79%	11,50%	11,21%	sum:	SEE:
error ²	0,00001	0,00006	0,00005	0,00006	0,00006	0,00002	0,00003	0,00164	0,75%
K_AA									
t/c from WEISSHAAR	6,72%	10,20%	9,14%	12,67%	13,35%	8,01%	5,97%	sum:	SEE:
error ²	0,00183	0,00004	0,00035	0,00001	0,00055	0,00153	0,00335	0,04521	3,95%
t/c from RAYMER	4,00%	10,01%	8,25%	14,70%	15,65%	7,39%	4,93%	sum:	SEE:
error ²	0,00490	0,00006	0,00076	0,00030	0,00216	0,00205	0,00467	0,05982	4,54%
t/c from SHEVELL	10,93%	17,44%	13,90%	21,78%	22,63%	14,29%	10,46%	sum:	SEE:
error ²	0,00000	0,00441	0,00084	0,00776	0,01354	0,00056	0,00017	0,18854	8,06%
a									
b									
c									
d									
t/c from BÖTTGER	0,07074	0,13714	0,07908	0,16640	0,17115	0,11284	0,07999	sum:	SEE:
error ²	0,00154	0,00085	0,00096	0,00134	0,00374	0,00004	0,00142	0,06288	4,66%
y	0,76035	0,55004	0,94043	0,50977	0,50721	0,56083	0,71940		
M_DIV	0,87000	0,77154	0,76107	0,70989	0,73000	0,79931	0,83968		
ΔM_{DIV}	-0,06	-0,06	-0,06	-0,06	-0,06	-0,06	-0,06		
M_DIV_peaky = M_DIV + ΔM_{DIV}	0,81000	0,71154	0,70107	0,64989	0,67000	0,73931	0,77968		
M_CC	0,77924	0,68932	0,67778	0,63236	0,64972	0,71605	0,75292		
u	2,83550	2,83550	2,83550	2,83550	2,83550	2,83550	2,83550		
v	-1,58314	-1,67277	-1,50639	-1,68994	-1,69103	-1,66817	-1,60059		
w	0,15951	0,21284	0,16337	0,23713	0,24920	0,18856	0,15227		
arg in root	0,69717	0,38418	0,41630	0,16630	0,03317	0,64419	0,83483		
x	0,13193	0,18567	0,15186	0,22609	0,26607	0,15263	0,12113		
t/c from KROO	10,81%	16,89%	13,41%	21,84%	24,54%	13,84%	10,52%	sum:	SEE:
error ²	0,00000	0,00371	0,00058	0,00786	0,01834	0,00037	0,00016	0,05695	4,59%
ϕ_{25}	35,0	24,5	28,0	15,0	22,7	25,0	29,7		
C_L	0,51	0,46	0,73	0,48	0,43	0,46	0,54		
M_DIV	0,87000	0,77154	0,76107	0,70989	0,73000	0,79931	0,83968		
ΔM_{DIV}	-0,02	-0,02	-0,02	-0,02	-0,02	-0,02	-0,02		
M_DIV_supercrit = M_DIV + ΔM_{DIV}	0,85	0,75	0,74	0,69	0,71	0,78	0,82		
t/c from SCHAUFLELE (roughly from chart)	9,00%	14,00%	9,00%	14,00%	16,00%	12,00%	10,00%	sum:	SEE:
error ²	0,00040	0,00102	0,00040	0,00011	0,00250	0,00000	0,00031	0,03182	3,31%

standard
5,49

all
4,66%

Appendix E

Schaufele's Method

Supercritical Airfoil Sections

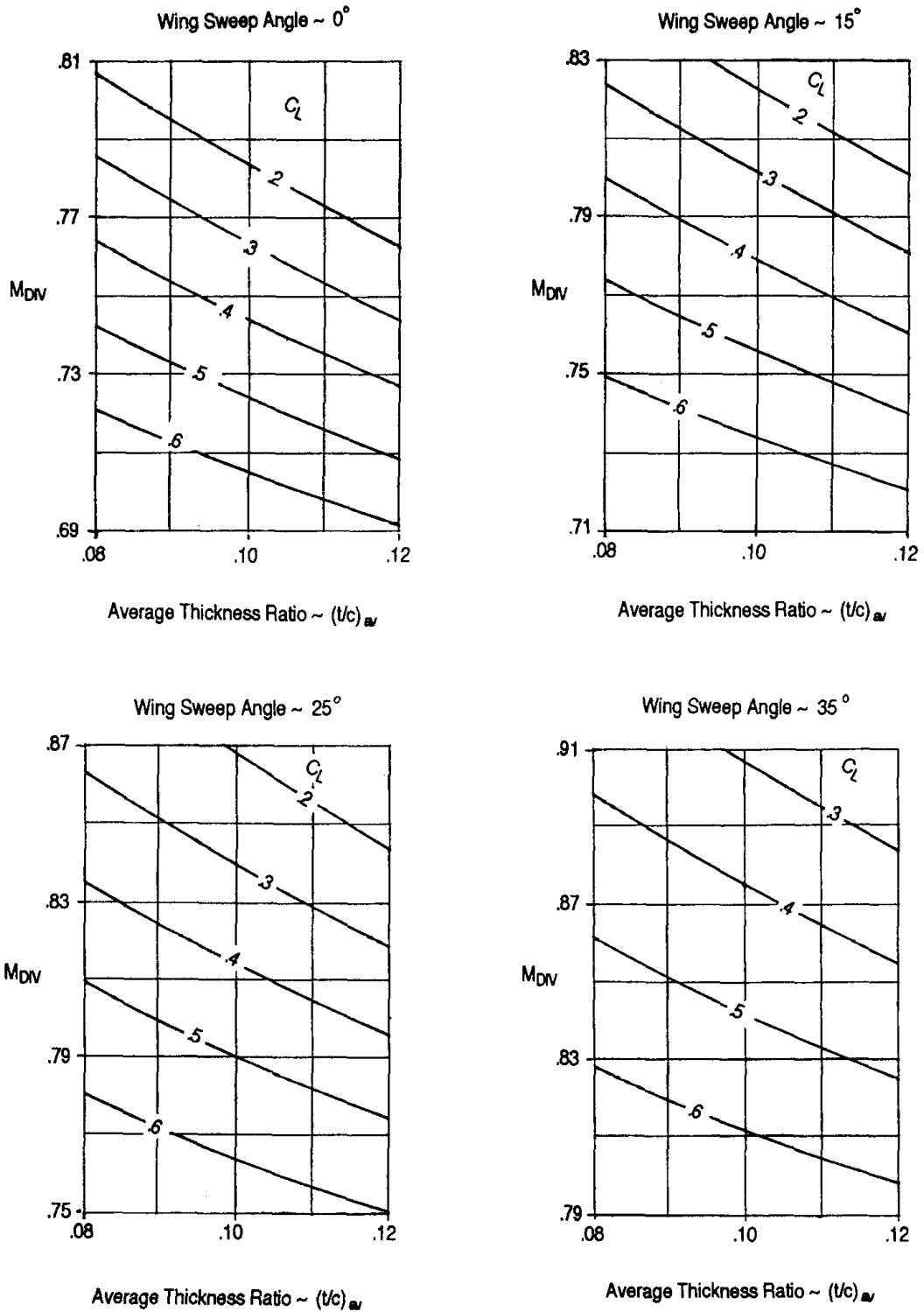


Figure E.1 Determination of M_{DIV} from Schaufele 2000